

NEURAMINIDASE-1 SIALIDASE AND MATRIX  
METALLOPROTEINASE-9 CROSSTALK IN ALLIANCE WITH  
INSULIN RECEPTORS IS AN ESSENTIAL MOLECULAR SIGNALING  
PLATFORM FOR INSULIN-INDUCED RECEPTOR ACTIVATION

by

Farah Gaber Alghamdi

A thesis submitted to the graduate program in Microbiology and Immunology  
In the Department of Biomedical & Molecular Sciences in conformity with the requirements for  
the degree of Master of Science

Queen's University  
Kingston, Ontario, Canada  
(February, 2013)

Copyright ©Farah Gaber Alghamdi, 2013

## Abstract

Molecular-targeting therapeutics directed towards growth factor receptors have become promising interventions in cancer. They include the family of mammalian receptor tyrosine kinases such as epidermal growth factor, TrkA and insulin. In particular, the insulin receptor (IR) is one of the most well-known members of the RTK family of receptors playing a role in cancer. IRs are covalently-linked heterodimers of  $\alpha\beta$  subunits on the cell membrane in the absence of insulin. The IR signaling pathways are initially triggered by insulin binding to the  $\alpha$  subunits followed by the interaction of  $\beta$  subunits and ATP. The parameter(s) controlling IR activation remains unknown. Here, we report a membrane receptor signaling platform initiated by insulin binding to its receptor to induce Neu1 in live HTC-IR and MiaPaCa-2 cell lines. Microscopy colocalization and co-immunoprecipitation analyses reveal that Neu1 and MMP9 form a complex with naïve and insulin-treated receptors. Tamiflu (neuraminidase inhibitor), galardin and piperazine (broad range MMP inhibitors), MMP9 specific inhibitor and anti-Neu1 antibody blocked Neu1 activity associated with insulin stimulated live cells. Moreover, Tamiflu, anti-Neu1 antibody, and MMP9 specific inhibitor blocked insulin induced insulin receptor substrate-1 phosphorylation (p-IRS1). The previous findings reveal a molecular organizational signaling platform of Neu1 and MMP-9 crosstalk in alliance with insulin receptors. It proposes that insulin binding to the receptor induces MMP9 to activate Neu1, which hydrolyzes  $\alpha$ -2,3 sialic acid in removing steric hindrance to generate a functional receptor. The results predict a prerequisite desialylation process by activated Neu1. A complete understanding of IR activation and the role of sialic acids in the

signaling pathways may provide a therapeutic strategy in the prevention of different diseases such as diabetes mellitus and cancer.

## **Acknowledgements**

Over the past two years I have received support from many great people. This thesis would not have been possible without their guidance. It gives me great pleasure to acknowledge their support and help.

First, it is with immense gratitude that I acknowledge the support and help of my supervisor, Dr. Myron Szewczuk. His support, guidance, patience and thoughts have made this a thoughtful and rewarding journey. Thank you for making working on my master degree an unforgettable experience. Thank you for helping me to develop my background in immunology, biochemistry and laboratory work. Besides my supervisor, I would like to acknowledge the support of my committee members, Dr. Katrina Gee and Dr. Chandra Tayade. Thank you for your thoughts, suggestions and help. I am very grateful for you and I really appreciate your insightful comments, encouragement, support, and your motivating discussions.

My sincere thanks also go to the Microbiology and Immunology department. Thank you to all the faculty members, all graduate students and the technical staff. I appreciate your support and guidance.

I am indebted to my friends who supported me through my journey in Queen's University especially, Samar Abdulkhalek, Masany Jung, Yan Ding and Vanessa Omana Moreno. I have learned a lot from you about friendship, life, research and how to solve research and life problems. Also, I would like to thank my best friend, Aiah Khateb, for her support when I have needed it the most. Thank you for being a great friend and a wonderful sister. Thank you with all my heart!

I would like to thank my mom, dad, my sisters, and my brother for their infinite support throughout everything in my life. Your care and love was the inspiration for me through my life journey. Despite the distance, you were always beside me and inside my heart.

Last but not the least, I cannot find words to express my gratitude to God. Thank you God for answering my prayers, helping me and for giving me the strength to get through all the hard times throughout my life.

This study was supported by a grant to M.R.S. from the Natural Sciences and Engineering Research Council of Canada (NSERC), and King Abdullah scholarship program from the Ministry of Higher Education, Saudi Arabia to Farah Alghamdi.

# Table of Contents

Abstract-----	ii
Acknowledgements -----	iv
List of Figures-----	ix
List of Tables-----	xi
List of Abbreviations -----	xii
Chapter 1 Introduction and Literature Review-----	1
1.1 Introduction-----	1
1.2 Insulin Receptor Family -----	3
1.2.1 Overview -----	3
1.2.2 Insulin-Like Growth Factor System -----	3
1.2.3 Insulin Receptor Isoforms -----	5
1.2.4 Insulin Receptors structure and Dimerization-----	10
1.2.5 Insulin -----	16
1.3 Insulin Activation of Insulin Receptor. -----	17
1.3.1 Ligand Binding to Insulin Receptors -----	17
1.3.2 Insulin Receptor Signaling Pathways-----	19
1.4 Receptor Glycosylation -----	22
1.5 Insulin Receptor Glycosylation -----	23
1.5.1 Overview -----	23
1.5.2 The Role of Glycosylation in Insulin Receptor activation-----	23
1.6 Sialic Acids-----	25
1.6.1 Functions of Sialic Acids -----	28
1.7 The Sialidases-----	29
1.7.1 Mammalian Neuraminidases -----	30
1.8 The Role of Neu1 Sialidase in Different Receptor Activation -----	33
1.9 Matrix Metalloproteinase Family-----	35
1.10 Insulin Receptor Activation Proposed Model-----	36
1.11 The Rational of this Project -----	38
1.12 Overall Hypothesis. -----	40
1.13 Main Objectives of Research Project-----	40
Chapter 2 Materials and Methods -----	41
2.1 Cell Lines:-----	41

2.2 Ligands:-----	41
2.3 Inhibitors: -----	42
2.4 Primary Antibodies: -----	43
2.5 Secondary Antibodies: -----	43
2.6 . Live Cell Sialidase Assay: -----	44
2.7 Immunocytochemistry for phosphorylation of IR $\beta$ in insulin-treated HTC-IR cells:-----	45
2.8 Preparation of Cell Lysates -----	46
2.9 Bradford Assay for Protein quantification -----	46
2.10 Western blot of insulin receptor $\beta$ (IR $\beta$ ) and human phosphorylated insulin receptor substrate-1 (pIRS-1):-----	47
2.11 Co-immunoprecipitation:-----	48
2.12 Neu1 and MMP9 colocalization with insulin receptor $\beta$ (IR $\beta$ ):-----	48
2.13 Statistical Analysis: -----	49
Chapter 3 Results -----	50
3.1 Expression of insulin receptors in different cell lines -----	50
3.2 Sialidase activity is associated with insulin stimulation of live HTC-IR cells-----	53
3.3 Oseltamivir phosphate inhibition of sialidase activity associated with insulin stimulated live HTC-IR -----	53
3.4 Neu1 sialidase activity is associated with insulin-treated HTC-IR cells-----	56
3.5 Neu1 sialidase activity is associated with insulin-treated live human pancreatic carcinoma MiaPaCa-2 cell line -----	61
3.6 Neu1 sialidase activity is associated with insulin-induced phosphorylation of insulin receptors (IR) in HTC-IR cells-----	61
3.7 Western blot analysis of Neu1 inhibition on insulin-induced insulin receptor phosphorylation in HTC-IR cells-----	64
3.8 Neu1 sialidase colocalizes with insulin receptor $\beta$ on the cell surface in naïve HTC-IR cells. -----	67
3.9 Co-immunoprecipitation of insulin receptors with mammalian sialidases (Neu-1,-2,-and 4) in naïve and insulin-stimulated HTC-IR cells.-----	70
3.10 Inhibition of insulin-induced sialidase activity by broad-range MMP inhibitors piperazine and galardin in live HTC-IR (Sialidase experiments). -----	76
3.11 MMP9 specific inhibitor blocks sialidase activity associated with insulin-treated live HTC-IR cells -----	76

3.12 MMP9 specific inhibitor blocks insulin-induced receptor phosphorylation in HTC-IR cells-----	81
3.13 MMP9 colocalizes with insulin receptor $\beta$ in HTC-IR cells-----	88
3.14 Co-immunoprecipitation of IR $\beta$ and MMP-9 in naïve and insulin-stimulated HTC-IR cells.-----	88
Chapter 4 Discussion-----	92
4.1 The Significance of the Project.-----	101
Literature Cited -----	103

## List of Figures

Figure 1.1	The structure of insulin super family and the homology between them.....	4
Figure 1.2	The ligand selectivity of the Insulin Receptors .....	6
Figure 1.3	Structure of insulin receptor isoforms, IR-A and IR-B .....	8
Figure 1.4	IR isoforms in different cancer tissue in comparison to normal tissues .....	9
Figure 1.5	Structure of IR heterotetramer extracellular portion of IR-A and IR-B. ....	13
Figure 1.6	Insulin receptor structure. ....	15
Figure 1.7	Insulin Binding to Insulin Receptors .....	18
Figure 1.8	Insulin Receptor Signaling Pathway.....	21
Figure 1.9	The primary forms of Sialic Acids .....	26
Figure 1.10	Sialic Acid Structure.....	27
Figure 1.11	A proposed model of insulin-induced IR Activation on the cell surface.....	39
Figure 3.1	HTC-IR, HTC-WT, and MiaPaCa-2 cell lines express insulin receptors.....	52
Figure 3.2	Insulin stimulation of insulin receptors induced sialidase activity in a dose dependent manner in live HTC-IR cells.....	55
Figure 3.3	Oseltamivir phosphate (Tamiflu) inhibition of insulin-induced sialidase activity in live HTC-IR cells.....	58
Figure 3.4	Insulin stimulation of insulin receptors induces only Neu1 sialidase activity in live HTC-IR cells.....	60
Figure 3.5	Induction of sialidase activity by insulin stimulation in live MiaPaCa cells.....	63
Figure 3.6	Inhibition of insulin-induced insulin receptor phosphorylation by oseltamivir phosphate (Tamiflu).....	66
Figure 3.7	Oseltamivir phosphate (Tamiflu) and Neu1 specific inhibitor were able to block insulin receptor phosphorylation in HTC-IR cell line .....	69
Figure 3.8	The colocalization between IR $\beta$ and Neu1 in naïve HTC-IR cells .....	72
Figure 3.9	Insulin IR $\beta$ receptors co-immunoprecipitate with Neu1 in cell lysates from naïve and insulin-stimulated HTC-IR cells.....	75
Figure 3.10	Inhibition of insulin-induced sialidase activity by piperazine (broad range MMP inhibitors) in live HTC-IR .....	78

Figure 3.11 Inhibition of insulin-induced sialidase activity by galardin (broad range MMP inhibitors) in live HTC-IR .....	80
Figure 3.12 Effect of MMP-3 specific inhibitor on insulin-induced sialidase activity in live HTC-IR. ....	83
Figure 3.13 Inhibition of insulin-induced sialidase activity by MMP-9 specific inhibitor in live HTC-IR .....	85
Figure 3.14 MMP-9 specific inhibitor was able to block insulin receptor phosphorylation in HTC-IR cell line .....	87
Figure 3.15 MMP9 colocalization with IR $\beta$ in naïve HTC-IR cells .....	89
Figure 3.16 Insulin receptors and MMP9 co-immunoprecipitate in naïve and insulin-stimulated HTC-IR cells.....	91
Figure 4.1 Proposed model for IR activation.....	100

## List of Tables

Table 1 The differences among mammalian sialidases.....	31
---	----

## List of Abbreviations

4-MUNANA	2 <sup>o</sup> -(4-methylumbelliferyl)- $\alpha$ -D-N-acetylneuraminic acid
Akt, PKB	Protein Kinase B, a serine/threonine-specific protein kinase
ATP	adenosine triphosphate
$\beta$ .Gal	$\beta$ -galactosides
BSA	bovine serum albumin
CR	Cystine rich domain
CT	Carboxy terminal
CTP	cytidine 5-triphosphate
EBP	Elastin binding protein
EGFR	Epidermal growth factor receptor
ER	endoplasmic reticulum
FBS	Fetal bovine serum
FnIII	Fibronectin type III domains
GLUT4	Glucose transporter type 4
GPCR	G-protein coupled receptor
Grb2	Growth factor receptor-bound protein 2
HTC-IR	A rat hepatoma cell line that overly express insulin receptors
HTC-WT	Wild type rat hepatoma cell line
HRP	horse radish peroxidase
IGF	Insulin like growth factor
IGF-BPs	Insulin like growth factor binding proteins
IGF-IR, IGF-IIR	Insulin like growth factor receptor I and II
Ins	Insulin
IR	Insulin receptors
IR $\beta$	Insulin receptor $\beta$ subunit
IR-A, IR-B	Insulin receptor isoform A and B
IRR	insulin related receptors
IRS	Insulin receptor substrates
JAK	Janus Kinase
JM	jaxtamembrane domain
KDN	2-keto-3-deoxy-D-glycero-D-galactononic acid
L1, L2	Leucine-rich repeats
LPS	lipopolysaccharide
MAPK	Mitogen-activated protein kinase
MiaPaCa-2	human pancreatic carcinoma cell line
MMP	Matrix metalloproteinase
NGF	Nerve growth factor
Neu	Neuraminidase
Neu5Ac	2-keto-5-acetamido-3,5-dideoxy-D-glycero-D-galactononulosonic acid
P85	The regulatory subunit of PI3k

P110	The catalytic subunit of PI3k
PBS	Phosphate-buffered saline
PDK1	Phospho-inositol dependent kinase 1
PI3K	Phosphoinositide 3-kinase
PIP2	Phosphatidylinositol biphosphate
PIP3	Phosphatidylinositol 3,4,5- biphosphate
PIPZ	Piperazine
pIR	Phosphorylated Insulin receptor
PPCA	Protective protein cathepsin A
PPP	Cyclolignan picropodophyllin
pTyr	Phosphorylated tyrosine
PVDF	Polyvinylidene difluoride membrane
RAS	RAt Sarcoma
RTK	Receptor tyrosine kinase
RLF	Relaxin-like factor
SH2	Sarcoma Cc homology2
STAT	Signal transducer and activator of transcription
Tami	Oseltamivir phosphate
TBS	Tris-buffered saline
T.cruzi	Trypanasoma cruzi
TK	Tyrosine kinase
TLR	Toll-like receptor
TS	Trans sialidase

# Chapter 1

## Introduction and Literature Review

### 1.1 Introduction

Mammalian receptor tyrosine kinases (RTKs) are high affinity cell surface receptors which bind many growth factors, cytokines and hormones (1). There are approximately twenty different RTK classes (2). Most RTKs are single (monomeric) in the absence of their ligands (3). However, there are some exceptions such as the insulin receptor and insulin-like growth factor receptor that exist as multimeric complexes (4). The binding between a growth factor and the extracellular domain of an RTK leads to dimerization with the adjacent RTKs (5). Dimerization triggers a rapid activation of the receptor's cytoplasmic kinase domains. The activated receptor then undergoes autophosphorylation on specific intracellular tyrosine residues (6). Although the signaling pathways of RTKs are well characterized, the parameters controlling dimerization and the interactions between the receptors and their ligands remain poorly defined. For instance, glycosylation of the nerve growth factor (NGF) TrkA receptors is required to localize the receptor to the cell surface where glycosylation is proposed to prevent receptor autophosphorylation (7). Indeed, glycosylation of most cell membrane bound RTKs may be an important requirement for their transport and function. In support of this, glycosylation is an important requirement for at least the processing, hormonal regulation

and binding activity of insulin receptor (8). However, the precise role of glycosylation in RTK receptor activation has not been fully determined.

Insight for the role of glycosylation in RTK receptor activation originated from the well-characterized model of TrkA family of receptors, demonstrating the role of the removal of sialyl  $\alpha$ -2,3 residues linked to  $\beta$ -galactosides of TrkA by an exogenous sialidase (9-11). These reports presented a novel role of glycosylation for receptor dimerization and activation. Three important findings were presented in these reports. Firstly, recombinant *Trypanosoma cruzi* (*T. cruzi*) trans-sialidase (TS) treatment of TrkA-expressing PC12 cells led to TrkA phosphorylation (pTrkA), sufficient to promote cell differentiation (neurite outgrowth) and this activation process was independent of the TrkA natural ligand NGF (12). Secondly, trypanosome TS mimicked Trk related neurotrophic factors in cell survival responses (10). Thirdly, a membrane sialidase-controlling mechanism was reported to be dependent on ligand binding to its receptor to induce sialidase activity. Activated sialidase on the cell surface was shown to target and desialylate the receptor with subsequent induction of Trk dimerization and activation (9). These observations suggested that RTK activation is regulated by a cell surface mammalian sialidase induction and thus, critical parameters were identified to be involved with ligand binding to RTKs.

Since glycosylation is an important requirement for at least the processing and/or hormone-binding activity of RTK insulin receptor (13), the first objective of the literature review is to present an overview of the insulin receptor with a particular focus on the

structure, its different isoforms and functions. The second objective is to review the activation of the insulin receptor by its ligand and the subsequent signaling pathways involved in cell functions. The third objective is to discuss the role of glycosylation in the activation of the insulin receptor by its ligand.

## **1.2 Insulin Receptor Family**

### **1.2.1 Overview**

The insulin receptor family is composed of the insulin receptor, insulin-like growth factor I receptor, insulin-like growth factor II receptor, and insulin receptor related receptor (14). There is a high percentage of homology between insulin receptors and insulin-like growth factor I receptors. There are also functional overlaps between these two receptors. Therefore, several studies have focused on attempting to understand the relationship between insulin receptors and insulin-like growth factors.

### **1.2.2 Insulin-Like Growth Factor System**

Insulin-like growth factors (IGFs) are members in the insulin peptide superfamily. This family includes structurally related peptide hormones that play important roles in the growth, development, metabolism and survival of the cells (15) (see Figure 1.1). In humans, they are insulin, IGF-I, IGF-II, relaxin, a relaxin-like factor (RLF) and placentin (16). Both IGF-I and IGF-II are produced by the liver and are

## A-Chain

Insulin		G	I	V	E	Q	C	C	T	S	I	C	S	L	Y	Q	L	E	N	Y	C	N					
Relaxin-1		R	P	Y	V	A	L	F	E	K	C	C	L	I	G	C	T	K	R	S	L	A	K	Y	C		
Relaxin-2		Z	L	Y	S	A	L	A	N	K	C	C	H	V	G	C	T	K	R	S	L	A	R	F	C		
IGF-1	~	A	P	Q	T	G	I	V	D	E	C	C	F	R	S	C	D	L	R	R	L	E	M	Y	C	A	~
IGF-2	~	R	R	S	R	G	I	V	E	E	C	C	F	R	S	C	D	L	A	L	L	E	T	L	C	A	~
INSL3		A	A	A	T	N	P	A	R	Y	C	C	L	S	G	C	T	Q	Q	D	L	L	T	L	C	P	Y
INSL4	R	S	G	R	H	R	F	D	P	F	C	C	E	V	I	C	D	D	G	T	S	V	K	L	C		
INSL5			Q	D	L	Q	T	L			C	C	T	D	G	C	S	M	T	D	L	S	A	L	C		
INSL6			G	Y	S	E	K				C	C	L	T	G	C	T	K	E	E	L	S	I	A	C		
Relaxin-3		D	V	L	A	G	L	S	S	S	C	C	K	W	G	C	S	K	S	E	I	S	S	L	C		

## B-chain

Insulin					F	V	N	Q	H	L	C	G	S	H	L	V	E	A	L	Y	L	V	C	G	E	R	G	F	F	Y	T	P	K	A	
Relaxin-1		K	W	K	D	D	V	I	K	L	C	G	R	E	L	V	R	A	Q	I	A	I	C	G	M	S	T	W	S						
Relaxin-2	D	S	W	M	E	E	V	I	K	L	C	G	R	E	L	V	R	A	Q	I	A	I	C	G	M	S	T	W	S						
IGF-1		~	G	P	E	T	L				C	G	A	E	L	V	D	A	L	Q	F	V	C	G	D	R	G	F	Y	F	N	K	P	~	
IGF-2		~	P	S	E	T	L				C	G	G	E	L	V	D	T	L	Q	F	V	C	G	D	R	G	F	Y	F	S	R	P	~	
INSL3		P	T	P	E	M	R	E	K	L	C	G	H	H	F	V	R	A	L	V	R	V	C	G	G	P	R	W	S	T	E	A			
INSL4		Z	S	L	A	A	E	L	R	G	C	G	P	R	F	G	K	H	L	L	S	Y	C	P	M	P	E	K	T	F	T	T	T	P	
INSL5			S	K	E	S	V	R	L		C	G	L	E	Y	I	R	T	V	I	Y	I	C	A	S	S	R	W							
INSL6		S	D	I	S	S	A	R	K	L	C	G	R	Y	L	V	K	E	I	E	K	L	C	G	H	A	N	W	S	F	R				
Relaxin-3		R	A	A	P	Y	G	V	R	L	C	G	R	E	F	I	R	A	V	I	F	T	C	G	G	R	W								

**Figure 1.1 The structure of insulin super family and the homology between them.**

This figure represents the primary structure of insulin superfamily members. Members of this family share six cysteines that give three disulfide bonds and a single glycine residue within B-chain (6).

essential for growth and development of somatic tissues as skeletal muscles and bone (17).

Since IGFs show structural homology to insulin, IGF-IRs are also very closely related to the IR (18). Both IGF-IR and IR share the structure of a covalently linked  $2\alpha 2\beta$  tetramer (19). They are both transmembrane receptors and they belong to the RTK superfamily of receptors (16). IGF-IR and IR also share functions such as glucose homeostasis and the proliferative effects of normal and abnormal neoplastic cells (19). Both receptors have the ability of combining and forming heterodimeric hybrid IR/IGF-IR receptors (16).

Unlike IGF-IR, IGF-IIR shows a structural homology with the cation independent mannose-6-phosphate receptors. IGF-IIR also lacks the tyrosine phosphorylation activity (20). IGFs bind to both the insulin receptor and the type I and II IGF receptors. Type I IGF receptors bind IGF I and IGF II with high affinity, while type II IGF receptors bind IGF I with high affinity and IGF II with low affinity (see Figure 1.2). Insulin receptors also bind IGF-I with about 100-fold less affinity than insulin. Thus, only high concentrations of IGFs trigger signaling via insulin receptor (21).

### **1.2.3 Insulin Receptor Isoforms**

Insulin receptors are represented by twenty-two exon-encoded sequences (22). Depending on the alternative mRNA splicing of exon 11, two IR isoforms are formed (23). The first one is the IR-A isoform, which lacks exon 11, the second isoform

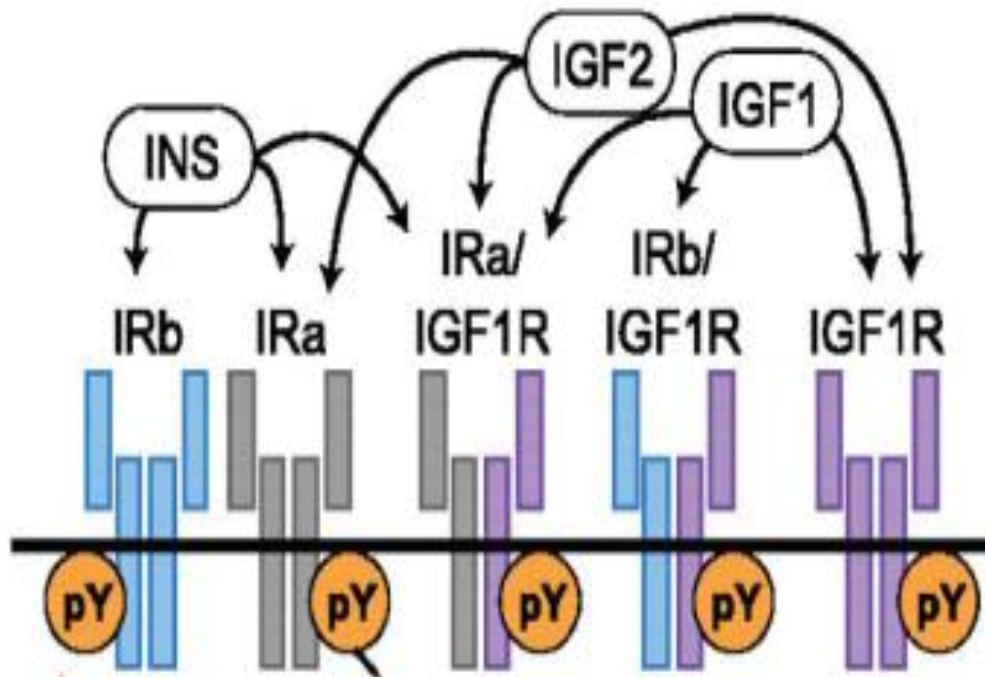


**Figure 1.2 The ligand selectivity of the Insulin Receptors**

Insulin (Ins) stimulation can activate IRa, IRb and IRa/IGF1R. IGF1 stimulation can activate IGF1R, IRa/IGF1R and IRb/IGF1R. IGF2 can activate IR-A, IR-A/IGF1R and IGF1R. Activation of the previously mentioned receptors lead to the autophosphorylation (pY) of beta subunits (24)

is IR-B, which includes this exon (24) (see Figure 1.3). IR-A is predominantly expressed during embryogenesis and fetal development. It enhances the embryonic life, growth and development. Thus, IRs function metabolically and non-metabolically (25). Different studies suggested that IR-A has two-fold higher affinity to bind insulin than IR-B (18,26). IR-A also has a faster internalization process and recycling time (27). The upregulation of IR-A is associated with the decrease of insulin signaling and the gain of insulin growth factor signaling (28). IR-A triggers mitogenic and anti-apoptotic signals (18). Numerous studies have linked IR-A overexpression with several serious diseases such as diabetes mellitus, different types of cancer and myotonic dystrophy (18,29). Interestingly, the overexpression of IR-A in cancer cells has been linked to the upregulation of hnRNP-A1 (splicing factor) (18).

In contrast, IR-B is predominantly expressed in well-differentiated tissues, where it plays an important role in the metabolic action of insulin. IR-B upregulation is associated with a predominant metabolic insulin signaling (30).

The main physiological function of the insulin receptor (IR) is involved in metabolic regulation. IR regulates glucose metabolism homeostasis (31). Failure to maintain metabolic homeostasis results in metabolic disorders such as diabetes mellitus (32). The alteration in the balanced ratio between IR-A and IR-B and the overexpression of IR-A has been linked to different cancer types such as breast cancer, lung cancer and colon cancer (30,33) (see Figure 1.4) . Thus, numerous studies are focusing on the role of these receptors in cancers and diabetes mellitus (28,30,33,34).

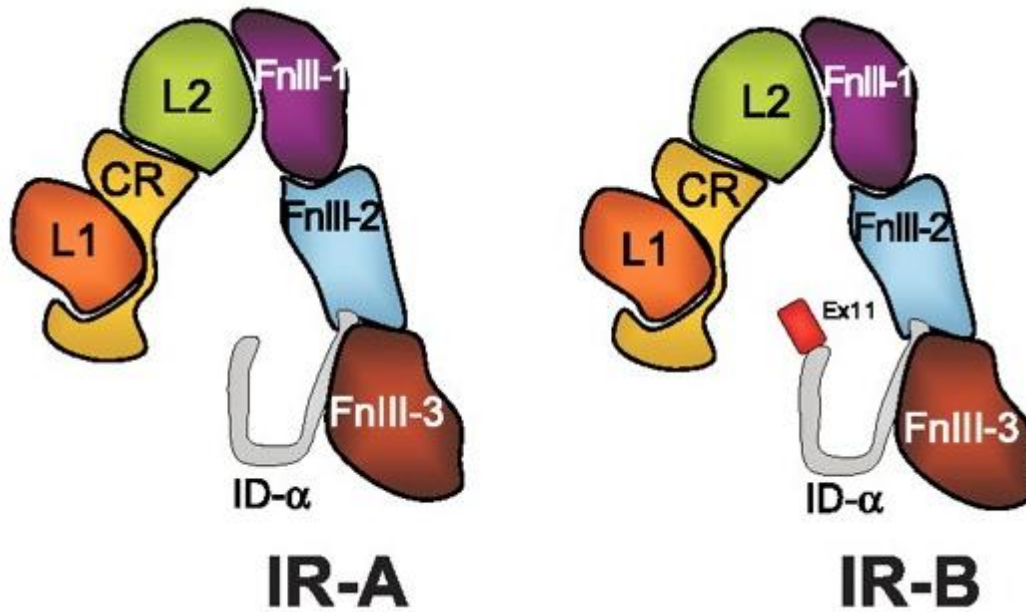


**Figure 1.3 Structure of insulin receptor isoforms, IR-A and IR-B**

Both forms A and B consist of leucin rich repeat 1(L1), cysteine rich domain (CR), leucin rich repeat 2 (L2), and three fibronectin domains (FnIII 1, FNIII 2 and FnIII 3). The red part represents the exon 11 which lacks in IR isoform A (30).

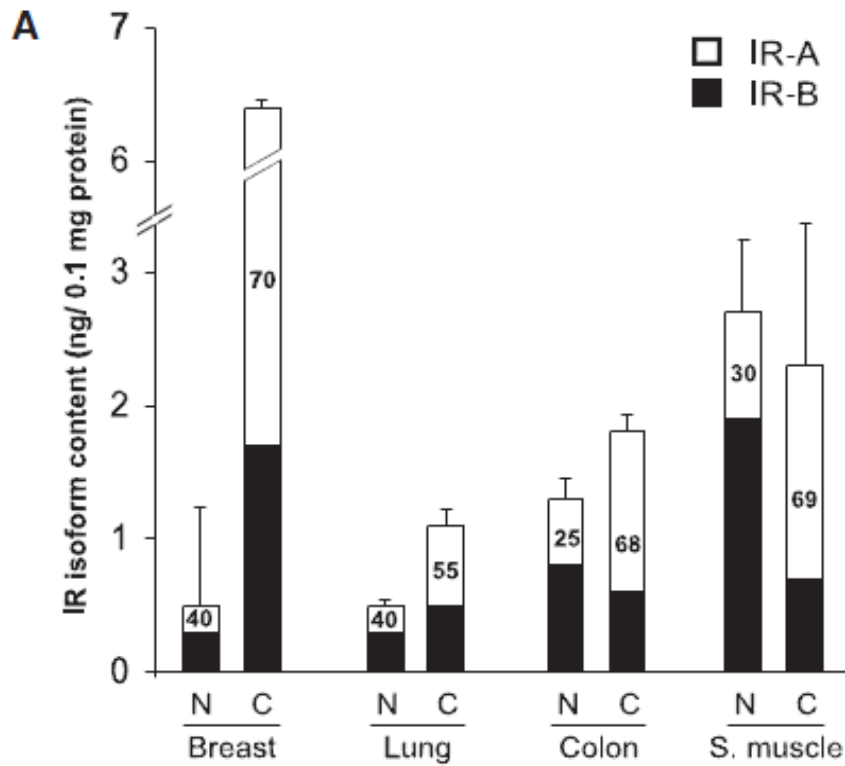


**Figure 1.4 IR isoforms in different cancer tissue in comparison to normal tissues**

The alteration in the balanced ratio between insulin receptor isoform A (IR-A) and insulin receptor isoform B (IR-B) and the over expression of insulin receptor isoform A have been linked to breast cancer, lung cancer, colon cancer and s.muscle cancer. IR isoform content has been calculated by determining the total IR protein content(30)

#### **1.2.4 Insulin Receptors structure and Dimerization**

Insulin receptors are transmembrane glycoprotein complexes or tetrameric proteins that play essential roles in different biological cell functions (35). IRs belong to the insulin family of receptors: insulin receptor, insulin-like growth factor-1 receptor (IGF-1R) and insulin related receptors (IRR) (6). The IR family of receptors belong to subclass II of the RTK superfamily of receptors (36).

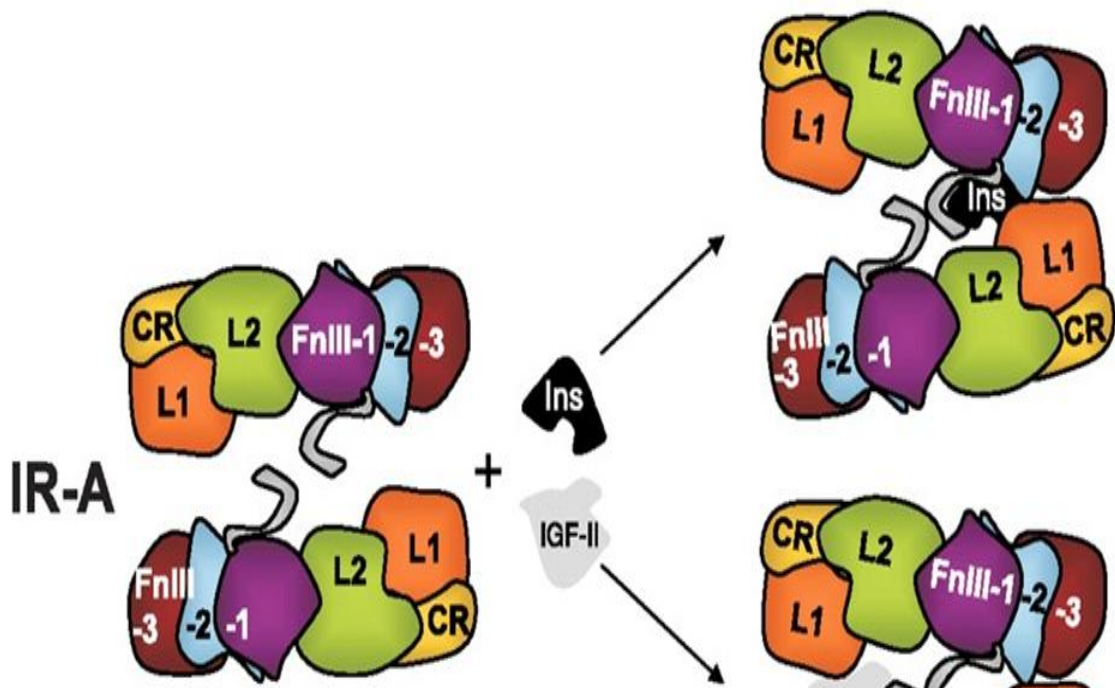
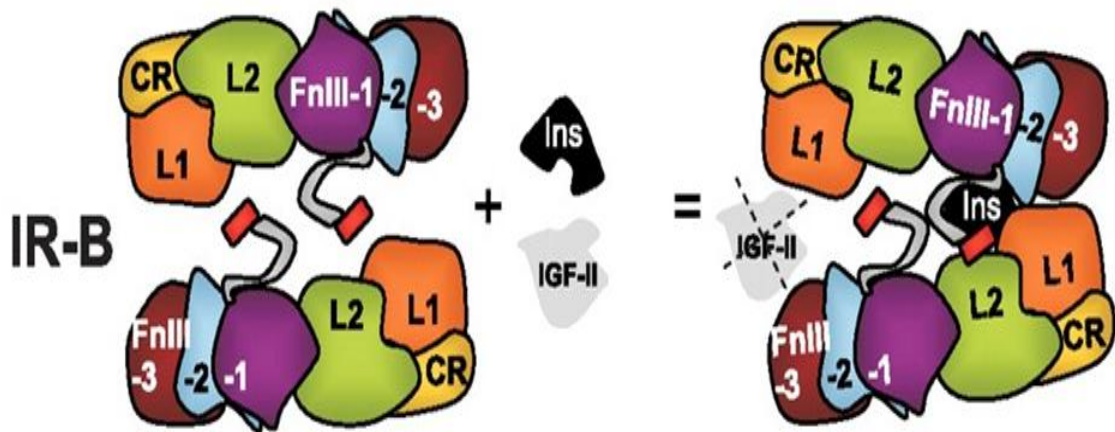
Generally, most RTKs are single highly glycosylated receptors and upon ligand binding, they undergo dimerization step. IR and IGF-1R are covalently-linked dimers in the absence of their ligands (37). The dimerization of the RTKs plays an important role in the regulation of their functions (38). The IR biosynthesis pathway or dimerization is initiated by the synthesis of a single-chain pre-proreceptor, the initial product of the IR gene, INSR, into the endoplasmic reticulum (ER) (36,39). INSR has twenty-two exons, of which eleven exons are encoding  $\alpha$ -subunits and eleven exons are encoding  $\beta$ -subunits (16,40). The formation of this pre-proreceptor is followed by a cleavage of the pre-proreceptor (6). Following this final step, the N-linked glycosylation of the proreceptor occurs at seventeen different sites (41). Two of the  $\alpha\beta$  subunits will undergo dimerization by combining together to form the  $\alpha\beta$  dimer of the insulin receptor. This dimer is composed of two extracellular  $\alpha$  subunits that contain the insulin binding site, and two  $\beta$  subunits that include a tyrosine kinase (TK) domain and two inter-chain covalent disulphide bonds (6). N-linked oligosaccharide will undergo a maturation step and the

cleavage of the receptor will take its place at the prototypical furin cleavage site (42,43). After this, IRs will transfer to the plasma membrane as the  $\alpha\beta$  heterodimer complex.

The  $\alpha$  subunit contains 719 or 731 amino acids (depending on the alternative mRNA splicing of exon 11) and its molecular mass is about 130 kDa. The  $\beta$  subunit contains 620 amino acids and its molecular mass is about 95 kDa (42).  $\alpha$  and  $\beta$  subunits are linked by two interchain disulphide bonds, while the two  $\alpha$  subunits are linked by a single intra- $\alpha$  disulphide bonds (6).

There are six extracellular structural domains in IR. Two of the homologous domains L1, L2, are leucine-rich repeats that are flanked by a cystine rich domain (CR), and three fibronectin domains (FnIII0, FnIII 1 and FnIII 2) (31). The FnIII0 domain is the location of the disulphide link between the  $\alpha$  subunits. The FnIII 2 domain is the site for cleavage, while FnIII 1 and FnIII 2 are sites for  $\alpha\beta$  disulphide links (31). Adjacent to the CR, a 12 amino acid sequence that is encoded by exon 11 is spliced and it gives two isoforms, IR-A and IR-B (23,42) (see Figure 1.5). The  $\beta$  subunit is composed of fibronectin type III domains (FN III), transmembrane domains (TM), jaxtamembrane domain (JM), Tyrosine Kinase domain (TK), and C terminal domain (44) (16) (see Figure 1.6).

There are similarities in the structure of both the insulin and IGF I and II receptors. The homology between IR and IGF-IR is 45–65% in the ligand binding domains and 60–85% in the tyrosine kinase domains (30). This homology may provide an explanation for



**“Free”**

**“Bound”**

**Figure 1.5 Structure of IR heterotetramer extracellular portion of IR-A and IR-B.**

This picture represents the extracellular portion of IR-A and IR-B. The extracellular portion of insulin receptor is composed of leucine-rich repeats (L1,L2) that are flanked by a cystine rich domain (CR), and three fibronectin domains (FnIII0 , FnIII 1 and FnIII 2). This picture is also shown that IR-B can bind to insulin, but not IGF-II. The reason why IR-B cannot bind to IGF-II is that IR-B has exon 11 (represented in the figure as a red fragment), which does not allow the binding between IR-B and IGF-II. On the other hand, IR-A can bind both insulin and IGF-II because it lacks exon 11(30).

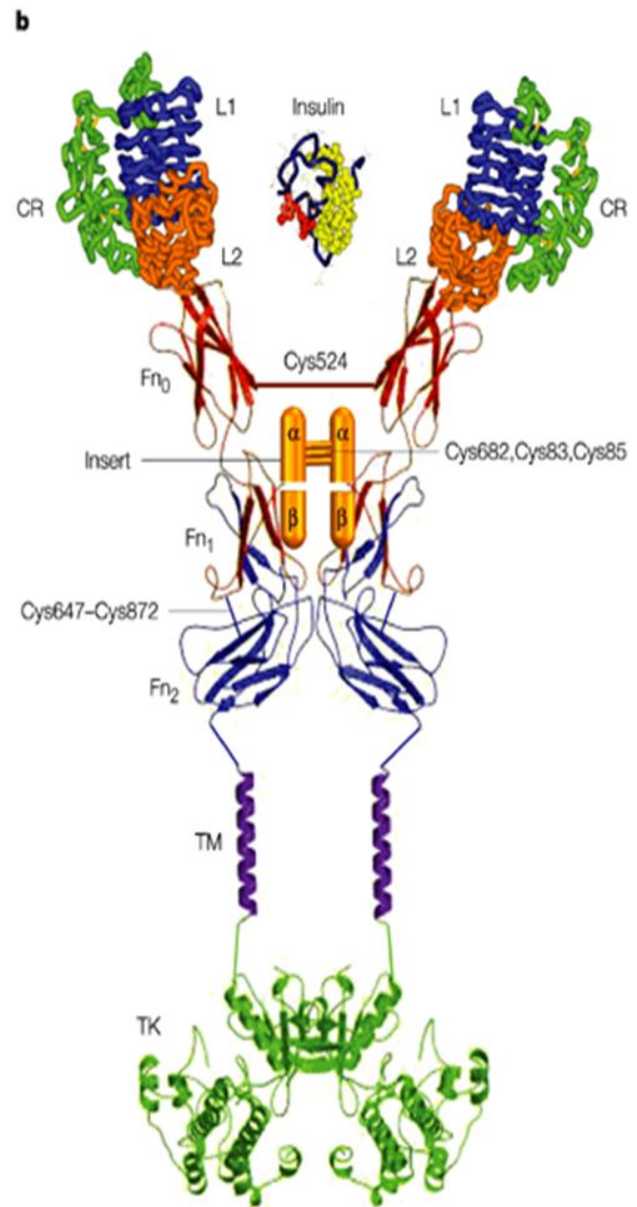
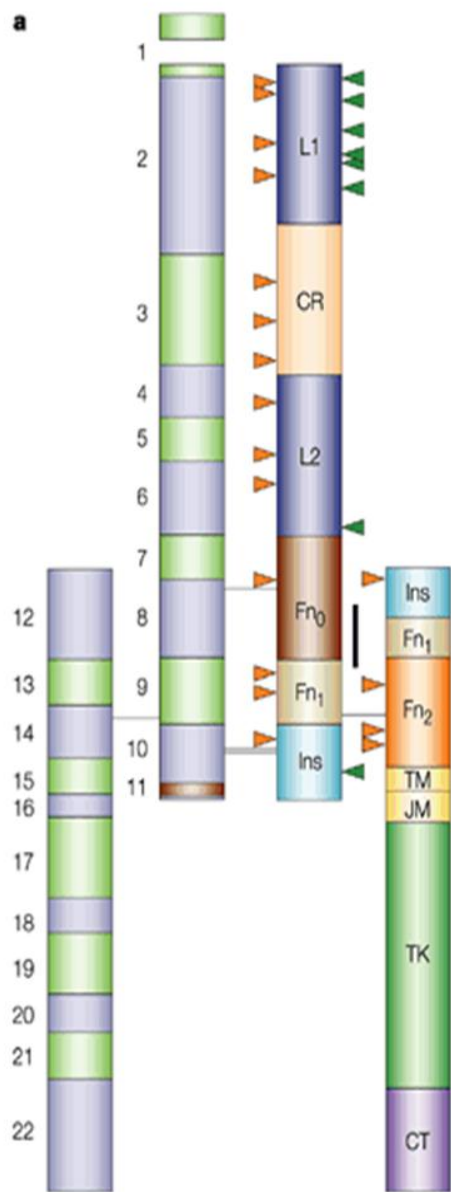


**Figure 1.6 Insulin receptor structure.**

Diagram A: shows the 22 exons that encode sequences of Insulin Receptor. Insulin receptor consists of two extracellular  $\alpha$  subunits and two transmembrane  $\beta$  subunits. Insulin receptor has three disulphide bonds; one bond between the two  $\alpha$  subunits and two bonds between the  $\alpha$  subunits and the  $\beta$  subunits. The orange arrowheads indicate the glycosylation sites: 14 at  $\alpha$  chain and four at  $\beta$  chain. The green arrowheads represent the ligand-binding hotspots. The major immunogenic region in the insulin receptor is represented in this diagram by a black bar along FN0. Diagram B: shows a modular structure of insulin receptors. Protein modules are composed of leucine-rich repeats 1 (L1), cystine rich domain (CR), leucine-rich repeats 2 (L2), fibronectin type III domains (FN III), transmembrane domains (TM), jaxtamembrane domain (JM), Tyrosine Kinase domain (TK) and C terminal domain (45) .

the cross reaction and overlapping between both insulin receptor and insulin like growth factor receptors (46).

### **1.2.5 Insulin**

The insulin hormone maintains the body's metabolic homeostasis by regulating energy storage and glucose metabolism (47). It plays crucial roles for cells such as the increase of glycogen and fatty acid synthesis, the increase of fatty acid esterification, decreasing proteolysis, lipolysis and gluconeogenesis and increasing amino acid and potassium uptake (6,35). Insulin is a peptide hormone that is released by the pancreatic  $\beta$  cells directly into the hepatic portal blood (48). Insulin biosynthesis is initiated by the synthesis of preproinsulin, the initial translation product of the insulin gene, INSR gene (6). Pre-proinsulin is synthesized into the cytoplasm with a signal peptide (49). This is followed by the cotranslocation of the pre-proinsulin into the endoplasmic reticulum (49). Proinsulin will then produce by the cleavage of the signal peptide in the pre-proinsulin (50). A protein folding step will result in three disulphide bonds (49). The proinsulin will then transfer to the Golgi apparatus and packaged into secretory molecules, where it convert from proinsulin into insulin (51). Exocytosis is responsible for the release of mature insulin (52).

Fifty-one amino acids make up insulin. The A chain consists of 21 amino acids, while the B chain consists of 30 amino acids, giving it a molecular weight of 5808 Daltons. The A and B chains are covalently linked by disulphide bonds that maintain the stability and the biological activity of the insulin (53). Two bonds are interchain

disulphide linked bridges at the A7-B7 and at A20-B19 domains. The third is an intra A-chain that bonds A6 and A11 (53).

The insulin molecule is composed of hydrophobic core and the canonical elements of secondary structure (54). The hydrophobic core has four structural features: a central helix at B chain between B9 and B19, a disulphide bond between A20 and B19, a C-terminal A chain helix between A13 and A19, and a  $\beta$ -turn at B20 and B23 (53). Insulin molecules are produced and stored in a hexameric inactive, crystal form (53). This inactive structure provides the insulin molecule with long term protection and stability (53).

### **1.3 Insulin Activation of Insulin Receptor.**

#### **1.3.1 Ligand Binding to Insulin Receptors**

In each IR monomer, there are two non-identical binding sites, each of which is in a different region (55). When insulin binds to the low affinity site on the  $\alpha$  subunit, this promotes another insulin association with the alternative insulin receptor subunits (56). High affinity binding can occur only between the paired sites on one side of the insulin receptor dimer, for example, site 1 and 2' or site 1' and 2. This pairing process causes the negative co-operativity of the insulin receptor dimerization (42). The formation of site (1' and 2) cross-linking is responsible for opening up the initial site (1 and 2') and dissociation of the ligand bond at the previous initial site (55) (see Figure 1.7).

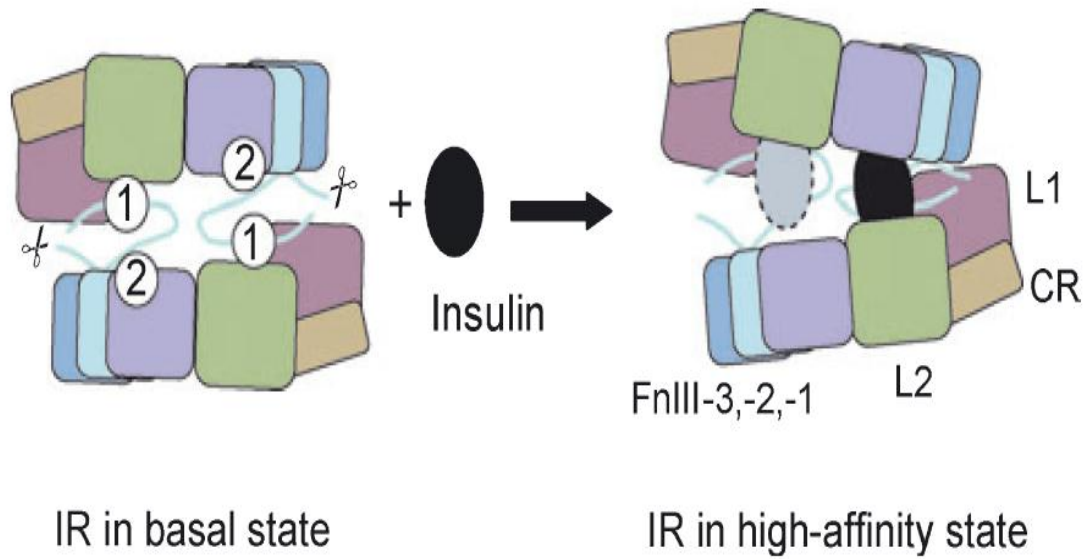


**Figure 1.7 Insulin Binding to Insulin Receptors**

This figure shows how insulin binds insulin receptor. The 'scissors' symbol represents the cleavage site. In case of high affinity state, insulin molecules can crosslink 1 and 2 on one side of the dimer. As a result, two monomers will close up on that side and open at the other side. Formation of the alternate cross-link will cause the negative co-operativity(55)

In addition, insulin binding to the receptor causes conformational changes within the receptor, ligand and N-terminal region. The carboxy-terminus of the insulin receptor moves in order to expose its hydrophobic surface. The N-terminal region then changes from an extended, stable, less active form to a less stable, more active form, resulting in the extension of the IR  $\beta$  chain (55).

Insulin binding to the insulin receptor, IR, results in the phosphorylation of a complex network of intracellular effector molecules that are involved in glucose metabolism and glucose transporter type 4 (GLUT4) translocation (25). The activation of the insulin receptor by insulin triggers the signaling cascade, a crucial step in hormonal regulation (53).

### **1.3.2 Insulin Receptor Signaling Pathways**

IR signaling pathways are triggered by the binding of insulin to the extracellular portion of the IR  $\alpha$  subunits which is followed with the association of the  $\beta$  subunits with the adenosine triphosphate (ATP) domain (6). This process leads to a cascade of autophosphorylation of tyrosine kinase domain in the  $\beta$  subunits, this is followed by the phosphorylation of insulin receptor substrate proteins (57).

The insulin receptor substrate (58) proteins are a family of cytoplasmic adaptor proteins, this family is composed of four members; IRS-1, IRS-2, Irs-3, and IRS-4 (57). IRS-1 and IRS-2 are essential mediators of insulin-dependent mitogenesis and the regulation of glucose metabolism in most cell types (59). The third member is Irs-3, which is expressed in rodents but not human (60). The last member is IRS-4, the

expression of IRS-4 is restricted to the liver, brain, kidney, and thymus (61). In insulin receptor signaling pathway, the phosphorylation of IRS proteins stimulates two signaling pathways: the phosphatidylinositol 3 kinase (PI3K) pathway, and the mitogen activated protein kinase (MAPK) pathway (6) (see Figure 1.8)

The PI3K is a heterodimeric protein that involves two subunits: p110, the catalytic subunit and p85, the regulatory subunit (46). The activation of the PI3K signaling pathway plays important roles in glucose metabolism, glycogen, lipid and protein synthesis (21). The phosphorylation of PI3K triggers the subsequent signaling cascade. The phosphorylation of IRS leads to the release of a subsequent cellular signaling pathway, resulting in the association of the PI3K regulatory subunit, p85, and the phosphorylated tyrosine residues of IR or IRS adaptor proteins (6). This association of p85 with IR or IRS results in conformational changes in the catalytic p110 subunit of PI3K (6,40). The phosphatidylinositol biphosphate (PIP<sub>2</sub>) is then catalyzed by PI3K into phosphatidylinositol 3,4,5- biphosphate (PIP<sub>3</sub>) (40). Accumulation of PIP<sub>3</sub> on the plasma membrane results in the recruitment and colocalization of phospho-inositol dependent kinase 1 (PDK1) and protein kinase B (PKB1/Akt). As a result (PDK)1 will phosphorylate and activate PKB1/Akt (46). PKB/Akt will then phosphorylates several target proteins, including glycogen synthase kinase 3 (GSK-3) (62).

The second pathway is Ras / MAPK. Ras proteins are composed of small guanosine triphosphate (GTP)/guanosine diphosphate (GDP)-binding GT (63). Ras proteins control a major intracellular signaling network affecting several cellular

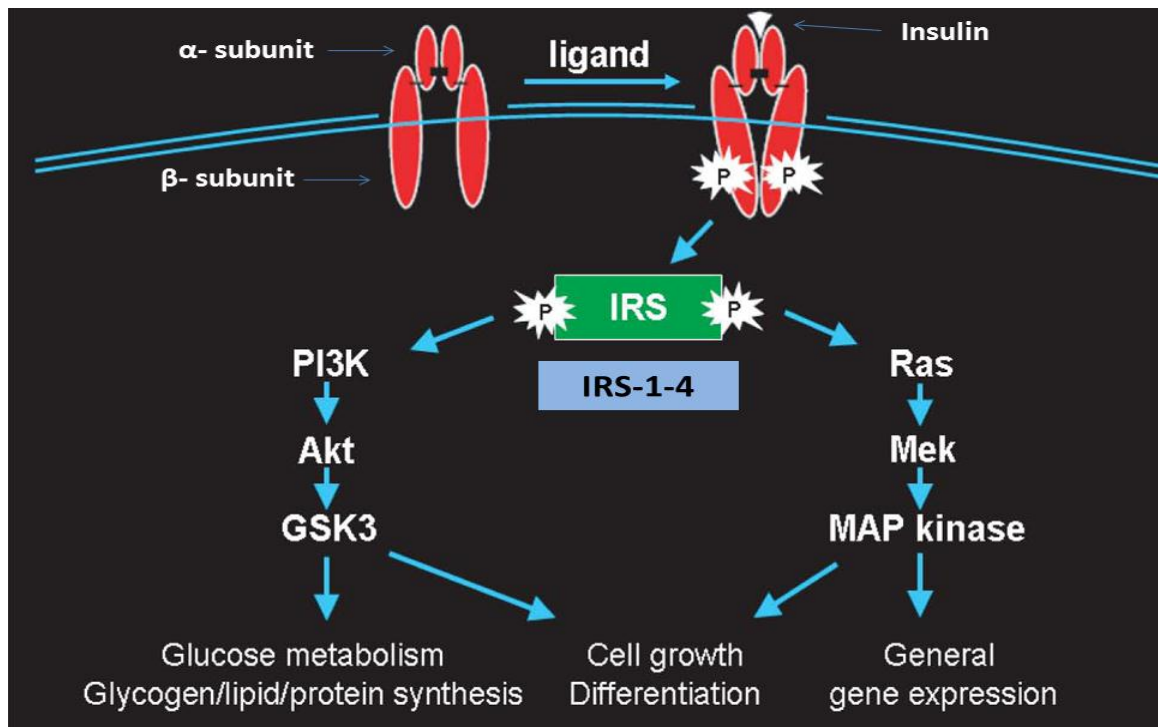


**Figure 1.8 Insulin Receptor Signaling Pathway**

This figure represents the cell signaling through insulin receptor substrate 1-4 (IRS-1-4). Insulin receptor pathway is initiated with insulin binding to insulin receptors, which leads to conformational changes in beta subunit of the receptor. Then, autophosphorylation of beta subunit will occur and that will lead to the phosphorylation of insulin receptor substrate 1-4. Phosphorylation of IRS proteins will then lead to two pathways; PI3K and MAPK.. PI3K activation leads to the recruitment of protein kinase B (PKB1/Akt). Akt will then phosphorylates several target proteins, including glycogen synthase kinase3 (GSK-3). PI3K pathway plays an important role in the metabolism of glucose, the synthesis of; glycogen, lipid, and protein. The second major insulin receptor signaling pathway is MAPK pathway. The phosphorylation of IRS proteins leads to the activation of Ras proteins. Ras proteins are composed of small guanosine triphosphate (GTP)/guanosine diphosphate (GDP)-binding GT. This is followed by the activation of Mek and the the release of MAP kinase. MAP kinase pathway plays an important role in gene expression. Both insulin receptor pathways affect the cell growth and differentiation. The picture was modified from (24).

functions such as proliferation, migration, survival, cell fate determination, differentiation, senescence and gene expression (24,64). Activation of cell surface receptors via extracellular ligands initiates the Ras/MAPK pathway (63). The activation of the Ras/MAPK pathway creates docking sites for adaptor molecules, such as Grb2, which bind to phosphorylated IR via their SH2 domain (30). As a result, activation of Ras/Raf occurs, triggering MAPK activation (65).

#### **1.4 Receptor Glycosylation**

Glycosylation is an enzymatic process that attaches glycan structures to protein, lipid and other organic molecules (66). There are five glycan classes. First, N-linked glycans are attached to a nitrogen of asparagine or arginine side-chains (67). Second, O-linked glycans are attached to the hydroxy oxygen of serine, threonine, tyrosine, hydroxylysine, or hydroxyproline side-chains, or to oxygens on lipids such as ceramide (66,68). Third, phospho-glycans are linked through the phosphate of a phospho-serine (66). Fourth, C-linked glycans are an infrequent glycan type, where a sugar is added to a carbon on a tryptophan side-chain (69). The last glycan class is glypiation, which is the addition of a GPI anchor that links proteins to lipids through glycan linkages (66).

Insulin receptors have 18 asparagine residues (glycosylation sites) that have the ability to accept N-linked glycosylation and some serine/threonine amino acids that are involved in O-linked glycosylation (55). The N-linked glycosylation process is crucial for folding and oligomerization of complex- multi-domain proteins (8). In 2000, Frankel et al. used site-directed mutagenesis in order to remove the N-linked glycosylation sites at

15 various regions. Interestingly, they found that individual mutations did not affect IR expression, processing or ligand binding. Mutation of a combination of sites results in impaired protein folding and processing.

## **1.5 Insulin Receptor Glycosylation**

### **1.5.1 Overview**

Receptor glycosylation is one of the essential aspects in a receptor's biosynthesis and functions. In particular, insulin receptor (IR) glycosylation is crucial for the folding, processing and trafficking of the receptor. In the following sections, the first objective is to investigate the role of glycosylation in IR biosynthesis and activation. The second objective is to present an overview of the sialic acids and the mammalian sialidases. Mammalian sialidases are enzymes that have the capability of cleaving the sialic acids from the glycosylated molecules in the cell. Sialidases play an important role in the activation of different receptors, such as insulin receptors (IR), insulin-like growth factor receptors (IGFRs) and epidermal growth factor receptors (EGFR). The third objective is to provide an overview of the role of glycosylation in the activation of different receptors. Finally, a particular focus of the following sections will be on the role of neuraminidase-1 (Neu1) in the IR activation.

### **1.5.2 The Role of Glycosylation in Insulin Receptor activation**

The insulin receptor is considered to be a highly glycosylated receptor, as it includes 18 asparagine residues (glycosylation sites). Fourteen of those glycosylation sites are localized on the  $\alpha$  subunits, while the rest are on the  $\beta$  subunits (8). Specifically,  $\alpha$  subunits contain the N-linked carbohydrate only, while  $\beta$  subunits contain both O- and N-linked carbohydrates (37).

During IR biosynthesis, and specifically at the endoplasmic reticulum (ER), N-linked glycans (Glc3Man9GlcNAc2) are moved from the dolichol-P-P derivative to the asparagine chain of the growing polypeptide (70). The reversible trimmers of the N-linked glycans are controlled by two enzymes: glucosidase and glucosyl transferase (71). These two enzymes play an important role in the transient glycosylation of the glycoprotein at the ER level (72). Dimerization of IR will then occur in the ER. After this, additional processing of the glycans occurs in the ER and the golgi. Following the additional processing step, further maturation steps are required in order to synthesize the mature functional IR. These maturation steps include the cleavage of the pre-proreceptor and the transport of the mature insulin receptor to the cell surface.

N-linked glycans that attach to IR have several biological functions. For instance, they are essential for the correction of the polypeptide folding chain. They are important for the correction of the  $\alpha\beta$  chain processing (71). They are also responsible for the transportation of the mature IR to the cell surface (71).

## 1.6 Sialic Acids

The sialic acid (neuraminic acid) family contains about 50 members that share a nine-carbon amino sugar backbone and a carboxylic acid group at the C1 position (66). This carboxylate gives the negative charge to the sialic acid. (73). Sialic acids are widely distributed among both invertebrates and vertebrates, as they are present in all cell surfaces, specifically at the outermost end of glycan chains (74).

There are two primary sialic acids: 2-keto-5-acetamido-3,5-dideoxy-D-glycero-D-galactononulosonic acid (Neu5Ac) and 2-keto-3-deoxy-D-glycero-D-galactononic acid (KDN) (66). (See figure 1.9). The rest of the sialic acid family members are derived from those primary sialic acids. Neu5Ac is the most common sialic acid among vertebrates (75).

The carbon number five position (C5) in the sialic acids is considered to be modification site, because distinct functional groups can attach to it. At this position, sialic acids can undergo different modification processes, such as acylation, methylation and hydroxylation (76,77). For instance, the modification (substitution) of Neu5Ac carbon number 5 results in KDN (66) The modification of C5 is essential for the diversity of sialic acids (see Figure 1.10). This diversity in sialic acids allows sialic acids to perform different biological functions such as; recognition and contact between cells and molecules, neuronal transmission, and ion transport (78).

Synthesis of sialic acid occurs in the cytosol as Neu5Ac and later, Neu5Ac transfers to the nucleus (66). Then, Neu5Ac attaches to cytosine 5-triphosphate (CTP) in order to

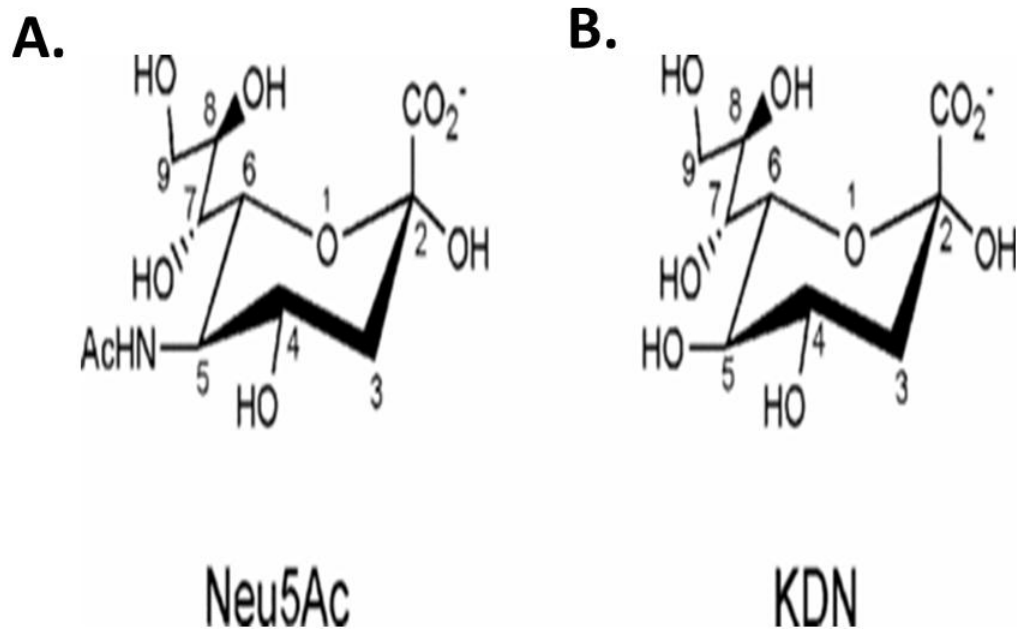
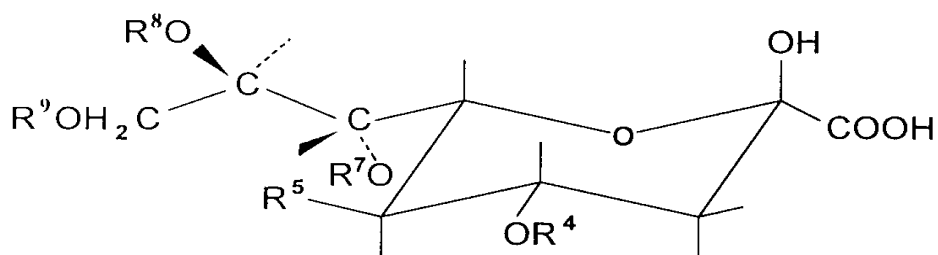


**Figure 1.9 The primary forms of Sialic Acids**

A, 2-keto-5-acetamido-3,5-dideoxy-D-glycero-D-galactononulosonic acid (Neu5Ac). B, 2-keto-3-deoxy-D-glycero-D-galactononic acid (KDN). The modification (substitution) in Neu5Ac carbon number 5 results in KDN. Neu5Ac is the most common sialic acid among vertebrates. Both Neu5Ac and KDN are primary sialic acids and all the rest of sialic acids family are derived from those primary sialic acids (79).



$R^5$	$R^{4,7,8,9}$
— NH — C — CH <sub>3</sub>    O	— H (4,7,8,9)
— NH — C — CH <sub>2</sub>                O          OH	— C — CH <sub>3</sub> (4,7,8,9)    O
— NH — C — CH <sub>2</sub>               O          O = O   CH <sub>3</sub>	— C — CH — CH <sub>3</sub> (9)                O          OH
— OH	— CH <sub>3</sub> (8)
	— SO <sub>3</sub> H (8)
	— PO <sub>3</sub> H <sub>2</sub> (9)

**Figure 1.10 Sialic Acid Structure**

This figure represents the structure of sialic acid. Sialic acids are composed of nine-carbon amino sugar backbone and carboxylic acid group at C1 position. The figure also represents a list of a possible nature substituents in the following modification sites: C4, C7, C8, C9, C5 (78)

produce CMP-Neu5Ac, which transfers to Golgi apparatus to be used by sialyl transferases (ST) (78). ST will then attach to CMP-Neu5Ac and give the sialic acid its specific glycoside linkage (66).

In humans, most of sialic acids are linked to galactose, as a terminal, non-reducing end of either glycolipids or glycoproteins (80). The rest of the sialic acids are in a free state (81). Both C-5 and the carboxyl group at the position number create negatively charged molecules of sialic acids (80). Human IR contains two types of oligosaccharides: high mannose oligosaccharide and a complex type. The complex type oligosaccharide includes N-acetylglucosamine, additional fructose, and sialic acid residues (8).

### **1.6.1 Functions of Sialic Acids**

Sialic acids play important roles in cell to cell interaction; the signaling, recognition, attachment, transportation, stabilization of the cell membrane and finally control of the permeability of the glomerular basement membrane (66). The most important function of sialic acids is cellular and molecular recognition (82). Sialic acids function as a recognition sites for host and pathogen receptors, which help the immune system to differentiate between self and non-self-cells (78). On the other hand sialic acids also have the capability of disguise and conceal recognition sites (75). For instance, some tumors are sialylated more than the normal tissue, this sialylation helps the tumor cells to escape from being recognized by the immune system (78).

Sialic acids have special features that affect their functions. For instance, as part of the membrane and as negative molecules, sialic acids are implicated in the transport of the positively charged molecules by using  $\text{Ca}^{+2}$  mobilizations (83,84). Sialic acids size, their negative charge and their exposed terminal position in the carbohydrate chain allow them to function as protective shields for the sub-terminal part of the sialic acid molecule (78). This protective shield prevents protease degradation of glycoproteins (78).

The increase in sialic acid levels is associated with many conditions such as malignancies, inflammations, cardio-vascular diseases, diabetes mellitus type I and II. Additionally, some studies have shown that sialic acid is increased in insulin resistance, which suggests a relation between the elevation in sialic acid level and the insulin resistance (66). One of the main features of cancer cells is the alteration in glycosylation. For example, different studies show that malignant metastatic potential and invasiveness are accompanied by the alteration of sialylation (85).

### **1.7 The Sialidases**

Sialidases or neuraminidases are enzymes that belong to the exo-glycosidase family (80). Neuraminidases play important roles in regulating several cell functions, such as proliferation, differentiation, antigenic properties, catabolism, infection and signal transduction (86). In order to perform these functions, neuraminidases catalyze the hydrolysis of the terminal sialic acid from oligosaccharides, glycoproteins, or glycolipids (87). Neuraminidases are capable of cleaving the  $\alpha$ -2,3,  $\alpha$ -2,4,  $\alpha$ -2,6,  $\alpha$ -2,8, and  $\alpha$ -2,9 linkages. However, the  $\alpha$ -2,3 and  $\alpha$ -2,6 linkages are the essential neuraminidase substrate

(77). Neuraminidases can be found in viruses, bacteria, protozoa and mammalian cells (88).

According to the differences in their localization, pH, response to the ions and detergent, kinetic properties and the specificity of the substrate, mammalian neuraminidases can be classified into four types; Neu1, Neu2, Neu3 and Neu4 (80) (See (see Table 1.1). Human neuraminidases share three important structural features with viral and bacterial neuraminidases. First, they involve the F/YRIV/P motif that is localized in the N-terminal end (86). Second, they include the Asp boxes [consensus sequence Ser/Thr-X-Asp-(Xb-Gly-X-Thr-Trp/Phe)], and this consensus sequence is repeated two to five times according to the protein type (89). Third, they also share the conserved six-bladed  $\beta$  propeller domain that includes the enzyme active site (90). The arginine of the F/YRIV/P motif is localized in the center of the  $\beta$  propeller, which implies that F/YRIV/P motif is part of the active site. Asp boxes on the other hand are localized on the peripheral end of the protein, which implies that they might play a role related to the structure (89).

### **1.7.1 Mammalian Neuraminidases**

Mammalian neuraminidases are involved in different cell functions, for instance, cellular proliferation, cellular differentiation and membrane function and antigenic masking (91). The first type of mammalian neuraminidase is the lysosomal neuraminidase-1 (Neu1), which can be found on the cell surface as well (92,93). The majority of vertebrate tissues express Neu1: pancreas, skeletal muscle, kidney, heart,

	Neu1	Neu2	Neu3	Neu4
Major location	Lysosomes	Cytosol	Plasma membranes	Lysosomes (?)
Substrate specificity	Oligosaccharides 4MU-NeuAc	Oligosaccharides 4MU-NeuAc Glycoproteins Gangliosides	Gangliosides	Oligosaccharides 4MU-NeuAc Glycoproteins Gangliosides
Optimal pH	4.4-4.6	6.0-6.5	4.6-4.8	4.4-4.5
Total amino acids (human)	415	380	428	496 (484)
Chromosome location (human)	6p 21.3	2q 37	11q13.5	2q37.3

**Table 1** The differences among mammalian sialidases

lung, liver and brain cells are expressing Neu1 (89). In order to perform its functions, Neu1 forms a multienzyme complex that contains two hydrolases: the protective protein/cathepsin A (PPCA) and the glycosidase beta-galactosidase ( $\beta$ -GAL) (80). Neu1 is the only sialidase known to have direct involvement in the two neurodegenerative metabolism defects: sialidosis and galactosialidosis (80). Sialidosis is an inherited metabolic disorder caused by Neu1 gene structural lesions (94). On the other hand, galactosialidosis is caused by the deficiency of both Neu1 and  $\beta$ -galactosidase (89). Both disorders share a metabolic biochemical defect that is characterized by the accumulation of sialylated oligosaccharides and glycopeptides in fibroblast tissues. Furthermore an enormous amounts of these compounds appear in the urine and body fluids (95). The involvement of Neu1 in these two neurodegenerative metabolism defects implies that there is a role for Neu1 in intracellular catabolism of sialylated glucoconjugates (96).

The second type of mammalian neuraminidase is the cytosolic neuraminidase-2 (Neu2) (97). Neu2 is expressed in skeletal muscles (98). Neu2 has the capability of recognizing distinct substrates, such as glycoproteins, gangliosides, and oligosaccharides (99). Neu2 is implicated in myoblast differentiation and muscle regeneration (80).

The third type of mammalian neuraminidase is the membrane associated neuraminidase3 (Neu3), which recognizes gangliosides (80). Neu3 is expressed in the adrenal glands, testis, skeletal muscle, thymus, and fetal tissues (100). The fourth type of mammalian neuraminidase is the neuraminidase-4 (Neu4). Neu4 is localized in the

mitochondria, lysosome, and the cell membrane (80). According to the presence of the twelve amino acids sequence localized in the N-terminus, Neu4 can be sub-classified into two isoforms: the long isoform (Neu4L) that has the sequence and the short isoform (Neu4S) which lacks the sequence (101). Neu4 is expressed in CNS cells, colon, liver, kidney, and small intestine (80). Neu4 is implicated in the regulation of neuronal differentiation (80).

### **1.8 The Role of Neu1 Sialidase in Different Receptor Activation**

Numerous studies suggested that Neu1 mediated desialylation has an important role in the activation of different receptors. For instance, *Woronowicz et al.,( 2004)* presented the role of glycosylation in TrkA receptor dimerization and activation. This study demonstrated the role of the removal of sialyl  $\alpha$ -2,3 residues linked to  $\beta$ -galactosides of Trk by an exogenous sialidase. Treatment of TrkA-expressing PC12 cells with recombinant *T. cruzi* trans-sialidase (TS) resulted in TrkA phosphorylation (pTrkA) sufficient to promote cell differentiation (neurite outgrowth). This activation process was independent of TrkA natural ligand, nerve growth factor (NGF). In addition, trypanosome TS mimicked Trk related neurotrophic factors in cell survival responses (10,12).

In 2007, *Woronowicz et al.* suggested a novel signaling paradigm for NGF TrkA receptor activation. They reported that the cleavage of the  $\alpha$ 2,3- linked galactose residues by a sialidase enzyme is essential for receptor activation. In this study, they treated cells with oseltamivir phosphate, a broad range sialidase inhibitor, before stimulating them

with the ligand. Oseltamivir phosphate was able to inhibit phosphorylation of TrkA, thus implying that TrkA activation requires sialidase activity (9).

In 2010, Jayanth et al, reported unprecedented membrane sialidase mechanism initiated by nerve growth factor (NGF) binding to TrkA to potentiate GPCR-signaling via membrane G $\alpha$ i subunit proteins and matrix metalloproteinase-9 (MMP-9) activation in order to induce Neu1 sialidase activation in live primary neurons and TrkA- and TrkB-expressing cell lines. They were able to block the sialidase activity in live TrkAPC12 cells treated with NGF with subsequent inhibition of Trk activation in primary neurons and neurite outgrowth in TrkA-PC12 cells by using Tamiflu (neuraminidase inhibitor). These findings reveal a Neu1 and MMP-9 cross-talk on the cell surface that is essential for neurotrophin-induced Trk tyrosine kinase receptor activation and cellular signaling (102).

In 2010, Amith et al. extended this research to the activation of the Toll-like receptors (TLRs). They have shown that Neu1 sialidase forms a complex with TLR 2, 3 and 4 on the cell surface of macrophages. They demonstrated that upon ligand (lipopolysaccharide, polyinosinic-polycytidylic acid and killed *Mycobacterium butyricum*) stimulation, Neu1 sialidase becomes activated. This activation of Neu1 results in the cleavage in the  $\alpha$ -2,3 linked sialic acid on the ecto-domain of TLR. Also, they have shown that Neu1 sialidase plays an important role in TLR activation and dimerization (93).

## **1.9 Matrix Metalloproteinase Family**

The metalloproteinase family is composed of transmembrane metalloproteinases with a disintegrin domain (ADAM proteins), secreted metalloproteinases with thrombospondin repeats (ADAMTS proteins) and matrix metalloproteinases (MMPs) (103). Metalloproteinases have the ability of processing cytokines, collagen and growth factors and form an integral part of the pathological and physiological processes in the extracellular matrix environment (103). Matrix metalloproteinases (MMPs) are a family of enzymes, capable of regulating cell-matrix composition by using zinc for their proteolytic activities (104). MMPs are responsible for different cellular functions such as tissue remodeling and degradation of the extracellular matrix (104).

There are 26 human matrix metalloproteinases. Human MMPs are classified according to their specificity into collagenases such as MMP-1, gelatinases such as MMP-9, stromelysins such as MMP-3, and matrilysins such as MMP-26 (105). MMP-9 is a 92 kDa gelatinase B matrix metalloproteinase (106). MMP9 is implicated in the breakdown of extracellular matrix in several biological processes. For instance, during reproduction, tissue remodeling and embryonic development (107). Several studies have looked at the involvement of MMP-9 with different pathological disorders such as insulin resistance, systemic lupus erythematosus, Sjogren's syndrome, systemic sclerosis, rheumatoid arthritis, multiple sclerosis, polymyositis and atherosclerosis (104,108-111).

Different studies have focused on the role of MMP-9 in the activation of different receptors such as Toll-like receptors. In 2012, Abdulkhalek et al. reported that

Neu1 and MMP-9 crosstalk is essential for Toll-like receptor activation. They knockdown MMP-9 and reported that Neu1 activity associated with addition of the TLR4 ligand LPS, bombesin or LPA in siRNA MMP9 knockdown cells was reduced to low levels compared to wild-type RAW-blue cells (112).

In 2012, Purushothaman et al. showed that heparanase mediated upregulation of IRS1 regulates ERK activation, which leads to the enhancement of activated MMP-9 level and syndecan-1 shedding. In their experiment, they used zymography technique with IRS-1 knockdown and control cells. Compared to the control, IRS-1 knockdown cells exhibited low gelatinolytic activity corresponding to pro-MMP-9. They confirm the previous finding by using heparanase that mediated upregulation of IRS-1 regulates ERK activation, leading to the enhancement in the levels of activated MMP-9 and syndecan-1 shedding (113). The data from this study suggested that MMP-9 plays a role in insulin receptor activation. Also they indicated that the inhibition of the IRS-1 affects the MMP-9 level, which suggested that there is a relation between MMP-9 and insulin receptor activation. Further studies need to be done in order to identify the mechanism of MMP-9 activation and its role in insulin receptor activation.

### **1.10 Insulin Receptor Activation Proposed Model**

As both TrkA and IR belong to the receptor tyrosine kinases (RTKs) superfamily, we hypothesize that IR might follow the same activation paradigm as TrkA. Accordingly, sialidases might be the key for IR activation together with the MMP9. IR is

a heavily glycosylated receptor as it contains 18 glycosylation sites. The studies of IR glycosylation sites mutation have also shown the importance of glycosylation in IR biosynthesis, binding and activation (71,114). In 1992, Leconte et al. presented a study that focused on the potential contribution of N-linked oligosaccharides of the  $\beta$ -subunit in the processing, structure and function of the IR. They used a mutated IR (IR- $\beta$ N<sub>1234</sub>), which was mutagenized on four potential N-glycosylation sites (ASn-X-Ser/Thr) of the  $\beta$ -subunit. They compared the IR- $\beta$ N<sub>1234</sub> with the wild type IR (115). The immunoprecipitation method was used for both insulin receptors (IR- $\beta$ N<sub>1234</sub> and IRT), with two monoclonal antibodies that targeted the IR  $\alpha$  and  $\beta$  subunits. There were no differences on the molecular weight of  $\alpha$  subunits between both receptors. However, they reported a reduction in the molecular weight of the IR- $\beta$  subunit in the mutated IR, as the molecular weight had been reduced from 95 kDa to 80 kDa. These results showed that the mutation of the four glycosylation sites in IR- $\beta$  subunit has no effect on the  $\alpha$ -subunit, but it causes a reduction in the  $\beta$ -subunit molecular weight. It was reported that this mutation in the  $\beta$ -subunit had no effect on IR cell surface expression or on the insulin binding to the IR. However, the IR- $\beta$ N<sub>1234</sub> had major defect on tyrosine kinase activation by the insulin (114). These results prove the importance of the glycosylation in the structure and the activation of the insulin receptor.

Arabkhari et al. (2010) have shown that Neu1 inhibitors were able to inhibit the proliferative response of L6 cells (rat skeletal myoblast cells) to insulin (1-10 nM). Specifically, they used competitive Neu1 inhibitors such as anti-Neu1 Ab. and dd.

NANA (2,3-dehydro-2-deoxy-N-acetylneuraminic acid, a competitive inhibitor of the endogenous mammalian sialidases). They compared dermal fibroblast cells from sialidosis patients (i.e. patients who have Neu1 deficiency) with normal dermal fibroblast in order to determine the effect of Neu1 deficiency in the metabolic response to the insulin. In this study, they measured the Akt phosphorylation, because Akt is one of the end products of PI3K pathway. In Neu1 deficient samples, they reported a reduction in the Akt phosphorylation response to the same low dose of insulin, compared to the normal samples. Moreover, Arabkhari et al. were able to restore the normal level of Akt phosphorylation by pre incubating the Neu1 deficient samples with exogenous Neu1 and c-PNase (clostridium perfringens neuraminidase, exogenous neuraminidase) (116). The previous findings suggested that Neu1 plays a role in the activation of insulin receptor.

Insulin binding to the insulin receptors initiates the IR signaling cascade. This binding triggers the activation of MMP9. Activated MMP9 will activate Neu1. Neu1 sialidase, which in turn requires protective protein/cathepsin A (PPCA) to facilitate Neu1 recruitment from the lysosome to the cell membrane. The  $\alpha$ -2,3-linked sialic acid then undergoes a cleavage step after the activation of Neu1 sialidase. As a result, the receptor activation occurs and this is followed by autophosphorylation of insulin receptor  $\beta$  subunits, resulting in initiation of insulin receptor signaling cascades (See Figure 1.11).

### **1.11 The Rational of this Project**

IR overexpression is implicated in several pathological disorders, such as tumors and diabetes mellitus. Upon regulating IR expression, we could cure those disorders. In order

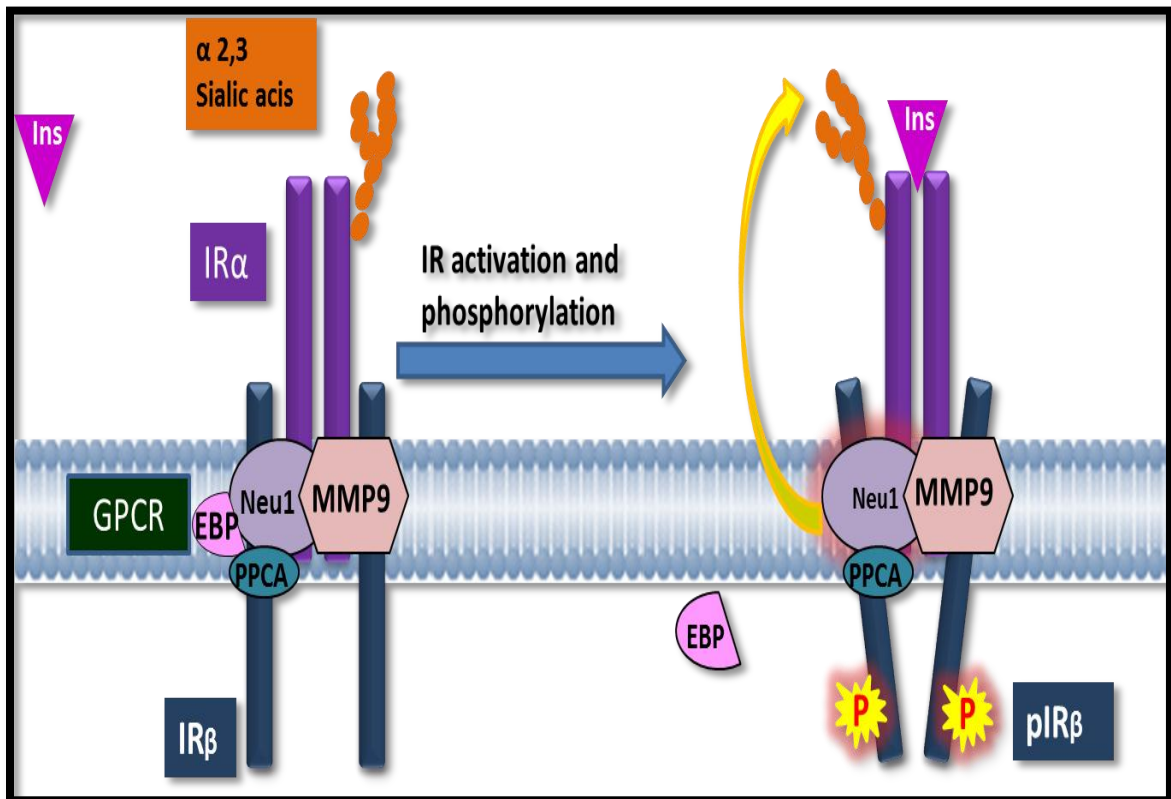


**Figure 1.11 A proposed model of insulin-induced IR Activation on the cell surface.**

Upon insulin binding to the IR, MMP9 become activated. Activated MMP9 will then activate Neu1. Activated Neu1 cleaves the terminal  $\alpha$ -2,3 sialic acids. This leads to the auto-phosphorylation of  $\beta$  subunit. Consequently, two major IR pathways will be initiated.

to regulate IR expression we have to regulate the key players in the IR activation process, such as Neu1 and MMP9.

### **1.12 Overall Hypothesis.**

Neu1 sialidase and MMP9 crosstalk in alliance with insulin receptors is an essential molecular signaling platform for insulin-induced receptor activation.

### **1.13 Main Objectives of Research Project**

Objective 1) To determine if a sialidase is activated upon insulin stimulation of the IR, and if so, which sialidase is activated (Neu1, -2, -3, or -4).

Objective 2) To examine if Neu1 sialidase and MMP9 form a complex with insulin receptors.

Objective 3) To investigate the possibility of a crosstalk between Neu1, MMP9 and insulin receptors.

## Chapter 2

### Materials and Methods

#### 2.1 Cell Lines:

Three different cell lines were used in these studies. The HTC-IR cells are rat hepatoma cell lines that overexpress the human insulin receptors (kindly provided by Dr Leda Raptis, Department of Biomedical and Molecular Sciences at Queen's University). The HTC-WT is the wild-type rat hepatoma cell line (kindly provided by Dr Leda Raptis, Department of Biomedical and Molecular Sciences at Queen's University). The MiaPaCa-2 cells are a human pancreatic carcinoma cell line (ATCC number: CRL-1420™). All cell lines were cultured in Dulbecco's modified eagle's medium (DMEM;GIBCO) containing 1.0 g/L glucose supplemented with 10% fetal calf serum (FCS, HyClone) and 5 µg/mL plasmocin. Cells were cultured at 37°C in a 5 % CO<sub>2</sub> enriched humidified atmosphere. For the HTC-IR cell line, the medium was supplemented with 400 µg/mL of G418 as selection marker for IR expression.

#### 2.2 Ligands:

Human insulin (Novolin®ge Toronto) is an injectable solution, 3.5 mg (100 IU) of the natural ligand of the insulin receptors, and stored at 4°C. The injectable insulin solution was used in our experiments at a concentration range of 10-100 nM. This concentration was determined to produce optimal ligand-induced sialidase activity based

on the results of our live cell sialidase assay. Incubation times vary between experiments and are indicated.

### **2.3 Inhibitors:**

Oseltamivir phosphate, Tamiflu (99% pure oseltamivir phosphate, Hoffmann-La Roche Ltd.), a broad-range sialidase inhibitor was used to inhibit Neu1, -2, -3, and -4. It was used at 300 µg/mL unless otherwise indicated. Galardin (GM6001; Calbiochem-EMD Chemicals Inc., Darmstadt, Germany) is a potent, cell-permeable, broad-spectrum hydroxamic acid inhibitor of matrix metalloproteinases (MMPs). Galardin inhibits MMP1, MMP2, MMP3, MMP8, and MMP9. Galardin was used at a concentration of 12.5ng/mL to 125µg/mL for the indicated incubation times. Piperazine (PIPZ; MMP-II inhibitor; Calbiochem-EMD Chemicals Inc.) is a potent, reversible, broad range inhibitor of matrix metalloproteinases. PIPZ inhibits MMP3, MMP7, and MMP9. PIPZ was used at a concentration of 12.5ng/mL to 125µg/mL for the indicated incubations times. MMP-9-inhibitor (MMP-9i; Calbiochem) is a specific inhibitor of MMP-9. MMP-9i was used at concentrations of 50µg/mL or 100µg/mL. MMP-3-inhibitor (MMP-3i; Calbiochem) is a specific and reversible inhibitor of MMP-3. MMP-3i was used at concentrations of 125ng/mL to 125µg/mL. Cyclo lignan picropodophyllin (PPP; Calbiochem) was used to discriminate between insulin receptor phosphorylation and insulin-like growth factor-1 receptor phosphorylation by inhibiting IGF-1. PPP is a non-competitive inhibitor that was used at a concentration of 50nM.

## **2.4 Primary Antibodies:**

The expression of insulin receptors was determined by using antibodies specific for IR $\beta$  (C-19; Santa Cruz Biotechnology). IR $\beta$  antibody is a rabbit anti-human antibody that is raised against a peptide mapping at the C- terminus of IR $\beta$  of human origin. Insulin receptor activation and tyrosine kinase phosphorylation was determined by using two specific antibodies. The anti-phosphorylated insulin receptor  $\beta$  (p-IR $\beta$ ; MBL International, Woburn, MA 01801) antibody is a rabbit anti-human antibody that is raised against a chemically synthesized phospho-peptide derived from the region of the human insulin receptor that contains tyrosine 972 .The anti-phosphorylated insulin receptor substrate-1 (p-IRS-1; Cell Signaling Technology, Inc.) is a rabbit anti-human antibody specific for phosphorylated insulin receptor substrate-1 (p-IRS). Four neutralizing antibodies were used to inhibit sialidase activity in live HTC-IR and MiaPaCa cell lines. The neutralizing antibodies are rabbit-anti-human Neu1 IgG antibody (Santa Cruz Technologies), mouse anti-human Neu2 IgG antibody (Santa Cruz), mouse anti-human Neu3 IgG antibody (MBL) and rabbit anti-human Neu4 IgG antibody (Proteintech Group, Inc., Chicago, IL 60612, USA). Goat anti-human MMP9 IgG antibody (Santa Cruz) was used in order to identify the role of MMP9 in insulin receptor activation and its effect on the phosphorylation of the receptor.

## **2.5 Secondary Antibodies:**

In western blot experiments, horse radish peroxidase (HRP) conjugated goat anti-rabbit IgG antibody (Sigma Aldrich) was used as a secondary antibody. In the co-

immunoprecipitation experiments, CleanBlot IP detection reagent (Pierce, Cell Signaling Technology, Inc.) was used as a secondary antibody. CleanBlot reagent is a conjugated HRP antibody that has the ability to bind to the native antibody and not the denatured antibody fragments from the immunoprecipitation processing step. In the immunocytochemistry and the co-localization experiments, donkey anti-rabbit AlexaFluor 488, donkey anti-rabbit AlexaFluor 594, donkey anti-goat Alexa 594 antibodies (Molecular Probes, Life Technologies, Carlsbad, CA, 92008. United States) and goat anti-mouse Alexa 594 (invitrogen) were used as secondary antibodies.

## **2.6 Live Cell Sialidase Assay:**

HTC-IR or MiaPaCa cells were cultured on 12 mm glass coverslips in a sterile 24 well plate. After cells reached ~75% confluence, cells were serum starved for 6 hours. Cells were divided into three groups: control, stimulated, and inhibited group. The control group was neither stimulated nor inhibited. The stimulated group was treated with insulin at indicated concentrations (10-100 nM) accompanied with PPP (IGF-1 inhibitor). The inhibited group was treated with different inhibitors (oseltamivir phosphate, anti-Neu-1, -2, -3, and -4 neutralizing antibodies, piperazine, galardin, MMP9 inhibitor or MMP3 inhibitor) at indicated concentrations with insulin stimulation. 2-(4-methylumbelliferyl)- $\alpha$ -D-N-acetylneuraminic acid (4-MUNANA; Biosynth Intl.) is a sialidase substrate that was used at a concentration of 0.318 mM in order to detect the sialidase activity. The substrate is hydrolyzed by sialidase to give free 4-methylumbelliferone, which has a fluorescence emission at 450 nm (blue color) following an excitation at 365 nm.

Fluorescent images were taken after 1 minute using epi-fluorescent microscopy (Zeiss Imager M2, x40 objective). Sialidase activity of live HTC-IR cells was indicated by the blue fluorescence surrounding the periphery of the cells. The mean fluorescence of 50 random points surrounding the cells was calculated using Image J software.

## **2.7 Immunocytochemistry for phosphorylation of IR $\beta$ in insulin-treated HTC-IR cells:**

HTC-IR cells were cultured on 12 mm glass coverslips in a sterile 24 well plate in conditional medium as previously described. After cells reached about 70% confluence, cells were serum starved for 6 hours. Cells were either control non-treated cells or secondary antibody only control, or pretreated cells. Pretreated cells were either stimulated by (100 nM) insulin accompanied with PPP for 5 minutes, or treated with oseltamivir phosphate (350 $\mu$ g/mL) for 30 minutes followed by 100nM insulin. Cells were fixed with 4 $\mu$ g/mL paraformaldehyde for 30 min and permeabilized with 0.2 % Triton-X for 5 min. Cells were blocked with 4 % bovine serum albumin (BSA) in 0.1% tween-TBS for 40 minutes on ice. The fixed cells were immunostained with 4  $\mu$ g/mL rabbit anti-human pIR $\beta$  antibody for 1 hour at 37C $^{\circ}$ , followed with Alexa 488 conjugated donkey anti-rabbit IgG antibody for 1 hour at 37C $^{\circ}$ . In order to detect the non-specific fluorescence background, control cells were incubated with secondary antibody only. Stained cells were viewed by epi-fluorescence microscopy (40X objective). The density of the cell staining (green fluorescence) was measured by Corel Photo Paint 8.0 software.

## **2.8 Preparation of Cell Lysates**

HTC-IR cells were cultured in 75 cm<sup>2</sup> flasks at 37 °C until confluent. Cells were treated with insulin, pretreated with different inhibitors followed with insulin, or left untreated as control cells. Cells were removed and re-suspended in 100µl of RIPA lysis buffer cocktail which contained 1x RIPA buffer, 1mM PMSF, 0.2 mg/mL leupatin, 1% β mercaptoethanol and 1 µl protease inhibitor cocktail on ice for 30 minutes. Cell suspension were then transferred into other eppendorf tubes and stored at -80 °C.

## **2.9 Bradford Assay for Protein quantification**

Protein concentration of cell lysates was determined using the Bradford Assay for protein quantification. A standard curve was obtained by using different concentrations of bovine serum albumin (BSA) ranged from 0 to 80 µg/mL diluted in double-distilled water. In separate set of tubes, cell lysates were diluted into 1:10. 2 µL of each (1:10) diluted samples was added to 798µL double-distilled water. 200 µL of Bradford reagent (Sigma Adrich) was added into each sample. The (bound) form of the Bradford reagent dye has an absorption spectrum at 595 nm. The increase of absorbance at 595 nm is directly proportional to the amount of bound dye, and thus to the amount or concentration of protein present in the sample. Using Graph Pad Prism 5 software, protein concentration of each cell lysates was obtained by comparing the absorbance values to the standard BSA curve.

## **2.10 Western blot of insulin receptor $\beta$ (IR $\beta$ ) and human phosphorylated insulin receptor substrate-1 (pIRS-1):**

Cell lysates were prepared from the following cell lines: HTC-IR, HTC-WT and MiaPaCa-2. 60  $\mu$ g proteins from the cell lysates were resolved by 8% Bis-Tris SDS-PAGE gel. Semi dry transfer technique was performed to transfer the resolved proteins on PVDF transfer membrane blot at 100 mA. The membrane blot was blocked for 2 hrs at room temperature or overnight at 4°C using 5% BSA or fat-free skim milk in 0.1% Tween- Tris buffered saline (TBS) to block non-specific background binding. The blot was probed with rabbit anti-insulin receptor  $\beta$  (IR $\beta$ ) antibody or rabbit anti-human phosphorylated insulin receptor substrate-1 (pIRS-1) antibody (Cell Signaling) as primary antibody overnight at 4°C. After incubating, the blot was washed three times followed with horse radish peroxidase (HRP) conjugated secondary goat anti-rabbit IgG antibody for 60 minutes at room temperature. Western Lightning Chemiluminescence Reagent Plus was added to the blot for 5 minutes, and chemiluminescence was measured with x-ray film. The blot was washed, stripped and re-probed with anti- $\beta$ -actin antibody (Cell Signaling) as an internal control protein for loading of the cell lysate. Quantitative analysis was done by assessing the density of a band corrected for background in each *lane* using Corel Photo Paint 8.0 software. Each *bar* in the graphs represents the mean ratio of IR $\beta$  to  $\beta$ -actin of band density  $\pm$ S.E. (*error bars*) for 5–10 replicate measurements.

### **2.11 Co-immunoprecipitation:**

HTC-IR cells were left cultured in medium or in medium containing 100 nM insulin for the indicated time intervals. Cells ( $1 \times 10^7$  cells) were pelleted and lysed in lysis buffer. For immunoprecipitation, Neu-1, -2, -4, MMP9 and insulin receptor in cell lysates from HTC-IR cells using 100 $\mu$ g of cell lysates were immunoprecipitated with either 1 $\mu$ g of rabbit-anti-human Neu1 antibody, mouse anti-human Neu2 antibody, rabbit anti-human Neu4 antibody or goat anti-human MMP9 antibody overnight at 4°C. Following immunoprecipitation, complexes were isolated using protein A or G magnetic beads for 90 min, washed three times in lysis buffer and resolved by 8% Bis-Tris gel electrophoresis (SDS-PAGE). The gel's running time was 90 minutes at 150 V. The proteins were transferred onto PVDF transfer membrane blot via semi-dry blotting technique for 75 minutes at 100 mA. The blot was blocked with 5% BSA in 0.1% Tween-TBS as blocking buffer for 2 hr at room temperature. The blot was incubated with rabbit anti-human IR $\beta$  antibody overnight at 4°C followed with Clean-Blot IP Detection Reagent for immunoprecipitation/Western blots (Pierce, Thermo Fisher Scientific) for 60 minutes at room temperature and Western Lightning Chemiluminescence Reagent Plus for 5 minutes. The chemiluminescence reaction was analyzed with x-ray film.

### **2.12 Neu1 and MMP9 colocalization with insulin receptor $\beta$ (IR $\beta$ ):**

HTC-IR cells were cultured on 12 mm circular glass coverslips in a sterile 24 well plate in conditional medium as described. After cells reached about 70% confluence, cells were serum starved for 6 hours. Cells were fixed with 4  $\mu$ g/mL paraformaldehyde,

permeabilized with Triton-X, and blocked with 4% BSA in 0.1% Tween-TBS for 40 minutes on ice. Cells were incubated with 4  $\mu\text{g}/\text{mL}$  of one of the following combinations of antibodies ( $\text{IR}_\beta$  antibody and Neu1 antibody;  $\text{IR}_\beta$  antibody and Neu2 antibody;  $\text{IR}_\beta$  antibody and Neu3 antibody;  $\text{IR}_\beta$  antibody and Neu4 antibody; or  $\text{IR}_\beta$  antibody and MMP9 antibody) for 60 minutes at  $37^\circ\text{C}$ . Co-localization procedure is dependent on the primary antibody combination with respect to animal species. Cells were washed and incubated with 4  $\mu\text{g}/\text{mL}$  of AlexaFluor 594 and AlexaFluor 488 conjugated secondary antibodies for 60 minutes at  $37^\circ\text{C}$ . To account for background non-specific fluorescence, control cells with only Alexa Fluor 488 or Alexa Fluor 594 conjugated secondary antibodies were used. Stained cells were mounted on microscope slide using 3  $\mu\text{L}$  of mounting medium (DAKO). Stained cells were viewed using Zeiss M2 epi-fluorescent microscopy (40 $\times$  objective). Images were taken under two different channels; red channel and green channel. Overlay and co-localization visualization was done by using Adobe Photoshop software and Image J software. To calculate the amount of colocalization in the selected images, the Pearson correlation coefficient was measured and expressed as a percentage using ImageJ version 1.44x software.

### **2.13 Statistical Analysis:**

Statistical analysis was performed by using GraphPad Prism 5.0. Comparisons between two groups were made by one-way analysis of variance at 99.9% confidence using Dunnett's multiple comparison test for comparisons among more than two groups.

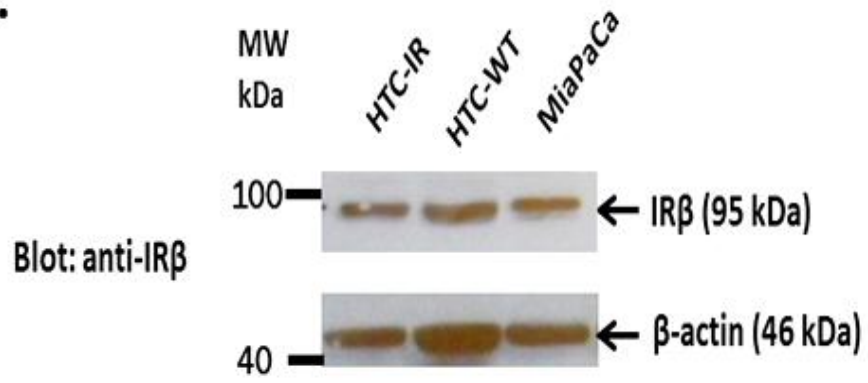
## Chapter 3

### Results

#### 3.1 Expression of insulin receptors in different cell lines

To study the role of glycosylation in the activation of insulin receptors, we initially investigated the expression level of insulin receptors in three different cell lines using western blot analysis. Cell lysates from rat hepatoma cell line over expressing human insulin receptors (HTC-IR), wild-type HTC (HTC-WT) cells and the human pancreatic carcinoma (MiaPaCa-2) cells were prepared. They were separated by SDS-PAGE, and the blot was probed with an antibody against insulin receptor  $\beta$  (anti-IR $_{\beta}$ ). After developing the blot, the same blot was washed, stripped and re-probed for  $\beta$ -actin as an internal control protein for loading of the cell lysate. The data in Figure 3.1A clearly show that all of the cell lines express IR $_{\beta}$  receptors. A quantitative analysis was done by assessing the density of a band corrected for background in each lane using Corel Photo Paint 8.0 software. Each bar in the graph Figure 3.1B represents the mean ratio of IR $_{\beta}$  to  $\beta$ -actin of band density  $\pm$  S.E. (*error bars*) for 5–10 replicate measurements. The highest expression of insulin receptors was found with HTC-IR cells Figure 3.1B.

**A.**



**B.**

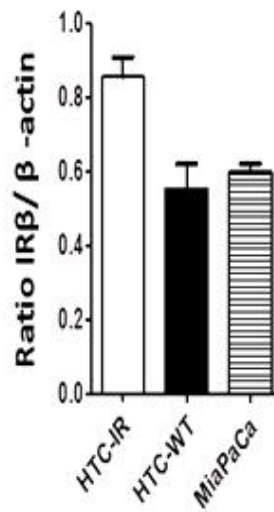


**Figure 3.1 HTC-IR, HTC-WT, and MiaPaCa-2 cell lines express insulin receptors.**

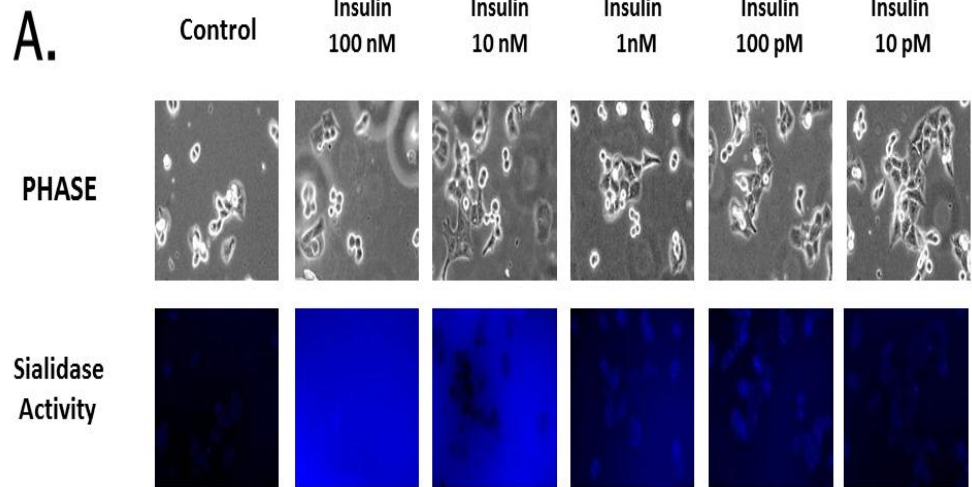
- A. IR $\beta$  in the cell lysates from HTC-IR, HTC-WT, and MiaPaCa-2 cell lines was resolved by 8% gel electrophoresis (SDS-PAGE). The blot was incubated with rabbit anti-human IR $\beta$  antibody overnight at 4°C, followed with HRP-conjugated secondary goat anti-rabbit IgG antibody and Western Lightning Chemiluminescence Reagent Plus. The chemiluminescence reaction was analyzed with x-ray film. The blot was also washed, stripped and re-probed for  $\beta$ -actin as an internal control protein for loading of the cell lysate.
- B. Quantitative analysis was done by assessing the density of a band corrected for background in each lane using Corel Photo Paint 8.0 software. Each bar in the graph represents the mean ratio of IR $\beta$  to  $\beta$ -actin of band density  $\pm$  *S.E.* (*error bars*) for 5–10 replicate measurements. The data are a representation of one out of three independent experiments showing similar results.

### **3.2 Sialidase activity is associated with insulin stimulation of live HTC-IR cells**

A report from our laboratory demonstrated that nerve growth factor (NGF) binding to TrkA receptors induced a cellular membrane associated sialidase(s) activity that specifically targeted and hydrolyzed sialyl  $\alpha$ -2-3-linked  $\beta$ -galactosyl residues of TrkA receptors (9). To determine whether a mammalian cellular sialidase is associated with insulin treated live HTC-IR cells, we used a recently developed assay to detect sialidase activity on the surface of viable cells (9). This sialidase activity is revealed in the periphery surrounding the cells using a fluorogenic sialidase specific substrate, 4-MUNANA [2'-(4-methylumbelliferyl)- $\alpha$ -D-N-acetylneuraminic acid], which fluoresces at 450 nm and caused by the emission of 4-methylumbelliferone. Cells were stimulated with different doses of insulin ranging from 10pM to 100nM. Cells that were stimulated with 10pM, 100 pM, 1nM, 10nM and 100nM of insulin showed significant dose-dependent increase in sialidase activity compared to the unstimulated cells. (see Figure 3.2).

### **3.3 Oseltamivir phosphate inhibition of sialidase activity associated with insulin stimulated live HTC-IR**

The results from the previous section (section 3.2) indicated that at least one of the mammalian sialidases was activated upon insulin stimulation of live HTC-IR cells.



★  $p < 0.0001$  (n=50)

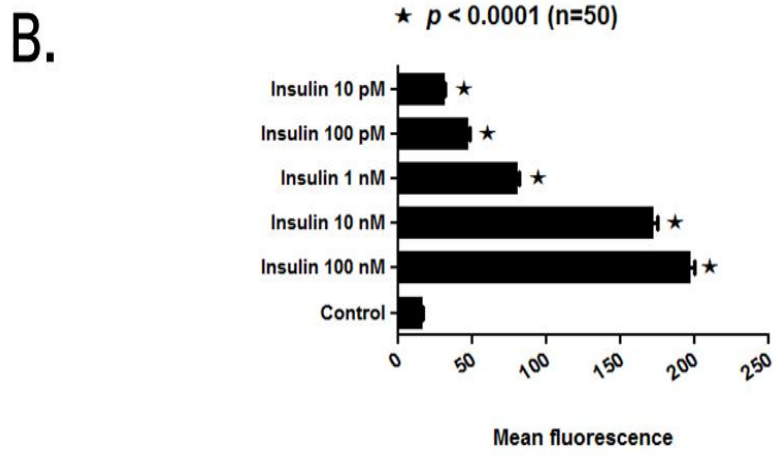


**Figure 3.2 Insulin stimulation of insulin receptors induced sialidase activity in a dose dependent manner in live HTC-IR cells.**

A. HTC-IR cells were cultured on 12 mm glass coverslips in a sterile 24 well plate in conditioned medium. After cells reached ~75% confluence, cells were divided into two groups: control cells (cells with no stimulation or inhibition) or stimulated cells with human insulin. Stimulated cells were treated with insulin at a concentration ranging from 10 pM to 100nM. 0.318 mM of 4-MUNANA substrate was added to the cells in order to detect the sialidase activity. Fluorescent images were taken at 1-min intervals using epifluorescent microscopy (x40 objective).

B. The mean fluorescence surrounding the cells after adding substrate for each of the images was measured using ImageJ software. mean±Error bars, *S.E.*. The data are a representation of one out of three independent experiments showing similar results. Significant differences at 99.9% confidence using the Dunnett multiple comparison test was used to compare inhibition with the insulin control in each group for n=50 replicates

Accordingly, by using a broad-range sialidase inhibitor such as oseltamivir phosphate (Tamiflu; inhibitor of Neu1, -2, -3, -4) we should be able to inhibit the sialidase activity associated with insulin treated live cells. Oseltamivir phosphate was able to inhibit the sialidase activity associated with 10 nM of insulin treated live cells in a dose-dependent manner, (see Figure 3.3). The effective inhibitory dose range of oseltamivir phosphate ranged from 250ng/mL to 250µg/mL..

### **3.4 Neu1 sialidase activity is associated with insulin-treated HTC-IR cells**

From our previous findings in section 3.2 and 3.3, the data indicated that there is a sialidase activity associated with insulin stimulated live HTC-IR cells. To identify the mammalian cellular sialidase associated with insulin treated HTC-IR cells, we used the live cell sialidase assay to detect sialidase activity on the cell surface. Specific antibodies against the four mammalian sialidases, known as lysosomal Neu1, cytosolic Neu2, the plasma membrane bound Neu3 and the fourth sialidase, Neu4, localized to either the mitochondrial compartment or the lysosomal lumen were used. The cells were pretreated with the neutralizing antibodies against Neu-1, -2, -3, and -4 at 100µg/mL for 30 minutes followed with 10nM of insulin. The cells that were pretreated with anti-Neu1 antibodies showed a significant decrease in the sialidase activity Figure3.4. The anti-Neu1 antibody is specific for the epitope corresponding to amino acids 116–415 mapping at the C-terminus of Neu1 of human origin. It also detects Neu1 of mouse, rat and human origin. In contrast, antibodies against the other three human sialidases had no blocking effect on insulin induced sialidase activity in HTC-IR cells, (see Figure 3.4).

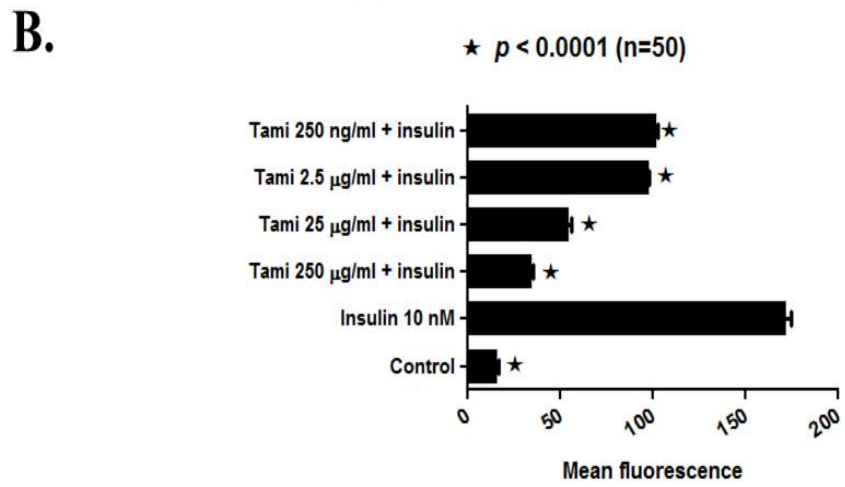
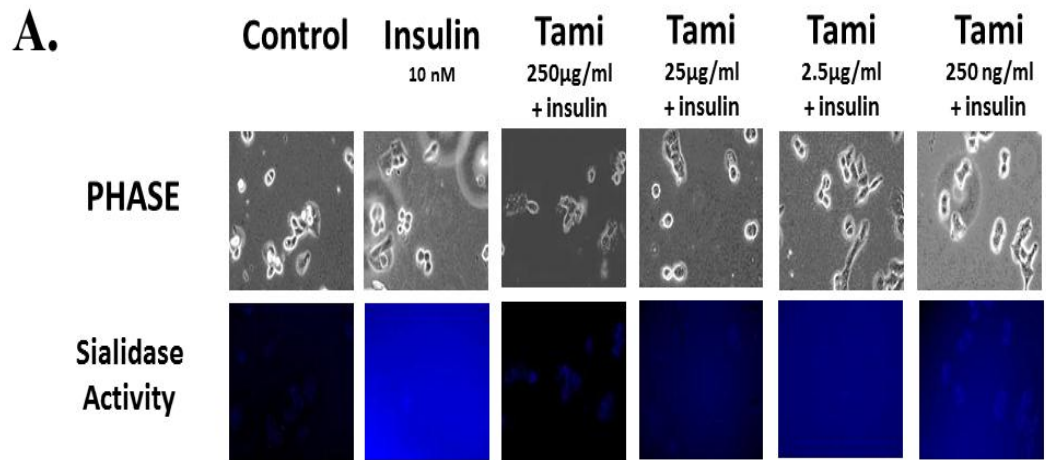


**Figure 3.3 Oseltamivir phosphate (Tamiflu) inhibition of insulin-induced sialidase activity in live HTC-IR cells**

A. HTC-IR cells were cultured on 12 mm glass coverslips in a sterile 24 well plate in conditioned medium as described. Cells were divided into three groups: control cells (cells with no stimulation or inhibition), stimulated cells with 10 nM insulin accompanied with 50 nM PPP , and inhibited group of cells with oseltamivir phosphate at concentration ranging from 250 ng/ml to 250 µg/ml accompanied with 10nM of insulin. 0.318 mM of 4-MUNANA was added to the cells in order to detect sialidase activity. Fluorescent images were taken at 1-min intervals using epifluorescent microscopy (x40 objective).

B. The mean fluorescence surrounding the cells after adding substrate for each of the images was measured using ImageJ software. mean±Error bars, *S.E.*. The data are a representation of one out of three independent experiments showing similar results. Significant differences at 99.9% confidence using the Dunnett multiple comparison test was used to compare inhibition with the insulin control in each group for n=50 replicates.

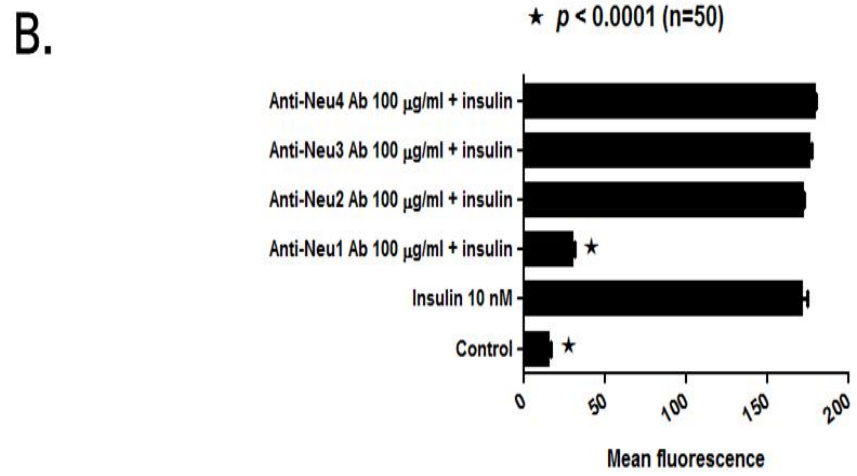
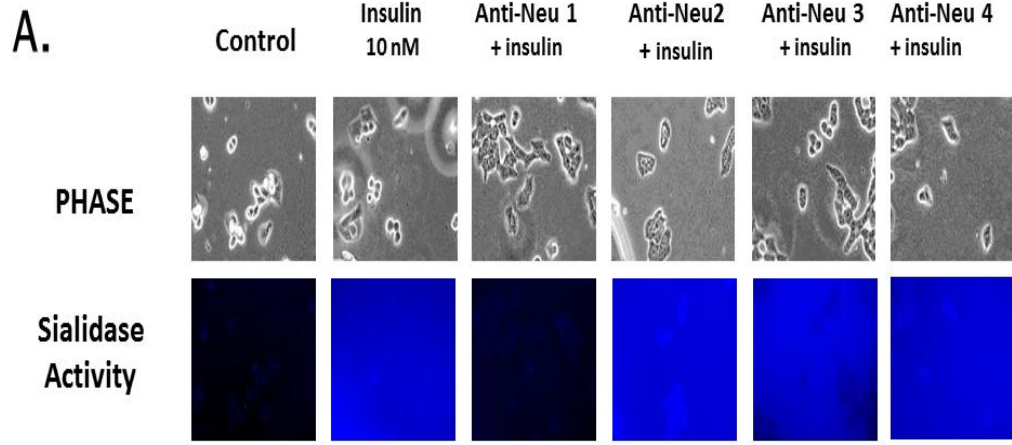


**Figure 3.4 Insulin stimulation of insulin receptors induces only Neu1 sialidase activity in live HTC-IR cells.**

A. HTC-IR cells were cultured on 12 mm glass coverslips in a sterile 24 well plate in conditioned medium as described. Cells were divided into three groups: control cells (cells with no stimulation or inhibition), stimulated cells with 10 nM insulin accompanied with 50 nM PPP , and inhibited group of cells with 100 µg/ml anti Neu1, -2,-3 or -4 neutralizing antibody were then stimulated with 10 nM of insulin. 0.318 mM of 4-MUNANA was added to the cells in order to detect sialidase activity. Fluorescent images were taken at 1-min intervals using epifluorescent microscopy (x40 objective).

B. The mean fluorescence surrounding the cells after adding substrate for each of the images was measured using ImageJ software. mean±Error bars, *S.E.*. The data are a representation of one out of three independent experiments showing similar results. Significant differences at 99.9% confidence using the Dunnett multiple comparison test was used to compare inhibition with the insulin control in each group for n=50 replicates.

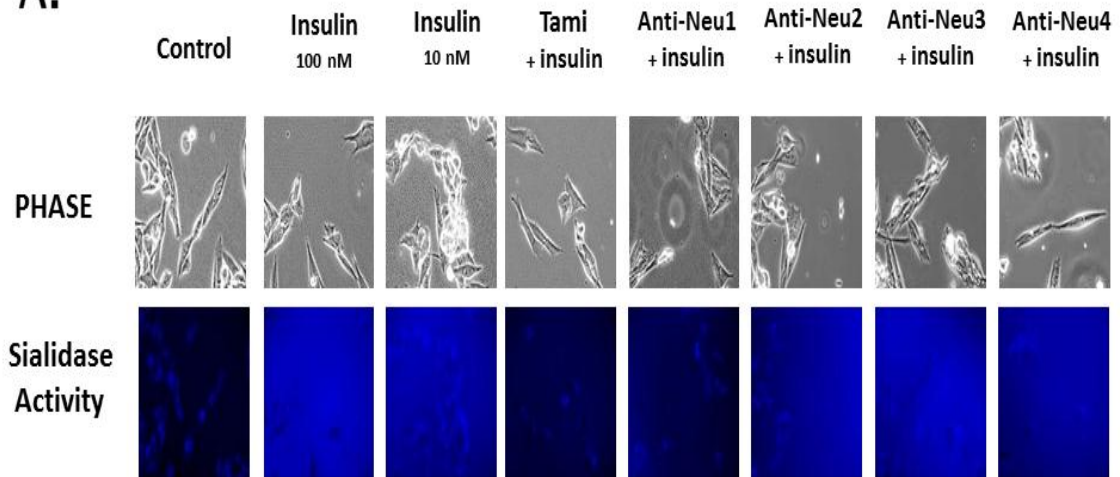
### **3.5 Neu1 sialidase activity is associated with insulin-treated live human pancreatic carcinoma MiaPaCa-2 cell line**

In the previous experiments, we used the HTC-IR cell line. We asked whether there is a similar Neu1 sialidase activity associated with the insulin-treated live pancreatic carcinoma MiaPaCa-2 cell line. The MiaPaCa-2 cells have been shown to express insulin receptors (section 3.1). Cells were left untreated as controls, and either stimulated with 10 nM insulin together with 50nM cyclolignan picropodophyllin (PPP), or inhibited using 100 µg/ml anti Neu1, -2,-3 or -4 neutralizing antibody prior to the stimulation with 10 nM of insulin. PPP was used to discriminate between insulin receptor and insulin like growth factor-1 (IGF-1) phosphorylations by inhibiting IGF-1. PPP is a non-competitive inhibitor that was used to inhibit the IGF-1 at a concentration of 50nM. Cells that were treated with 10 and 100nM insulin induced sialidase activity Figure 3.5. The addition of anti-Neu1 neutralizing antibody was able to inhibit sialidase activity, whereas the additions of anti-Neu-2,-3, and -4 antibodies were unable to significantly inhibit this sialidase activity associated with insulin-treated live cells. The findings indicate that MiaPaCa-2 cell line gave similar results as HTC-IR cells (see Figure3.5).

### **3.6 Neu1 sialidase activity is associated with insulin-induced phosphorylation of insulin receptors (IR) in HTC-IR cells**

From the previous sections (3.2, 3.3, 3.4 and 3.5), we observed that Neu1 sialidase activity is associated with insulin stimulation of HTC-IR cells. If insulin-

**A.**



**B.**

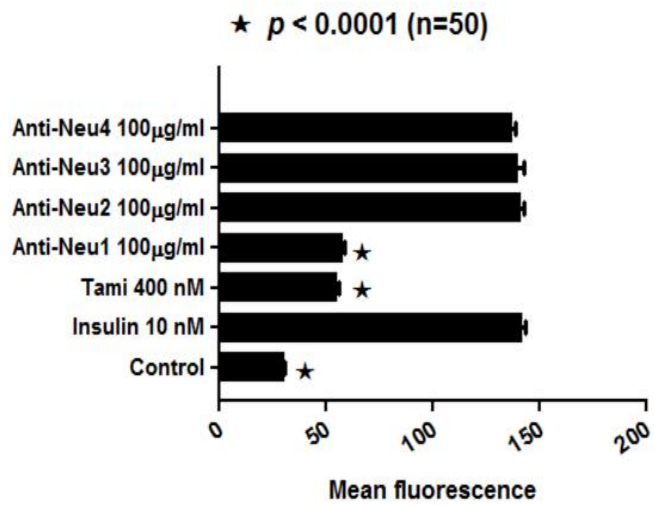


**Figure 3.5 Induction of sialidase activity by insulin stimulation in live MiaPaCa cells**

A. MiaPaCa cells were cultured on 12 mm glass coverslips in a sterile 24 well plate in conditioned medium. Cells were divided into three groups: control cells (cells with no stimulation or inhibition), stimulated cells with 10nM or 100 nM insulin accompanied with 50 nM PPP, and inhibited group of cells with either 100 µg/ml anti Neu1, -2,-3 or -4 neutralizing antibody accompanied with 10 nM of insulin or 400 nM oseltamivir phosphate accompanied with 10 nM insulin. 0.318 mM of 4-MUNANA was added to the cells in order to detect sialidase activity. Fluorescent images were taken at 1-min intervals using epifluorescent microscopy (x40 objective).

B. The mean fluorescence surrounding the cells after adding substrate for each of the images was measured using ImageJ software. mean±Error bars, *S.E.*. The data are a representation of one out of three independent experiments showing similar results. Significant differences at 99.9% confidence using the Dunnett multiple comparison test was used to compare inhibition with the insulin control in each group for n=50 replicates.

induced IR activation is dependent on Neu1 sialidase activity, then neuraminidase inhibitor like oseltamivir phosphate should have an inhibitory effect on insulin-induced phosphorylation of IR (pIR $\beta$ ) in HTC-IR cells. Immunocytochemistry analyses demonstrate that 100 nM of insulin was able to induce the phosphorylation of IR $\beta$  in HTC-IR cells. On the other hand, using 350  $\mu$ g/mL oseltamivir phosphate pretreated cells for 35 minutes, followed by 100nM insulin stimulation for 5 minutes accompanied with 50 nM PPP was able to significantly inhibit insulin-induced pIR $\beta$ , (see Figure 3.6). Unstimulated cells were used as negative control in this experiment. In addition, the non-specific fluorescence background was controlled by using secondary antibody only. Stained cells were viewed by epi-fluorescence microscopy (40X objective). The findings indicated that Neu1 is essential for insulin-induced receptor activation.

### **3.7 Western blot analysis of Neu1 inhibition on insulin-induced insulin receptor phosphorylation in HTC-IR cells**

Western blot analysis was performed to confirm and identify the alterations in the protein expression of phosphorylated insulin receptor substrate (58) under various conditions. HTC-IR cell lysates were prepared from unstimulated control cells, 100nM insulin stimulated cells accompanied with 50nM PPP, or cells pretreated with 200 $\mu$ g/mL oseltamivir phosphate (Tamiflu) for 35 minutes, or 33  $\mu$ g/mL anti-Neu1 antibody for 35 minutes followed by 100nM insulin stimulation for 5 minutes. Proteins in the cell lysates were separated by SDS-PAGE, and the blot was probed with an antibody against

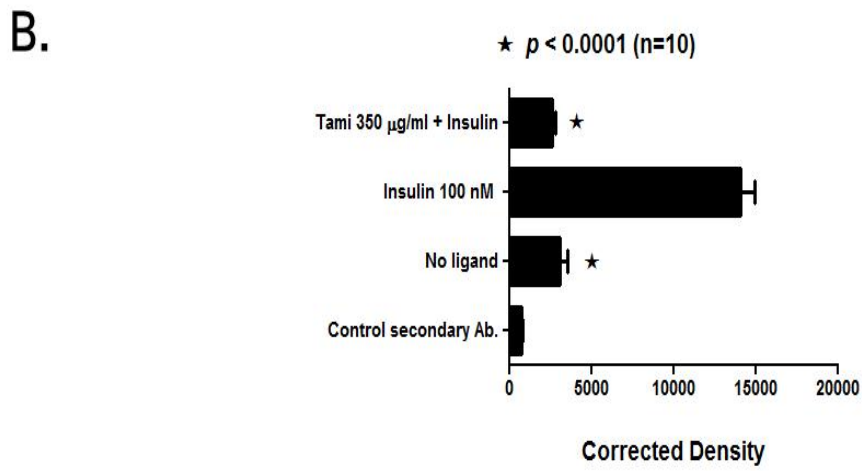
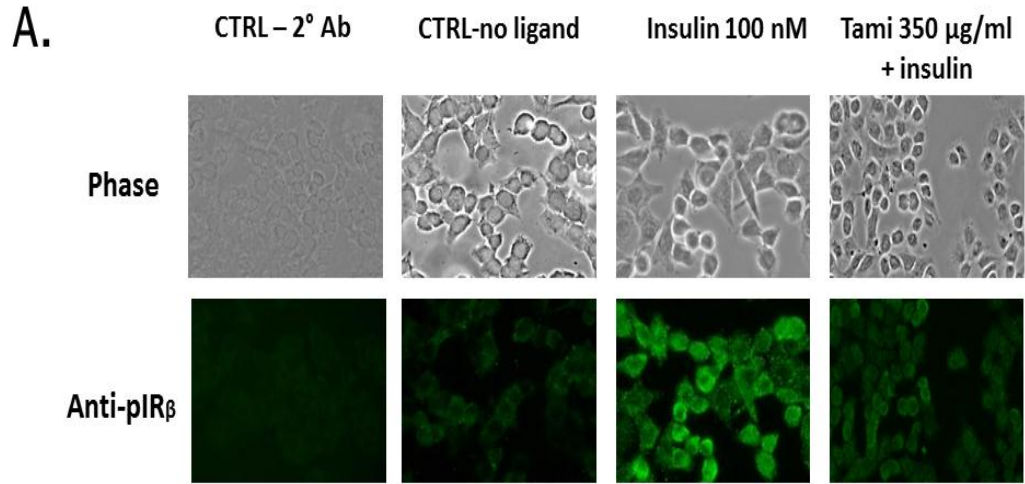


**Figure 3.6 Inhibition of insulin-induced insulin receptor phosphorylation by oseltamivir phosphate (Tamiflu).**

- A. HTC-IR cells were cultured on 12 mm glass coverslips in a sterile 24 well plate in conditioned medium. Cells were stimulated with 100 nM insulin accompanied with 50 nM PPP for 5 minutes, inhibited with 350  $\mu\text{g/ml}$  oseltamivir phosphate for 35 minutes followed by stimulation with 100 nM insulin for 5 minutes, or no ligand cells with no stimulation or inhibition. Cells were fixed, permabilized, blocked, and immunostained with 4  $\mu\text{g/ml}$  IR $_{\beta}$  rabbit anti-human antibody for 1 hour at 37C° followed with Alexa 488 donkey anti-rabbit IgG secondary antibody for 1 hour at 37C°. Control cells were incubated with secondary antibody only. Stained cells were visualized by epifluorescence microscopy using a 40x objective.
- B. Quantitative analysis was done by assessing the density of cell staining corrected for background in each panel using Corel Photo Paint 8.0 software. Each bar in the figure represents the mean corrected density of culture cell staining  $\pm$  SEM for equal cell density ( $5 \times 10^5$  cells) within the respective images. *P* values represent significant differences at 99.9% confidence using the Dunnett multiple comparison test compared to insulin treated cells.

phosphorylated insulin receptor substrate (anti-pIRS). After the developing the blot, the same blot was washed, stripped and re-probed for  $\beta$ -actin as an internal control protein for loading of the cell lysate. Insulin treated samples showed an increase in the phosphorylation of IRS1 in comparison to the control, while cells that were pretreated with oseltamivir phosphate or anti-Neu1 neutralizing antibody showed a decrease in the expression of pIRS (see Figure 3.7). The findings indicate that Neu1 sialidase activity is essential in the insulin-induced IR receptor activation process.

### **3.8 Neu1 sialidase colocalizes with insulin receptor $\beta$ on the cell surface in naïve HTC-IR cells.**

If Neu1 is localized to the cell surface of HTC-IR cells, we asked whether or not it is associated with IR $_{\beta}$  receptors. Confocal microscopy validated the predicted association of Neu1 with IR $_{\beta}$  receptors in naïve and insulin-treated HTC-IR cells (Fig. 3.8). Cells were fixed, permabilized, blocked and incubated with 4  $\mu$ g/mL of one of the following combinations of antibodies (IR $_{\beta}$  antibody and Neu1 antibody; IR $_{\beta}$  antibody and Neu2 antibody; IR $_{\beta}$  antibody and Neu3 antibody; or IR $_{\beta}$  antibody and Neu4 antibody). Cells were washed and incubated with 4  $\mu$ g/ml donkey anti-rabbit AlexaFluor 488, donkey anti-rabbit AlexaFluor 594, donkey anti-goat Alexa 594 antibodies and goat anti-mouse Alexa 594 secondary antibodies. To account for background non-specific fluorescence, control cells with only secondary antibody (Alexa Fluor 488 or Alexa Fluor 594) were used. Cells that were immunostained with (IR $_{\beta}$  antibody and Neu2 antibody; IR $_{\beta}$  antibody and Neu3 antibody; or IR $_{\beta}$  antibody and Neu4 antibody) were used as

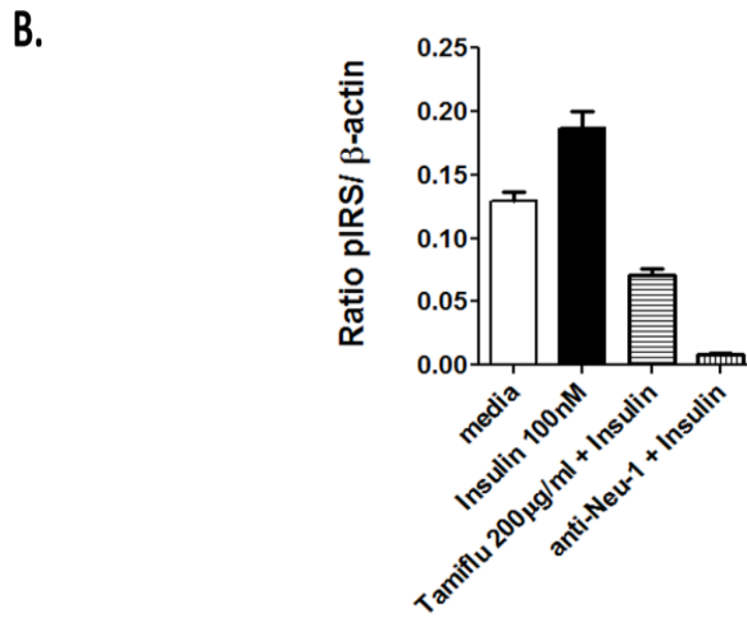
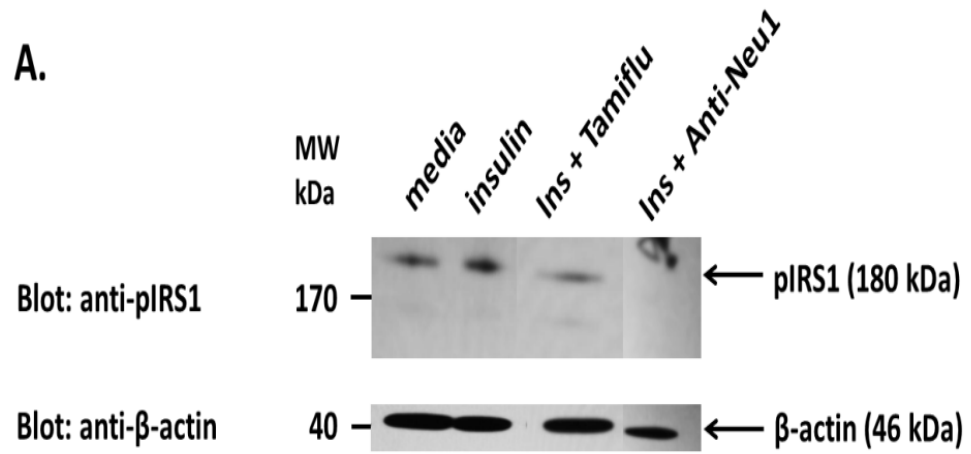


**Figure 3.7 Oseltamivir phosphate (Tamiflu) and Neu1 specific inhibitor were able to block insulin receptor phosphorylation in HTC-IR cell line**

- A. HTC-IR cell lysates were prepared from control cells (unstimulated cells), 100nM insulin stimulated cells in conjunction with 50 nM PPP, 200 $\mu$ g oseltamivir phosphate (tamiflu) treated cells for 35 minutes followed by 100 nM insulin stimulation for 5 minutes, or 33  $\mu$ g/ml anti-Neu1 antibody treated cells for 35 minutes followed by 100 nM insulin stimulation for 5 minutes. Unstimulated cells were performed as control in this experiment. For each sample, 60  $\mu$ g proteins were loaded into 8% Bis-Tris gel. The blot was incubated with pIRS1 antibody followed by secondary goat anti-rabbit IgG antibody. Later, Western Lightning Chemiluminescence Reagent Plus was added. The chemiluminescence reaction was analyzed with x-ray film. The blot was re-probed with  $\beta$ -actin as loading control.
- B. Quantitative analysis was done by assessing the density of a band corrected for background in each lane using Corel Photo Paint 8.0 software. Each bar in the graph represents the mean ratio of pIRS1 to  $\beta$ -actin of band density  $\pm$  S.E. (error bars) for 5–10 replicate measurements. The data are a representation of one out of three independent experiments showing similar results.

negative controls. Images were taken under two different channels; a red channel and a green channel. RGB overlay and colocalization visualization was done by using Photoshop software and Image J software. Colocalization was indicated by the presence of two fluorochromes on the same physical structure in the cell, which leads to the appearance of a yellow color in the overlay pictures. The data indicated that there was a colocalization between  $IR_{\beta}$  and Neu1 (see Figure 3.8). On the other hand, Neu2 and Neu3 showed no colocalization with  $IR_{\beta}$ . However, there was a slight colocalization between  $IR_{\beta}$  and Neu4. This slight colocalization between those two components ( $IR_{\beta}$  and Neu4) may not mean that they are interacting with each other; as it is possible that they might be in the same cellular structure but not interacting with each other. To further examine the interaction between them, we performed a co- immunoprecipitation assay as described in the next section.

### **3.9 Co-immunoprecipitation of insulin receptors with mammalian sialidases (Neu-1,-2,-and 4) in naïve and insulin-stimulated HTC-IR cells.**

The previous findings from the colocalization experiments suggested that Neu1 colocalizes with  $IR_{\beta}$ , and also suggested a possible colocalization between  $IR_{\beta}$  and Neu4. In order to examine the interaction between those molecules, several co-immunoprecipitation experiments were performed using HTC-IR cell lysates under different conditions. The Co-immunoprecipitation assay was utilized to determine whether or not Neu1 and the insulin receptors exist in a complex. HTC-IR cells were left

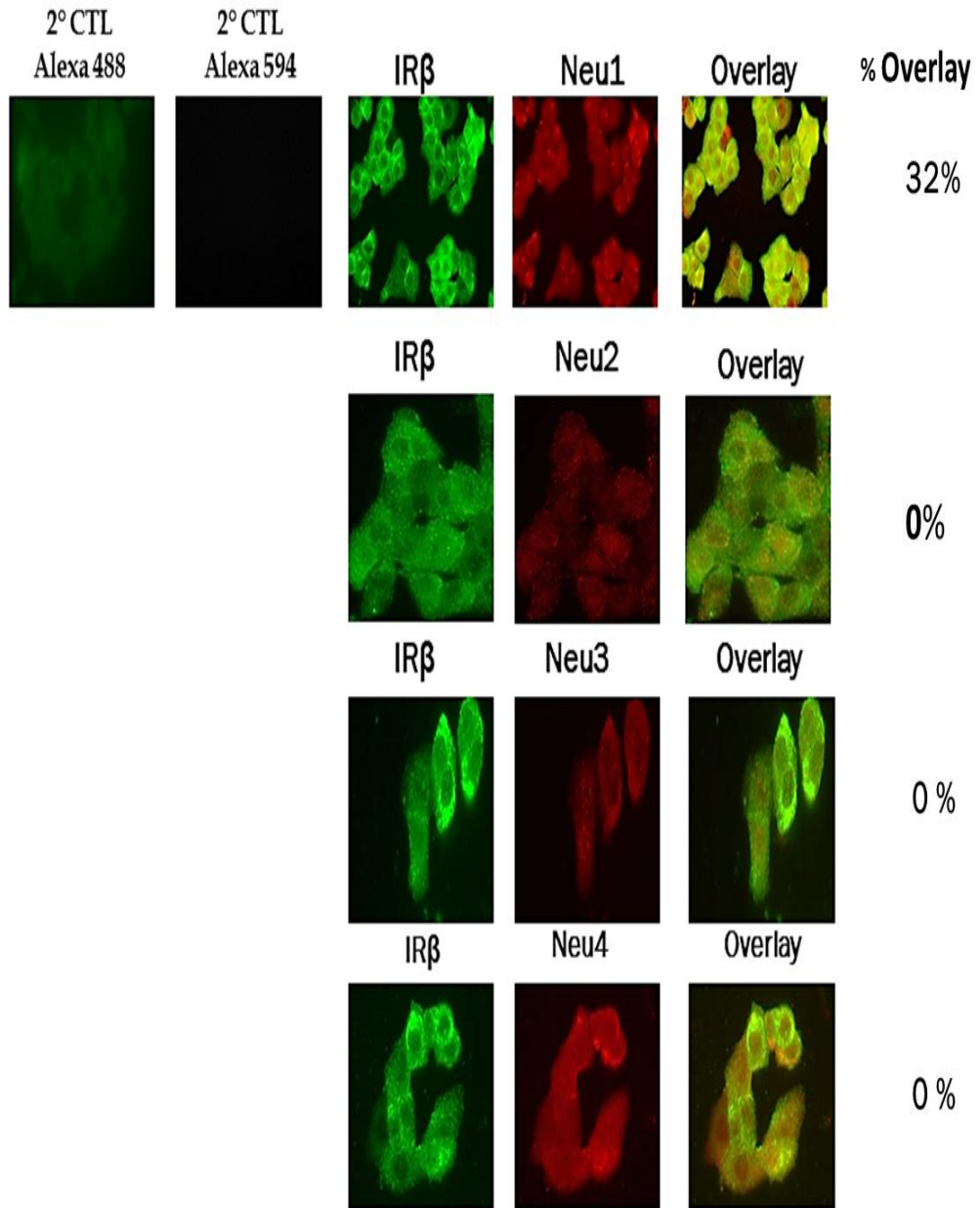
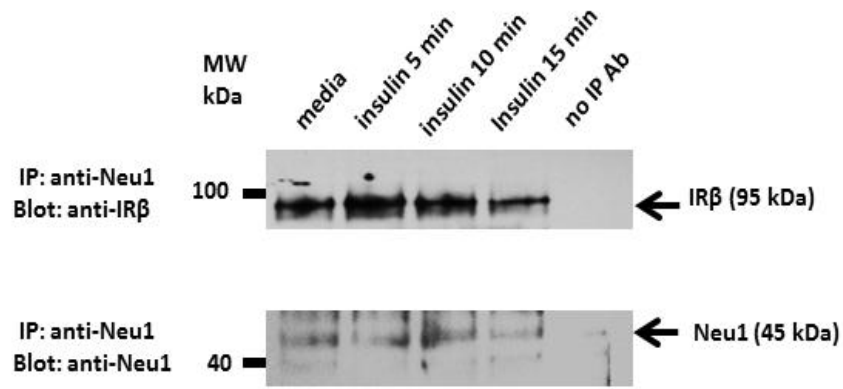


### **Figure 3.8 The colocalization between IR $\beta$ and Neu1 in naïve HTC-IR cells**

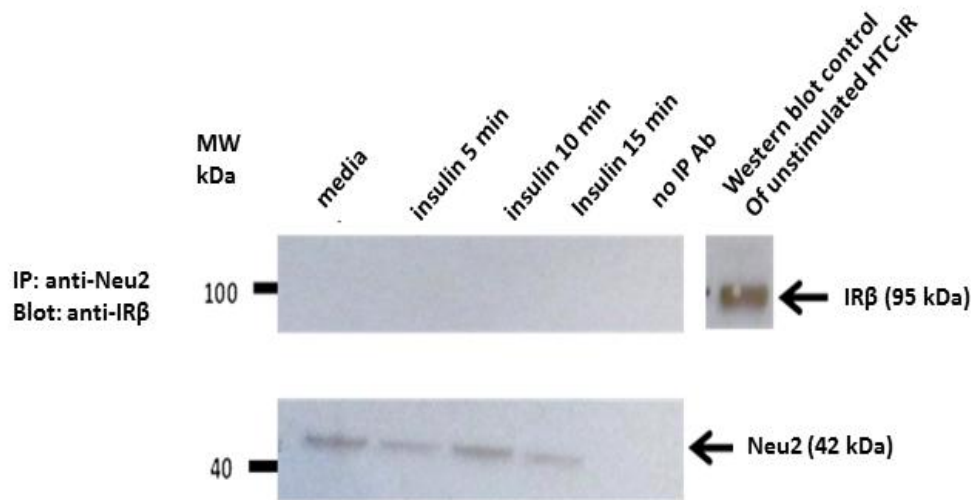
HTC-IR cells were cultured on 12 mm glass coverslips in a sterile 24 well plate in conditioned medium. Cells were fixed, permeabilized and blocked with 4 % bovine serum albumin (BSA) in 0.1% tween-TBS. Cells were incubated with 4  $\mu\text{g}/\text{mL}$  of one of the following combinations of antibodies (IR $\beta$  antibody and Neu1 antibody; IR $\beta$  antibody and Neu2 antibody; IR $\beta$  antibody and Neu3 antibody; or IR $\beta$  antibody and Neu4 antibody) for 60 minutes at 37°C. Cells were washed and incubated with 4  $\mu\text{g}/\text{ml}$  donkey anti-rabbit AlexaFluor 488, donkey anti-rabbit AlexaFluor 594, donkey anti-goat Alexa 594 antibodies and goat anti-mouse Alexa 594 secondary antibodies for 60 minutes at 37°C. To account for background non-specific fluorescence, control cells with only secondary antibody (Alexa Fluor 488 or Alexa Fluor 594) were used. Stained cells were visualized using epi-fluorescence microscopy with 40x objective. Images were taken under two different channels; a red channel and a green channel. RGB overlay and colocalization visualization was done by using Photoshop software and Image J software. The data are a representation of one out of three independent experiments showing similar results.

unstimulated or stimulated with 100nM insulin for 5, 10 or 15 minutes. Cell lysates were prepared as previously described. Proteins in the cell lysates were immunoprecipitated with 1 $\mu$ g of rabbit anti-human Neu1 antibody, mouse anti-human Neu2 antibody, or rabbit anti-human Neu4 antibody. Samples were resolved on SDS-PAGE gels, and the proteins were transferred onto PVDF membrane blots. The blots were incubated with rabbit anti-human IR $\beta$  antibody overnight at 4°C, followed with Clean-Blot IP Detection Reagent for immunoprecipitation/Western blots and Western Lightning Chemiluminescence Reagent Plus. The chemiluminescence reaction was analyzed with x-ray film. HTC-IR cell lysates that were not incubated with the anti-Neu-1,-2 or -4 antibodies prior to the immunoprecipitation step were used as negative controls in the co-IP experiments. For Neu1 IP blot; the blot was washed, stripped and re-probed with anti-Neu1 antibody in order to determine equal loading. In the co-immunoprecipitation experiments of IR with Neu2 and Neu4, a western blot of naïve HTC-IR cells was run simultaneous to the immunoprecipitation experiment in order to determine if the HTC-IR cells expressed detectable levels of Neu2 and Neu4 protein. Co-immunoprecipitation experiments using cell lysates from HTC-IR cells further demonstrated that Neu1 forms a complex with insulin receptors in naïve and insulin-treated cells (see Figure 3.9.A). In contrast, there was no co-immunoprecipitation between Neu2 and IR, or between Neu4 and IR (see Figure 3.9.A and 3.9 B). In light of our observations in Figure 3.8, this indicates that Neu4 and insulin receptors might be in the same cell compartment but they do not directly interact with each other.

**A.**



**B.**



**C.**

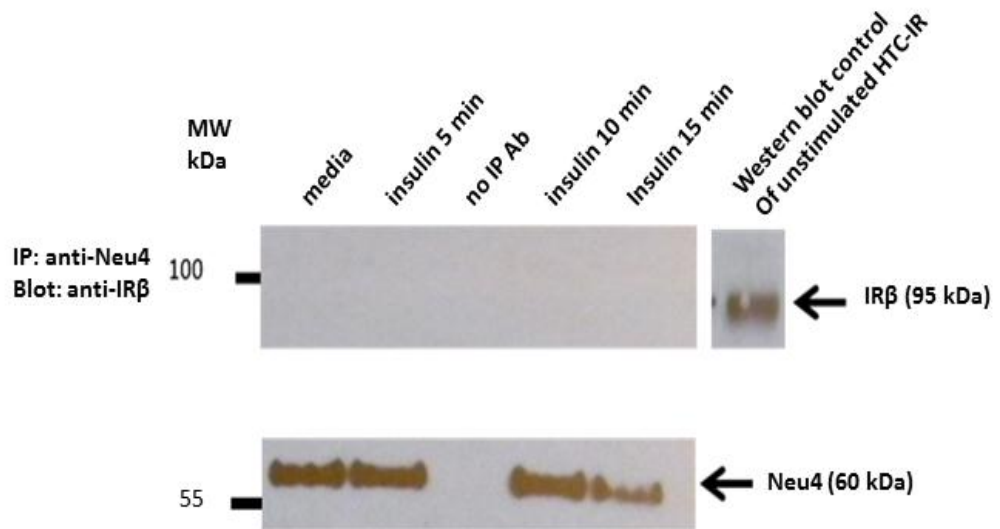


**Figure 3.9 Insulin IR $\beta$  receptors co-immunoprecipitate with Neu1 in cell lysates from naïve and insulin-stimulated HTC-IR cells.**

HTC-IR cells were left in culture medium or in medium containing 100nM insulin for 5, 10 or 15 minutes. Cells ( $1 \times 10^7$  cells) are pelleted and lysed in lysis buffer. 100 $\mu$ g of cell lysates were immunoprecipitate with 1 $\mu$ g of (A) rabbit-anti-human Neu1, (B) mouse anti-human Neu2, or (C) rabbit anti-human Neu4 antibodies overnight at 4°C. Following immunoprecipitation, complexes are isolated using protein A magnetic beads and resolved by 8% Bis-Tris electrophoresis (SDS-PAGE). The blot was probed for IR $\beta$  with anti-IR $\beta$  or Neu1 with anti-Neu1 overnight at 4°C followed by Clean-Blot IP Detection Reagent for immunoprecipitation/Western blots and Western Lightning Chemiluminescence Reagent Plus. The chemiluminescence reaction was analyzed with x-ray film. Sample concentration for gel loading was determined by Bradford assay. As a negative control, HTC-IR cell lysates were not incubated with antibody prior to the immunoprecipitation step in the co-IP. Western blot of cell lysates from naïve HTC-IR cells was run simultaneous with the immunoprecipitation experiment in order to determine detectable levels of Neu2 and Neu4 proteins. For Neu1 IP blot; the blot was washed, stripped and re-probed with anti-Neu1 antibody in order to determine equal loading. The data are a representation of one out of three independent experiments showing similar results.

### **3.10 Inhibition of insulin-induced sialidase activity by broad-range MMP inhibitors piperazine and galardin in live HTC-IR (Sialidase experiments).**

Reports have indicated that there is a Neu1 and matrix metalloproteinase-9 (MMP9) cross-talk in alliance with NGF TrkA (102) and TLR4 (112). To test whether MMP activation plays a role in Neu1 activity associated with insulin-stimulated HTC-IR cells, we initially asked whether galardin (GM6001), a broad specific inhibitor of MMP1, -2, -3, -8, and -9, and piperazine, an inhibitor of MMP-3, -7, and -9 would have an inhibitory effect on Neu1 activity associated with insulin-induced live HTC-IR cells. Using the live cell sialidase assay, galardin and piperazine at 12.5 ng/mL to 125 µg/mL blocked the sialidase activity associated with insulin-treated live HTC-IR cells compared with the insulin-positive control ( see Figure 3.10 and 3.11). Because the common MMPs between galardin and piperazine are MMP9 and MMP3, further experiments needed to be done to identify the role of those MMPs in the activation of insulin receptors.

### **3.11 MMP9 specific inhibitor blocks sialidase activity associated with insulin-treated live HTC-IR cells**

Next, we performed a sialidase assay on live HTC-IR cell line using specific inhibitors of MMP3 or MMP9. HTC-IR cells were left untreated as a control, treated with 10nM insulin or pretreated with 50nM PPP or MMP3i or MMP9i at a concentration range of 25ng/mL to 100 µg/mL followed with 10nM insulin. The sialidase activity associated

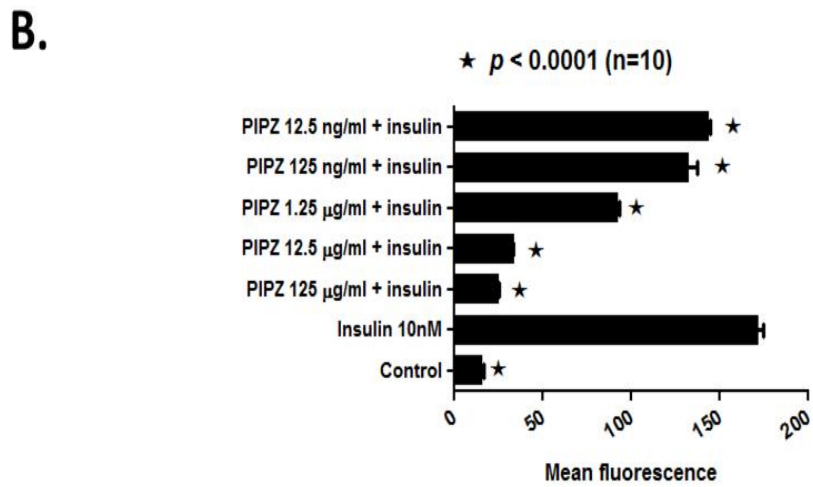
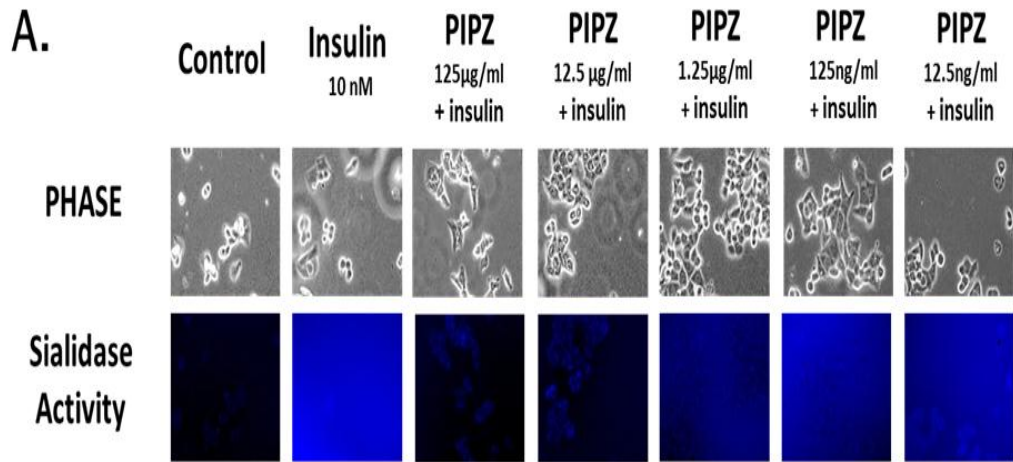


**Figure 3.10 Inhibition of insulin-induced sialidase activity by piperazine (broad range MMP inhibitors) in live HTC-IR**

A. HTC-IR cells were cultured on 12 mm glass coverslips in a sterile 24 well plate in conditioned medium. Cells were divided into three groups: control cells (cells with no stimulation neither inhibition), stimulated cells with 10nM insulin accompanied with 50 nM PPP , and inhibited group of cells with piperazine (inhibitor of MMP -3, -7,-9) at concentration ranging from 12.5ng/ml to 125 µg/ml accompanied with 10nM of insulin. 0.318 mM of 4-MUNANA was added to the cells in order to detect sialidase activity. Fluorescent images were taken at 1-min intervals using epifluorescent microscopy (x40 objective).

B. The mean fluorescence surrounding the cells after adding substrate for each of the images was measured using ImageJ software. mean±Error bars, *S.E.*. The data are a representation of one out of three independent experiments showing similar results. Significant differences at 99.9% confidence using the Dunnett multiple comparison test was used to compare inhibition with the insulin control in each group for n=50 replicates.

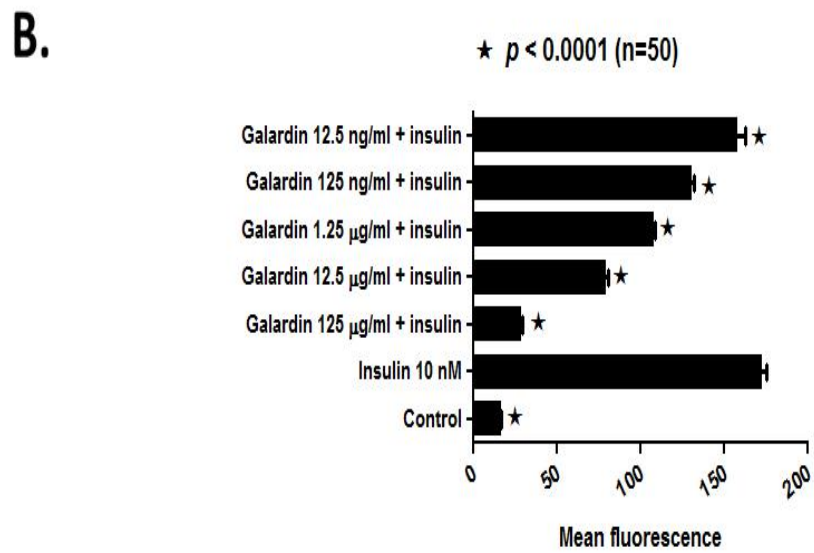
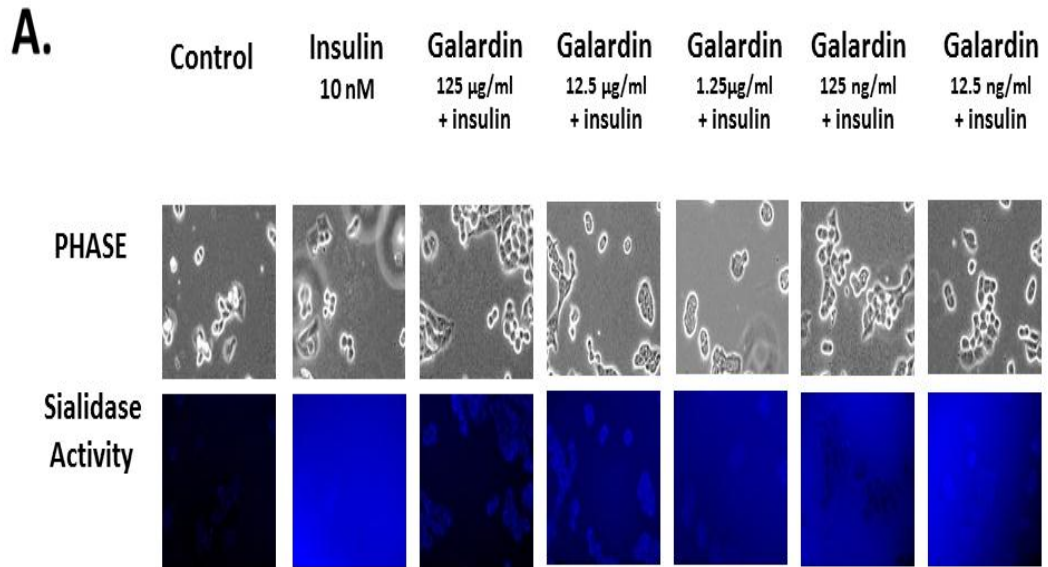


**Figure 3.11 Inhibition of insulin-induced sialidase activity by galardin (broad range MMP inhibitors) in live HTC-IR**

A. HTC-IR cells were cultured on 12 mm glass coverslips in a sterile 24 well plate in conditioned medium. Cells were divided into three groups: control cells (cells with no stimulation or inhibition), stimulated cells with 10nM insulin accompanied with 50 nM PPP , and inhibited group of cells with galardin (inhibitor of MMP-1, -2, -3, -8,-9) at concentration ranging from 12.5ng/ml to 125 µg/ml accompanied with 10nM of insulin. 0.318 mM of 4-MUNANA was added to the cells in order to detect sialidase activity. Fluorescent images were taken at 1-min intervals using epifluorescent microscopy (x40 objective).

B. The mean fluorescence surrounding the cells after adding substrate for each of the images was measured using ImageJ software. mean±Error bars, *S.E.*. The data are a representation of one out of three independent experiments showing similar results. Significant differences at 99.9% confidence using the Dunnett multiple comparison test was used to compare inhibition with the insulin control in each group for n=50 replicates.

with insulin-treated live HTC-IR cells revealed a blue fluorescence surrounding the periphery of the cells. The mean fluorescence was calculated using Image J software. In comparison to the control, cells that were treated with insulin showed an increase in the intensity of the fluorescence. In contrast, MMP9i was able to inhibit the insulin-induced sialidase activity in a dose-dependent manner (see Figure 3.13). While MMP3i was not able to inhibit the sialidase activity to significant values (see Fig. 3.12). These findings indicated that MMP9 might play an important role in insulin receptor activation by mediating sialidase activity associated with insulin-stimulated live cells.

### **3.12 MMP9 specific inhibitor blocks insulin-induced receptor phosphorylation in HTC-IR cells**

Western blot was performed to determine the role of MMP9 in the activation of insulin receptor. HTC-IR cell lysates were prepared from control, unstimulated cells, 100nM insulin-stimulated cells in conjunction with 50nM PPP, or inhibited with 50 or 100 µg/mL of specific MMP9i for 35 minutes followed by 100nM insulin stimulation for 5 minutes. The blot was probed with rabbit anti-human pIRS antibody as a primary antibody followed by secondary goat anti-rabbit IgG antibody. Insulin-treated samples showed an increase in the phosphorylation of IRS1 in comparison to the control, while the cells that were treated with MMP9i showed dose-dependent reduction in pIRS-1 expression in the cell lysates (see Figure 3.14). These findings suggest that MMP9 is an essential player in the insulin receptor activation.

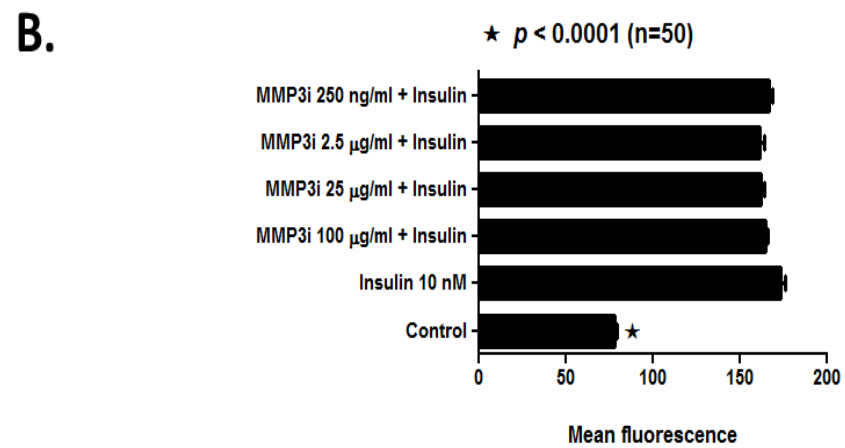
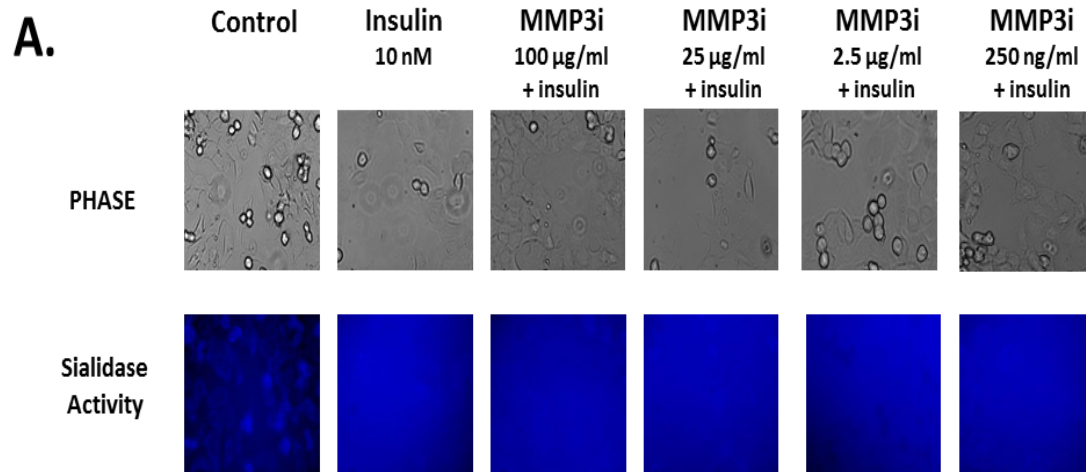


**Figure 3.12 Effect of MMP-3 specific inhibitor on insulin-induced sialidase activity in live HTC-IR.**

A. HTC-IR cells were cultured on 12 mm glass coverslips in a sterile 24 well plate in conditioned medium. Cells were divided into three groups: control cells (cells with no stimulation nor inhibition), stimulated cells with 10nM insulin accompanied with 50 nM PPP , and inhibited group of cells with MMP-3 specific inhibitor at concentration ranging from 250ng/ml to 100 µg/ml accompanied with 10nM of insulin. 0.318 mM of 4-MUNANA was added to the cells in order to detect sialidase activity. Fluorescent images were taken at 1-min intervals using epifluorescent microscopy (x40 objective).

B. The mean fluorescence surrounding the cells after adding substrate for each of the images was measured using ImageJ software. mean±Error bars, *S.E.*. The data are a representation of one out of three independent experiments showing similar results. Significant differences at 99.9% confidence using the Dunnett multiple comparison test was used to compare inhibition with the insulin control in each group for n=50 replicates.

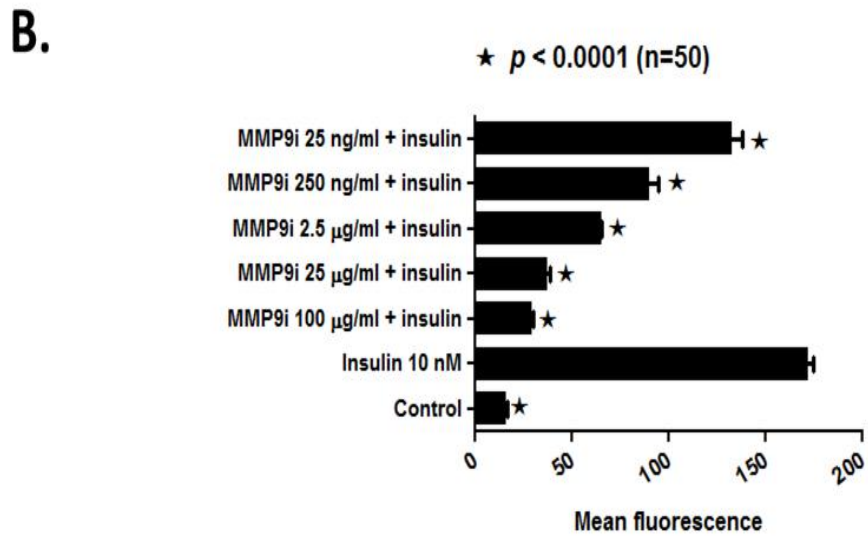
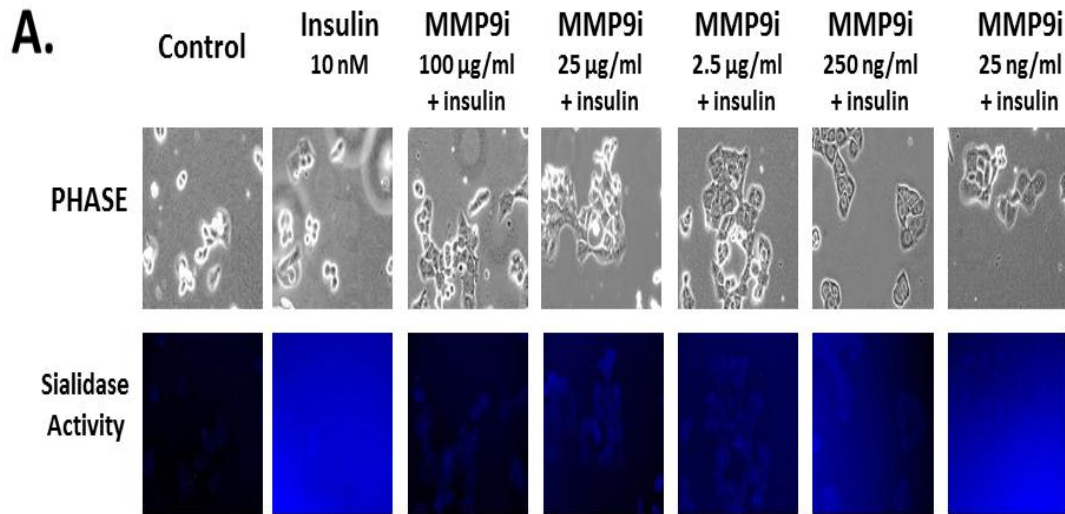
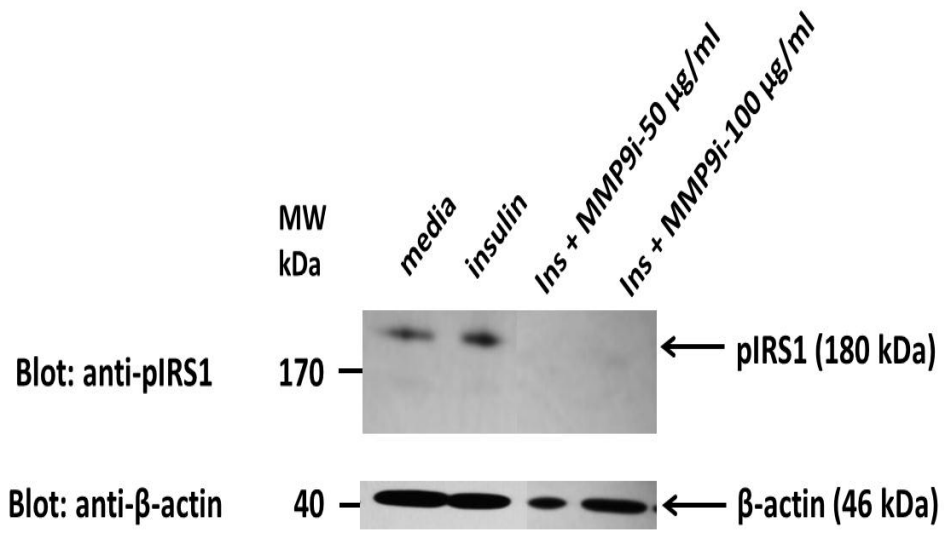


**Figure 3.13 Inhibition of insulin-induced sialidase activity by MMP-9 specific inhibitor in live HTC-IR**

A. HTC-IR cells were cultured on 12 mm glass coverslips in a sterile 24 well plate in conditioned medium. Cells were divided into three groups: control cells (cells with no stimulation or inhibition), stimulated cells with 10nM insulin accompanied with 50 nM PPP , and inhibited group of cells with MMP-9 specific inhibitor at concentration ranging from 25ng/ml to 100 µg/ml accompanied with 10nM of insulin. 0.318 mM of 4-MUNANA was added to the cells in order to detect sialidase activity. Fluorescent images were taken at 1-min intervals using epifluorescent microscopy (x40 objective).

B. The mean fluorescence surrounding the cells after adding substrate for each of the images was measured using ImageJ software. mean±Error bars, *S.E.*. The data are a representation of one out of three independent experiments showing similar results. Significant differences at 99.9% confidence using the Dunnett multiple comparison test was used to compare inhibition with the insulin control in each group for n=50 replicates.

**A.**



**B.**

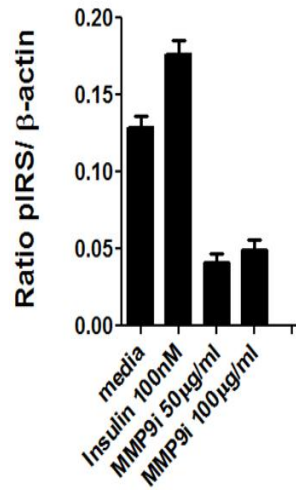


**Figure 3.14 MMP-9 specific inhibitor was able to block insulin receptor phosphorylation in HTC-IR cell line**

- A. HTC-IR cell lysates were prepared from control cells (unstimulated cells), 100nM insulin stimulated cells in conjunction with 50nM PPP, or (50 or 100  $\mu\text{g}/\text{ml}$ ) of specific MMP-9 inhibitor treated cells for 35 minutes followed by 100nM insulin stimulation for 5 minutes. Unstimulated cells were performed as control in this experiment. For each sample, 60  $\mu\text{g}$  proteins were loaded into 8% Bis-Tris gel. Then, the blot was incubated with rabbit anti-human pIRS antibody overnight at 4°C. The blot was incubated with secondary HRP conjugated goat anti-rabbit IgG antibody for 60 minutes at room temperature and Western Lightning Chemiluminescence Reagent Plus. The chemiluminescence reaction was analyzed with x-ray film. The blot was re-probed with  $\beta$ -actin as loading control.
- B. Quantitative analysis was done by assessing the density of a band corrected for background in each lane using Corel Photo Paint 8.0 software. Each bar in the graph represents the mean ratio of pIRS1 to  $\beta$ -actin of band density  $\pm$  S.E. (error bars) for 5–10 replicate measurements. The data are a representation of one out of three independent experiments showing similar results.

### **3.13 MMP9 colocalizes with insulin receptor $\beta$ in HTC-IR cells**

Next, we asked whether MMP9 would colocalize with the insulin receptors. Confocal microscopy revealed the cell surface colocalization of IR $\beta$  and MMP9 in naive and insulin treated HTC-IR cells (see Figure 3.15). Cells were fixed, permabilized, blocked and incubated with 4  $\mu\text{g}/\text{mL}$  rabbit anti-human IR $\beta$  antibody and 4  $\mu\text{g}/\text{mL}$  goat anti-human MMP9 antibody. Cells were then washed and incubated with 4  $\mu\text{g}/\text{mL}$  of AlexaFluor 594 and AlexaFluor 488 combination of secondary antibodies. To account for background non-specific fluorescence, control cells with only secondary antibody (Alexa Flur 488 or Alexa Flur 594) were used. Images were taken under two different channels; a red channel and a green channel. Overlay and co-localization visualization was done by using Photoshop software and Image J software. We observed from this experiment that there was a colocalization between IR $\beta$  and MMP9 Figure 3.15. To confirm the interaction between IR and MMP9 we performed co-immunoprecipitation assay.

### **3.14 Co-immunoprecipitation of IR $\beta$ and MMP-9 in naïve and insulin-stimulated HTC-IR cells.**

The results from the previous colocalization assay (section 3.13) suggested that MMP9 forms a complex with IR. To confirm these results, a co-immunoprecipitation experiment was performed to determine whether or not MMP-9 and the IR form a complex. Cell lysates were performed from HTC-IR cells which were left untreated as a control or stimulated with 100nM insulin for 5, 10 or 15 minutes. Proteins in the cell

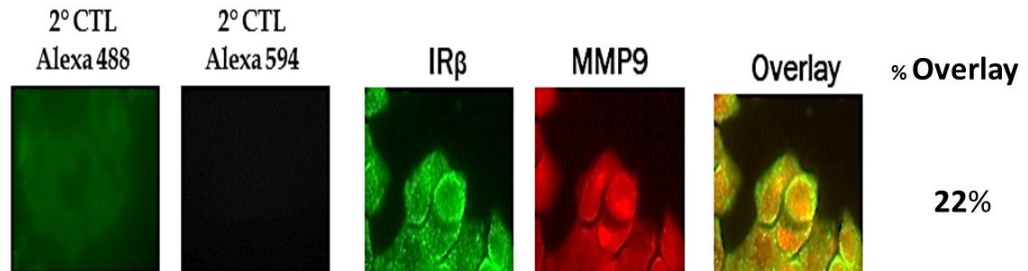


**Figure 3.15 MMP9 colocalization with IR $\beta$  in naïve HTC-IR cells**

HTC-IR cells were cultured on 12 mm glass coverslips in a sterile 24 well plate in conditioned medium as described. Cells were fixed, permeabilized and blocked with 4 % bovine serum albumin (BSA) in 0.1% tween-TBS. Cells were incubated with 4  $\mu$ g/mL of rabbit anti-IR $\beta$  antibody and goat anti-MMP9 antibody for 60 min at 37°C. Cells were washed and incubated with 4  $\mu$ g/mL of AlexaFluor 594 conjugated donkey anti-goat IgG and Alexa 488 conjugated donkey anti-rabbit IgG for 60 min at 37°C. To account for background non-specific fluorescence, control cells with only secondary antibody (Alexa Fluor 488 or Alexa Fluor 594) were used. Stained cells were visualized using epi-fluorescence microscopy with 40x objective. Images were taken under two different channels; a red channel and a green channel. RGB overlay and colocalization visualization was done by using Photoshop software and Image J software. The data are a representation of one out of three independent experiments showing similar results.

lysates were immunoprecipitated with 1 $\mu$ g of anti-MMP9 antibody. Protein samples were resolved on SDS-PAGE gels, and transferred onto the PVDF membrane blots. The blot was incubated with goat anti-human IR $\beta$  antibody overnight at 4°C followed with Clean-Blot IP Detection Reagent for immunoprecipitation/Western blots and Western Lightning Chemiluminescence Reagent Plus. The chemiluminescence reaction was analyzed with x-ray film. HTC-IR cell lysate that was not incubated with the anti-MMP9 antibody prior to the immunoprecipitation step was used as a negative control in the co-IP experiments. The data indicated that MMP9 and insulin IR $\beta$  co-immunoprecipitate in naïve and insulin-stimulated cells, (see Figure 3.16).

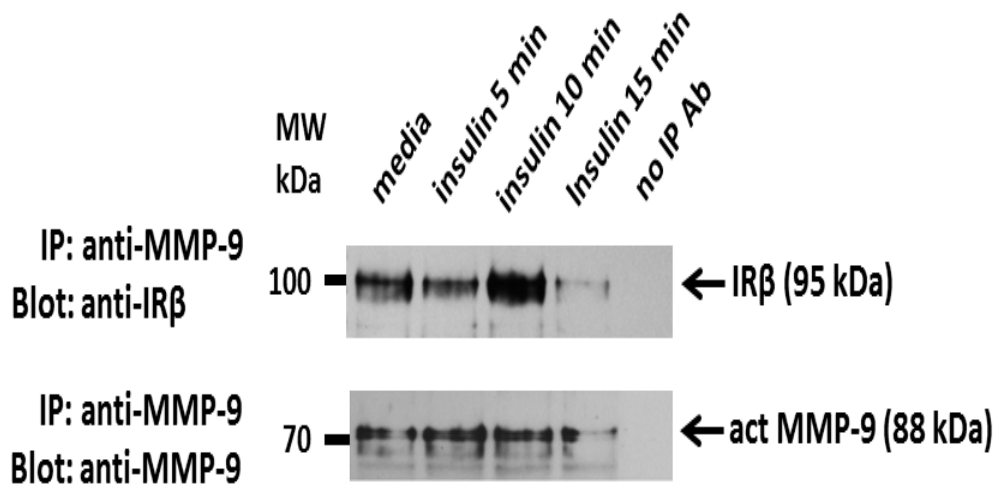


**Figure 3.16 Insulin receptors and MMP9 co-immunoprecipitate in naïve and insulin-stimulated HTC-IR cells**

HTC-IR cells were left unstimulated as a control or stimulated with 100nM insulin for 5, 10 or 15 minutes. Cell lysates were prepared as previously described. 100µg of each cell lysates was immunoprecipitate with 1µg of goat MMP9 antibody overnight at 4 °C. Then, samples were incubated with Protein A magnetic beads for 90 minutes at 4°C. Samples were washed in a magnetic rack and loaded to 8% Bis-Tris gel. The blot was incubated with rabbit anti-human IR<sub>β</sub> antibody overnight at 4°C. The next day, the blot was incubated with a CleanBlot HRP-conjugated secondary antibody for 60 minutes at room temperature and Western Lightning Chemiluminescence Reagent Plus. The chemiluminescence reaction was analyzed with x-ray film. HTC-IR cell lysates that was not incubated with the MMP9 antibody prior to the immunoprecipitation step was used as a negative control in the co-IP experiments. Blot was stripped and reprobed with anti-MPP9 antibody in order to determine equal loading. The data are a representation of one out of three independent experiments showing similar results.

## Chapter 4

### Discussion

The molecular mechanism(s) by which insulin receptors (IR) become activated or even inhibited are not well understood. The data presented in this thesis provide evidence that Neu1 sialidase is an important intermediate link in the initial process of insulin-induced receptor activation. They indicate an initial rapid activation of Neu1 activity which is only induced by insulin binding to the receptor. Central to this process is that Neu1 and not the other three mammalian sialidases, Neu-2, -3 and -4, forms a complex with IR $\beta$  subunit of the insulin receptor in naïve and insulin-stimulated IR-expressing cells. This would actually make Neu1 complexed with IR receptors readily available to be induced upon insulin binding. Our data support this premise because the sialidase activity induced by insulin-treated live cells occurs within a minute. The findings in this thesis also provide evidence for the involvement of matrix metalloproteinase-9 (MMP-9) activation in inducing Neu1 sialidase on the cell surface. Neu1 and MMP-9 form a complex with IR $\beta$  subunit of the insulin receptor on the cell surface of IR-expressing cells. This tripartite alliance would make Neu1 readily available to be induced by insulin binding to the receptor. My data support this premise. How Neu1 sialidase is rapidly induced by MMP-9 at the ectodomain of IR $\beta$  subunit of IR receptors remains unknown.

It can be speculated that insulin binding to the receptor on the cell surface initiates GPCR-signaling via GPCR G $\alpha$ i subunit proteins to activate MMP. It has been

documented that agonist-bound GPCRs have been shown to activate many MMPs (117), including MMP-3 (118), MMPs 2 and 9 (119,120), as well as members of the ADAM family of metalloproteases (121,122). This signaling paradigm would predict a conformational change following insulin binding. Others have reported that upon association of nerve growth factor (NGF) with TrkA, a minor conformational change can occur to form a complex (123). Other studies have determined that p75NTR binds along the homodimeric interface of NGF, which disables NGF's symmetry-related second p75 binding site through an allosteric conformational change (124). For the insulin receptor, several studies have indicated that the insulin receptor might have the ability to induce changes in the conformational state of G $\alpha$ i proteins (125,126). They have considered G $\alpha$ i proteins to function downstream of IR receptors (127). There are other indications for the possible involvement of GPCR signaling in tyrosine kinase receptors (RTKs). For an example, there is an association between  $\beta$ -arrestins (clathrin adaptor proteins that function as regulators of GPCR-dependent signaling) with several RTKs such as TrkA, PDGFRb, IGF-1R, EGFR and insulin receptor (128-131). The data in this thesis show that insulin binding to IR in HTC cells stably expressing IR receptors induces Neu1 sialidase activity which is inhibited by Tamiflu, anti-Neu1 antibodies and MMP inhibitors galardin and piperazine . Therefore, it appears that Neu1 is an intermediate link in the initial process of insulin induced IR activation, which has not been previously observed. In addition, this receptor signaling paradigm in my studies would also predict that insulin receptors are in alliance with a functional GPCR signaling complex.

To support this hypothesis, other reports (93,132,133) show that ligand binding to their respective receptors induces Neu1 sialidase activity within a minute, and that this activity is completely blocked by G $\alpha$ i-sensitive pertussis toxin. The rapidity of the ligand-induced Neu1 sialidase activity mediated by the ligand-bound receptor proposes that glycosylated receptors like NGF TrkA, brain-derived neurotrophin factor (BDNF) TrkB, and TOLL-like receptors (93,132) are forming a functional signaling complex with G $\alpha$ i proteins of GPCRs. Moreover, others have provided important evidence to show that first, the glycosylated platelet-derived growth factor- $\beta$  (PDGF $\beta$ ) receptor is tethered to an endogenous GPCR(s) and to a recombinant endothelial differentiation gene-1 protein (EDG1) in HEK 293 cells (128), second, the constitutively active lysophosphatidic acid (LPA) GPCR receptor enables G $\beta\gamma$  subunit proteins for use by the TrkA receptor (134). It has documented that G $\beta\gamma$  subunits enhance the ability of NGF to promote TrkA signaling and subsequently regulate p42/p44 MAPK signaling pathway in PC12 cells (135). Indeed, LPA1 GPCR was found to co-immunoprecipitate with naïve and NGF-treated TrkA receptors in cell lysates, which implies that LPA1 GPCR are forming a complex with TrkA (134), and (c) the G protein-coupled receptor kinase 2 (GRK2) is constitutively bound with the TrkA receptor, and that NGF stimulates the pertussis toxin-insensitive binding of  $\beta$ -arrestin I to the TrkA-GRK2 complex (129). Taken all together, these findings provide evidence for the first time that TrkA receptors utilize a classical GPCR signaling pathway to promote differentiation of neuronal cells, and thus establishes a molecular organizational platform of a novel tyrosine kinase receptor and

GPCR cross-talk in mammalian cells. It is still unknown whether this same GPCR signaling platform plays a role in insulin-induced activation of insulin receptors.

It is well known that the insulin receptors are heavily glycosylated receptors. They have 18 asparagine residues (glycosylation sites) that have the ability to accept N-linked glycosylation and some serine/threonine amino acids which are involved in O-linked glycosylation (55). Furthermore, the insulin receptors exist as preformed naïve signaling dimers. It is proposed that insulin binding to the ectodomain of the IR $\alpha$  subunits of the receptor induce conformational changes which enable subsequent signaling. However, the precise mechanism(s) of insulin activation of the receptor is unknown. Here, we hypothesize that the IR receptor signaling paradigm in my studies signifies a putative GPCR-signaling and MMP-9 activation in inducing Neu1 sialidase, all of which form a tripartite complex with IR $\beta$  subunits of the IR receptor on the cell surface. It is unknown whether this tripartite signaling complex is involved with the IR $\alpha$  subunits of IR receptors. However, it is proposed that active Neu1 in complex with IR $\beta$  hydrolyzes  $\alpha$ -2,3-sialyl residues enabling in removing a steric hindrance to IR $\beta$  receptor association for IR activation and cellular signaling, the process of which was previously observed for the NGF TrkA (9,93) and TOLL-like receptors (93). The premise for ligand activation of PDGF, TrkA and insulin receptors is that the dimerization is a prerequisite for the activation of the kinase. In conjunction with the dimerization and kinase activation, the IR receptor subunits undergo conformational changes following ligand binding, these conformational changes allow a basal kinase activity to phosphorylate the critical

tyrosine residue, thereby leading to full enzymatic activity directed toward other tyrosine residues in the receptor subunits as well as other substrates for the kinase. In this and our other report (9), it is proposed that an alternate molecular signaling platform exists at the cell surface receptor level in order to facilitate the initial IR subunit receptor dimerization process. These results in this thesis are consistent with other previous reports (9,12,93) in the laboratory supporting the glycosylation model in corroborating the importance of sialyl  $\alpha$ -2,3-linked  $\beta$ -galactosyl residues of IR $\beta$  subunits of IR receptors in the initial stages of insulin induced receptor activation.

In this thesis, Tamiflu (oseltamivir phosphate) which is the ethyl ester pro-drug of oseltamivir carboxylate was found to be highly potent ( $IC_{50}$  6.1  $\mu$ M) in inhibiting Neu1 activity induced by insulin treatment of live HTC-IR cells. The explanation for this inhibitory potency of Tamiflu on Neu1 sialidase activity is unrecognized. One possible explanation might be the unique orientation of Neu1 with the molecular multi-enzymatic complex that contains  $\beta$ -galactosidase and cathepsin A (136) and elastin-binding protein (EBP) (137), the complex of which would be associated within the ectodomain of IR receptors. Nan et al., have reported that the cell surface Neu1 is tightly associated with a subunit of cathepsin A and the resulting complex influences cell surface sialic acid in activated cells and the production of IFN $\gamma$  (138). Another possible explanation is that Tamiflu's may have direct effect on Neu1 sialidase with specificity for sialyl  $\alpha$ -2,3-linked  $\beta$ -galactosyl residues of IR receptors. In another report, Neu1 desialylation of  $\alpha$ -2,3-sialyl residues of TOLL-like receptors enables receptor dimerization (93). The report showed

that TLR ligand-induced NF $\kappa$ B responses were not observed in TLR deficient HEK293 cells, but were re-established in HEK293 cells stably transfected with TLR4/MD2, and were significantly inhibited by  $\alpha$ -2,3-sialyl specific *Maackia amurensis* (MAL-2) lectin,  $\alpha$ -2,3-sialyl specific galectin-1 and neuraminidase inhibitor Tamiflu but not by  $\alpha$ -2,6-sialyl specific *Sambucus nigra* lectin (SNA). Also, Tamiflu were able to inhibit LPS-induced sialidase activity in live BMC-2 macrophage cells with an IC<sub>50</sub> of 1.2 $\mu$ M compared to an IC<sub>50</sub> of 1015 $\mu$ M for its hydrolytic metabolite oseltamivir carboxylate (132). Tamiflu blockage of LPS-induced Neu1 sialidase activity was not affected in BMC-2 macrophage cells pretreated with anticarboxylesterase agent, clopidogrel. Moreover, Neu1 was found to have the ability of negatively regulate lysosomal exocytosis in hematopoietic cells where it processes the sialic acids on the lysosomal membrane protein LAMP-1 on the cell surface (139). Seyrantepe *et al.* have shown that Neu1 have the ability of activating phagocytosis in macrophages and dendritic cells through the desialylation of surface receptors, including Fc receptors for immunoglobulin G (Fc $\gamma$ R) (93).

The data presented in this thesis further signifies an important role of Neu1 sialidase as an intermediate link in the initial process of ligand induced insulin tyrosine kinase receptor activation and subsequent cellular signaling. The premise is that Neu1 forms a complex with glycosylated IR $\beta$  receptors within the ectodomain, which is consistent with other previous reports with Trk (93) and TLR receptors (132). Secondly, Neu1 may be a requisite intermediate in regulating IR activation following insulin

binding to the receptor. Thirdly, activated Neu1 by insulin binding to the receptor predicts a rapid removal of  $\alpha$ -2,3-sialyl residues linked to  $\beta$ -galactosides on IR $\beta$  ectodomain to generate a functional IR receptor. Although there are four identified mammalian sialidases, cytosolic sialidase (Neu2), plasma membrane bound sialidase (Neu3) (140-142) and Neu4 (94,101) are not involved in the sialidase activity associated with insulin treated live IR-expressing cells. Fourthly, the potentiation of GPCR-signaling and matrix metalloproteinase-9 activation by insulin binding to the IR receptor is involved in the activation process of Neu1 sialidase on the cell surface. Using colocalization microscopy on permeabilized naïve and insulin-treated cells and co-immunoprecipitation experiments, the additional intracellular and cell surface colocalization of Neu1, MMP-9 and IR receptors validated the predicted association of MMP-9 with Neu1 in alliance with IR receptors.

In conclusion, the data presented in this thesis suggest that at least for IR $\beta$  subunits of IR receptors the initial mechanism(s) for receptor activation and subsequent cellular signaling is dependent on Neu1 sialidase activity. Colocalization microscopy and co-immunoprecipitation data indicate that Neu1/IR $\beta$  complexes are already formed on the cell membrane in naïve IR-expressing cells. Secondly, insulin binding to its receptor may induce allosteric conformational changes in the receptor, which in turn potentiates GPCR-signaling and MMP-9 activation to induce Neu1 sialidase. Several studies have suggested that the insulin receptor might have the ability to induce changes in the conformational state of G $\alpha_i$  (125,126). GPCRs have been found to be in close proximity

to the receptor tyrosine kinases (RTKs) including the insulin receptors, and they can form a signaling platform (127). The functions of these signaling platforms are to share the protein signaling components for each receptor and to facilitate the production of an integrated response upon engagement to the ligands (127). Several studies have demonstrated that there is an overlapping signaling pathway between GPCRs and RTKs. This overlapping of GPCRs and RTKs is a result of the binding between GPCRs and their ligands and the binding between the growth factors and RTKs. This crosstalk between GPCRs and RTKs results in the tyrosine phosphorylation of the RTKs and the phospho-tyrosines function as adaptor sites for the recruitment of signaling molecules that contain SH2 domains (143,144). In this thesis, central to this process is that Neu1/MMP-9 complex in alliance with IR receptors is expressed on the cell surface of IR-expressing cells. This tripartite alliance would actually make Neu1 readily available to be induced by insulin binding to the receptor. The findings in this thesis suggest that Neu1 sialidase and MMP-9 cross-talk may be the key regulators of insulin-induced IR activation to generate a functional receptor.

Based on my findings in this thesis, the proposed model for insulin receptor activation is depicted in (see Figure 4.1). Firstly, insulin binding to the insulin receptor initiates the IR signaling cascade. This insulin binding to IR $\beta$ s triggers the activation of GPCR, which in turn cause conformational changes in the GPCR receptor. This conformational change in the GPCR in alliance with IR and MMP9 activates MMP9. Activated MMP9 in complex with IR induces Neu1 sialidase activity.

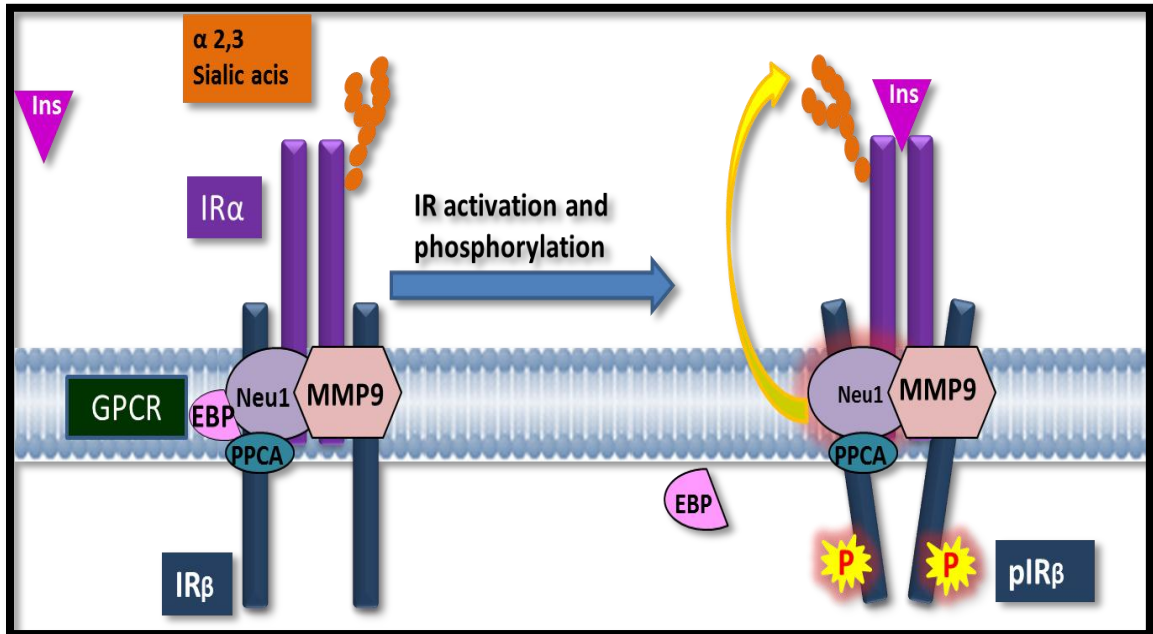


**Figure 4.1 Proposed model for IR activation.**

The figure represents the proposed model for IR activation. Insulin binds to IR results in a proposed conformational change that activates the GPCR signaling cascade at the receptor level to induce MMP9. Neu1 and MMP-9 have been found to form a complex with IR. Activated MMP-9 is proposed to remove the elastin binding protein (EBP) from the Neu1/cathepsin A/EBP complex and catalytically induces Neu1 sialidase. Activation of Neu1 sialidase leads to the cleavage of  $\alpha$ -2,3-linked sialic acid to facilitate the receptor phosphorylation and activation.

Neu1 sialidase in complex with IR exists as a multimeric partnership with elastin binding protein (EBP) and protective protein/cathepsin A (*PPCA* facilitates its recruitment from the lysosome to the cell membrane). In order to activate Neu1 sialidase, elastin binding protein has to be removed. Activated MMP9 with elastin substrate properties is proposed to remove the EBP to facilitate the activation of Neu1 sialidase. Activated Neu1 hydrolyzes  $\alpha$ -2,3-linked sialic acids at the ectodomain of IR $\beta$  subunits of IR receptors on the cell surface in removing steric hindrance to IR $\beta$  receptor association and allowing subsequent auto-phosphorylation of IR $\beta$  subunits.

#### **4.1 The Significance of the Project.**

The main physiological function of insulin receptor (IR) is involved in metabolic regulation. IR regulates glucose metabolism homeostasis (31). Failure to maintain the metabolic homeostasis is responsible for different metabolic disorders such as diabetes mellitus.

IR signaling pathways are triggered by the binding of the insulin to the extracellular portion of the IR  $\alpha$  subunits which is followed with the association of the  $\beta$  subunits with the ATP domain (6). This process leads to a cascade of autophosphorylation, which in turn stimulates two signaling pathways: the phosphatidylinositol 3 kinase pathway, PI3K, and the mitogen activated protein kinase pathway, MAPK, through the insulin receptor substrates, IRS (6). The activation of the PI3K signaling pathway plays important roles in glucose metabolism, glycogen, lipid and

protein synthesis (21). On the other hand, MAPK controls a major intracellular signaling network that affects several cellular functions such as proliferation, migration, survival, differentiation, senescence and gene expression (24,64).

Several studies have implicated insulin receptor over-expression with different cancers, such as breast cancer (145). Moreover, IR and IGF-1R are overexpressed in leukemia cells. It has been reported that the induction of PI3K/Akt pathways via the activation of IR, IGF-1R, or the hybrid form of IGF-1R can lead to the proliferation of leukemia cells (146).

A complete understanding of IR structure, activation and the role of sialic acids in the signaling pathways may provide therapeutic strategies in the prevention of different diseases such as diabetes mellitus and cancer.

## Literature Cited

1. Pawson, T., and Nash, P. (2000) *Genes & Development* **14**, 1027-1047
2. Robinson, D. R., Wu, Y. M., and Lin, S. F. (2000) *Oncogene* **19**, 5548-5557
3. Hubbard, S. R., Mohammadi, M., and Schlessinger, J. (1998) *Journal of Biological Chemistry* **273**, 11987-11990
4. Scott, M. P. (2003) *Molecular Cell Biology*,
5. Zwick, E., Bange, J., and Ullrich, A. (2001) *Endocrine-related cancer* **8**, 161-173
6. Litwack, G. (2009) *Insulin and IGFs*, Elsevier Science
7. Watson, F. L., Porcionatto, M. A., Bhattacharyya, A., Stiles, C. D., and Segal, R. A. (1999) *J.Neurobiol.* **39**, 323-336
8. Elleman, T. C., Frenkel, M. J., Hoyne, P. A., McKern, N. M., Cosgrove, L., Hewish, D. R., Jachno, K. M., Bentley, J. D., Sankovich, S. E., and Ward, C. W. (2000) *Biochem J.* **347**, 771-779.
9. Woronowicz, A., Amith, S. R., De Vusser, K., Laroy, W., Contreras, R., Basta, S., and Szewczuk, M. R. (2007) *Glycobiology* **17**, 10-24
10. Woronowicz, A., Amith, S. R., Davis, V. W., Jayanth, P., De Vusser, K., Laroy, W., Contreras, R., Meakin, S. O., and Szewczuk, M. R. (2007) *Glycobiology* **17**, 725-734
11. Woronowicz, A., De Vusser, K., Laroy, W., Contreras, R., Meakin, S. O., Ross, G. M., and Szewczuk, M. R. (2004) *Glycobiology*, cwh123
12. Woronowicz, A., De Vusser, K., Laroy, W., Contreras, R., Meakin, S. O., Ross, G. M., and Szewczuk, M. R. (2004) *Glycobiology* **14**, 987-998
13. Ronnett, G. V., Knutson, V. P., Kohanski, R. A., Simpson, T. L., and Lane, M. D. (1984) *J Biol Chem* **259**, 4566-4575
14. Hernández-Sánchez, C., Mansilla, A., de Pablo, F., and Zardoya, R. (2008) *Molecular Biology and Evolution* **25**, 1043-1053
15. Markus Leyck Dieken, M. F., Pierre De Meyts, Axel Wollmer. (2002) *Insulin and Related Proteins -- Structure to Function and*, Springer
16. Pierre De Meyts, W. S., Jane Palsgaard, Anne-Mette Theede, Lisbeth Gauguin, Hassan Aladdin, and Jonathan Whittaker. (2007) Insulin and IGF-I Receptor Structure and Binding Mechanism. in *Mechanisms of Insulin Action* (Pessin, A. R. S. a. J. E. ed.). pp
17. Maki, R. G. (2010) *Journal of Clinical Oncology* **28**, 4985-4995
18. Frasca, F., Pandini, G., Sciacca, L., Pezzino, V., Squatrito, S., Belfiore, A., and Vigneri, R. (2008) *Arch Physiol Biochem.* **114**, 23-37.
19. Annunziata, M., Granata, R., and Ghigo, E. (2010) *Acta Diabetol* **48**, 1-9
20. Weston, D. (2008) *Infection Prevention and Control*, Wiley-Interscience
21. Belfiore, A., and Frasca, F. (2008) *J Mammary Gland Biol Neoplasia* **13**, 381-406
22. Seino, S., Seino, M., and Bell, G. I. (1990) *Diabetes.* **39**, 123-128.
23. Zhang, H., Fagan, D. H., Zeng, X., Freeman, K. T., Sachdev, D., and Yee, D. (2010) *Oncogene* **29**, 2517-2527
24. Chiu, S. L., and Cline, H. T. (2010) *Neural Dev* **5**, 7
25. Belfiore, A., and Malaguarnera, R. (2011) *Endocrine-Related Cancer* **18**, R125-R147
26. Lee, J., and Pilch, P. F. (1994) *American Journal of Physiology - Cell Physiology* **266**, C319-C334
27. Lee, J. K., Tam, J. W., Tsai, M. J., and Tsai, S. Y. (1992) *J Biol Chem.* **267**, 4638-4645.

28. Belfiore, A. (2007) *Curr Pharm Des.* **13**, 671-686.
29. Pollak, M., and Russell-Jones, D. (2010) *International Journal of Clinical Practice* **64**, 628-636
30. Belfiore, A., Frasca, F., Pandini, G., Sciacca, L., and Vigneri, R. (2009) *Endocr Rev* **30**, 586-623
31. Whitten, A. E., Smith, B. J., Menting, J. G., Margetts, M. B., McKern, N. M., Lovrecz, G. O., Adams, T. E., Richards, K., Bentley, J. D., Trehwella, J., Ward, C. W., and Lawrence, M. C. (2009) *Journal of Molecular Biology* **394**, 878-892
32. Porte, D., Baskin, D. G., and Schwartz, M. W. (2005) *Diabetes* **54**, 1264-1276
33. Müssig, K., Staiger, H., Kantartzis, K., Fritsche, A., Kanz, L., and Häring, H. U. (2011) *Diabetic Medicine* **28**, 276-286
34. Azar, M., and Lyons, T. J. (2010) *F1000 Med Rep* **2**
35. Clark, S., Eckardt, G., Siddle, K., and Harrison, L. C. (1991) *Biochem J* **276 ( Pt 1)**, 27-33
36. Rentería, M. E., Gandhi, N. S., Vinuesa, P., Helmerhorst, E., and Mancera, R. L. (2008) *PLoS ONE* **3**, e3667
37. Mayer, J. P., Zhang, F., and DiMarchi, R. D. (2007) *Biopolymers* **88**, 687-713
38. Tertoolen, L. G., Blanchetot, C., Jiang, G., Overvoorde, J., Gadella, T. W., Jr., Hunter, T., and den Hertog, J. (2001) *BMC Cell Biol* **2**, 8
39. Ullrich, A., Bell, J. R., Chen, E. Y., Herrera, R., Petruzzelli, L. M., Dull, T. J., Gray, A., Coussens, L., Liao, Y. C., Tsubokawa, M., and et al. (1985) *Nature*. **313**, 756-761.
40. Rojek, A., and Niedziela, M. (2010) *Advances in Cell Biology*
41. Bass, J., Chiu, G., Argon, Y., and Steiner, D. F. (1998) *J Cell Biol* **141**, 637-646
42. Whittaker, J. (2011) *Uptodate*
43. Hwang, J. B., Hernandez, J., Leduc, R., and Frost, S. C. (2000) *Biochimica et Biophysica Acta (BBA) - Molecular Cell Research* **1499**, 74-84
44. Barbour, K., Boudreau, R., Danielson, M., Youk, A., Wactawski-Wende, J., Greep, N., LaCroix, A., Jackson, R., Wallace, R., Bauer, D., Allison, M., and Cauley, J. (2012) *Journal of bone and mineral research : the official journal of the American Society for Bone and Mineral Research* **27**, 1167-1176
45. De Meyts, P., and Whittaker, J. (2002) *Nat Rev Drug Discov* **1**, 769-783
46. Bertrand, L., Horman, S., Beauloye, C., and Vanoverschelde, J.-L. (2008) *Cardiovascular Research* **79**, 238-248
47. Taton, J., Czech, A., and Piatkiewicz, P. (2010) *Endokrynol Pol.* **61**, 388-394.
48. LeRoith, D. T., Simeon I.; Olefsky, Jerrold M. (2004) *Diabetes Mellitus: A Fundamental and Clinical Text*, Third ed., Lippincott Williams & Wilkins
49. Lipson, K. L., Fonseca, S. G., Ishigaki, S., Nguyen, L. X., Foss, E., Bortell, R., Rossini, A. A., and Urano, F. (2006) *Cell Metabolism* **4**, 245-254
50. Joslin, E. P., and Kahn, C. R. (2005) *Diabetes Mellitus*, Lippincott Williams & Wilkins
51. Najjar, S. (2001) *Insulin Action: Molecular Basis of Diabetes*. in *eLS*, John Wiley & Sons, Ltd. pp
52. LeRoith, D., Simeon I. Taylor, M. D., and Olefsky, J. M. (2004) *Diabetes Mellitus: A Fundamental and Clinical Text*, Lippincott Williams & Wilkins
53. Hua, Q. (2010) *Protein & Cell* **1**, 537-551
54. Baker, E. N., Blundell, T. L., Cutfield, J. F., Cutfield, S. M., Dodson, E. J., Dodson, G. G., Hodgkin, D. M. C., Hubbard, R. E., Isaacs, N. W., Reynolds, C. D., Sakabe, K.,

- Sakabe, N., and Vijayan, N. M. (1988) *Philosophical Transactions of the Royal Society of London. B, Biological Sciences* **319**, 369-456
55. Ward, C., Lawrence, M., Streltsov, V., Garrett, T., McKern, N., Lou, M. Z., Lovrecz, G., and Adams, T. (2008) *Acta Physiol (Oxf)* **192**, 3-9
  56. Wu, J. J., and Guidotti, G. (2004) *J Biol Chem* **279**, 25765-25773
  57. Mardilovich, K., Pankratz, S. L., and Shaw, L. M. (2009) *Cell Commun Signal* **7**, 14
  58. Lippe, R., Ohl, K., Varga, G., Rauen, T., Crispin, J., Juang, Y.-T., Kuerten, S., Tacke, F., Wolf, M., Roebrock, K., Vogl, T., Verjans, E., Honke, N., Ehrchen, J., Foell, D., Skryabin, B., Wagner, N., Tsokos, G., Roth, J., and Tenbrock, K. (2012) *Journal of molecular cell biology* **4**, 121-123
  59. White, M. F. (2002) *Am J Physiol Endocrinol Metab* **283**, E413 - 422
  60. Bjornholm, M., He, A. R., Attersand, A., Lake, S., Liu, S. C., Lienhard, G. E., Taylor, S., Arner, P., and Zierath, J. R. (2002) *Diabetologia* **45**, 1697 - 1702
  61. Lavan, B. E., Fantin, V. R., Chang, E. T., Lane, W. S., Keller, S. R., and Lienhard, G. E. (1997) *J Biol Chem* **272**, 21403 - 21407
  62. Roberts, M. S., Woods, A. J., Dale, T. C., van der Sluijs, P., and Norman, J. C. (2004) *Molecular and cellular biology* **24**, 1505-1515
  63. Tartaglia, M., and Gelb, B. D. (2010) *Annals of the New York Academy of Sciences* **1214**, 99-121
  64. Knowlden, J. M., Hutcheson, I. R., Barrow, D., Gee, J. M., and Nicholson, R. I. (2005) *Endocrinology* **146**, 4609-4618
  65. Huang, C. C., Lee, C. C., and Hsu, K. S. (2010) *Chang Gung Med J* **33**, 115-125
  66. Varki, A. (1999) *Essentials of Glycobiology*, Cold Spring Harbor Laboratory Press
  67. Herscovics, A. (1999) *Biochimica et Biophysica Acta (BBA) - General Subjects* **1473**, 96-107
  68. Lowe, J. B., and Marth, J. D. (2003) *Annual review of biochemistry* **72**, 643-691
  69. de Beer, T., Vliegthart, J. F., Löffler, A., and Hofsteenge, J. (1995) *Biochemistry* **34**, 11785-11789
  70. Fernandez, F., Jannatipour, M., Hellman, U., Rokeach, L. A., and Parodi, A. J. (1996) *Embo J* **15**, 705-713.
  71. Sparrow, L. G., Lawrence, M. C., Gorman, J. J., Strike, P. M., Robinson, C. P., McKern, N. M., and Ward, C. W. (2008) *Proteins: Structure, Function, and Bioinformatics* **71**, 426-439
  72. Kornfeld, R., and Kornfeld, S. (1985) *Annu Rev Biochem.* **54**, 631-664.
  73. Vimr, E. R., Kalivoda, K. A., Deszo, E. L., and Steenbergen, S. M. (2004) *Microbiology and Molecular Biology Reviews* **68**, 132-153
  74. Ajit, V. (2008) *Trends in Molecular Medicine* **14**, 351-360
  75. Schwerdtfeger, S. M., and Melzig, M. F. (2010) *Pharmazie*. **65**, 551-561.
  76. Buschiazzo, A., and Alzari, P. M. (2008) *Current Opinion in Chemical Biology* **12**, 565-572
  77. Achyuthan, K. E., and Achyuthan, A. M. (2001) *Comparative Biochemistry and Physiology Part B: Biochemistry and Molecular Biology* **129**, 29-64
  78. Traving, C., and Schauer, R. (1998) *Cell Mol Life Sci.* **54**, 1330-1349.
  79. Hao, J., Vann, W. F., Hinderlich, S., and Sundaramoorthy, M. (2006) *Biochem J* **397**, 195-201

80. Monti, E., Bonten, E., D'Azzo, A., Bresciani, R., Venerando, B., Borsani, G., Schauer, R., and Tettamanti, G. (2010) Sialidases in Vertebrates: A Family Of Enzymes Tailored For Several Cell Functions\*. in *Advances in Carbohydrate Chemistry and Biochemistry* (Derek, H. ed.), Academic Press. pp 403-479
81. Schauer, R., Kelm, S., and Reuter, G. (1995) *Biochemistry and role of sialic acids*,
82. Tavakkol, A., and Burness, A. T. (1990) *Biochemistry* **29**, 10684-10690
83. Schauer, R. (2000) *Glycoconj J.* **17**, 485-499.
84. Nakano, V., Fontes Piazza, R. M., and Avila-Campos, M. J. (2006) *Anaerobe.* **12**, 238-241. Epub 2006 Oct 2002.
85. Miyagi, T., Wada, T., Yamaguchi, K., Shiozaki, K., Sato, I., Kakugawa, Y., Yamanami, H., and Fujiya, T. (2008) *Proteomics* **8**, 3303-3311
86. Magesh, S., Suzuki, T., Miyagi, T., Ishida, H., and Kiso, M. (2006) *Journal of Molecular Graphics and Modelling* **25**, 196-207
87. Magesh, S., Moriya, S., Suzuki, T., Miyagi, T., Ishida, H., and Kiso, M. (2008) *Bioorganic & Medicinal Chemistry Letters* **18**, 532-537
88. Hinek, A., Bodnaruk, T. D., Bunda, S., Wang, Y., and Liu, K. (2008) *The American journal of pathology* **173**, 1042-1056
89. Bonten, E., van der Spoel, A., Fornerod, M., Grosveld, G., and d'Azzo, A. (1996) *Genes & Development* **10**, 3156-3169
90. Bass, J., Kurose, T., Pashmforoush, M., and Steiner, D. F. (1996) *J Biol Chem* **271**, 19367-19375
91. Monti, E., Preti, A., Venerando, B., and Borsani, G. (2002) *Neurochemical Research* **27**, 649-663
92. Pshezhetsky, A., and Hinek, A. (2011) *Glycoconjugate Journal* **28**, 441-452
93. Amith, S. R., Jayanth, P., Franchuk, S., Finlay, T., Seyrantepe, V., Beyaert, R., Pshezhetsky, A. V., and Szewczuk, M. R. (2010) *Cellular Signalling* **22**, 314-324
94. Seyrantepe, V., Poupetova, H., Froissart, R., Zabot, M.-T., Maire, I., and Pshezhetsky, A. V. (2003) *Human Mutation* **22**, 343-352
95. van Pelt, J., Kamerling, J. P., Vliegenthart, J. F., Hoogeveen, A. T., and Galjaard, H. (1988) *Clin Chim Acta.* **174**, 325-335.
96. Bonten, E. J., Arts, W. F., Beck, M., Covanis, A., Donati, M. A., Parini, R., Zammarchi, E., and d'Azzo, A. (2000) *Human Molecular Genetics* **9**, 2715-2725
97. Miyagi, T., Wada, T., Yamaguchi, K., and Hata, K. (2003) *Glycoconjugate Journal* **20**, 189-198
98. Monti, E., Preti, A., Rossi, E., Ballabio, A., and Borsani, G. (1999) *Genomics* **57**, 137-143
99. Parker, R. B., and Kohler, J. J. (2009) *ACS Chemical Biology* **5**, 35-46
100. Wada, T., Yoshikawa, Y., Tokuyama, S., Kuwabara, M., Akita, H., and Miyagi, T. (1999) *Biochemical and Biophysical Research Communications* **261**, 21-27
101. Yamaguchi, K., Hata, K., Koseki, K., Shiozaki, K., Akita, H., Wada, T., Moriya, S., and Miyagi, T. (2005) *Biochem J.* **390**, 85-93.
102. Jayanth, P., Amith, S. R., Gee, K., and Szewczuk, M. R. (2010) *Cellular Signalling* **22**, 1193-1205
103. de Laat, M. A., Kyaw-Tanner, M. T., Nourian, A. R., McGowan, C. M., Sillence, M. N., and Pollitt, C. C. (2011) *Veterinary Immunology and Immunopathology* **140**, 275-281
104. Ram, M., Sherer, Y., and Shoenfeld, Y. (2006) *J Clin Immunol* **26**, 299-307

105. Verma, R. P., and Hansch, C. (2007) *Bioorganic & Medicinal Chemistry* **15**, 2223-2268
106. Rybakowski, J. K. (2009) *Cardiovascular Psychiatry and Neurology* **2009**
107. Liu, Z., Li, L., Yang, Z., Luo, W., Li, X., Yang, H., Yao, K., Wu, B., and Fang, W. (2010) *BMC Cancer* **10**, 270
108. Fiscoeder, A., Meyborg, H., Stibenz, D., Fleck, E., Graf, K., and Stawowy, P. (2007) *Cardiovascular Research* **73**, 841-848
109. Fukuda, D., Shimada, K., Tanaka, A., Kusuyama, T., Yamashita, H., Ehara, S., Nakamura, Y., Kawarabayashi, T., Iida, H., Yoshiyama, M., and Yoshikawa, J. (2006) *The American Journal of Cardiology* **97**, 175-180
110. Marx, N., Froehlich, J., Siam, L., Ittner, J., Wierse, G., Schmidt, A., Scharnagl, H., Hombach, V., and Koenig, W. (2003) *Arteriosclerosis, Thrombosis, and Vascular Biology* **23**, 283-288
111. Haffner, S. M., Greenberg, A. S., Weston, W. M., Chen, H., Williams, K., and Freed, M. I. (2002) *Circulation* **106**, 679-684
112. Abdulkhalek, S., Guo, M., Amith, S. R., Jayanth, P., and Szewczuk, M. R. (2012) *Cellular Signalling* **24**, 2035-2042
113. Purushothaman, A., Babitz, S. K., and Sanderson, R. D. (2012) *Journal of Biological Chemistry* **287**, 41288-41296
114. Leconte, I., Auzan, C., Debant, A., Rossi, B., and Clauser, E. (1992) *J. Biol. Chem.* **267**, 17415-17423
115. Cheevers, W. P., Snekvik, K. R., Trujillo, J. D., Kumpula-McWhirter, N. M., Pretty On Top, K. J., and Knowles, D. P. (2003) *Virology* **306**, 116 - 125
116. Arabkhari, M., Bunda, S., Wang, Y., Wang, A., Pshezhetsky, A. V., and Hinek, A. (2010) *Glycobiology* **20**, 603-616
117. Fischer, O., Hart, S., and Ullrich, A. (2006) Dissecting the Epidermal Growth Factor Receptor Signal Transactivation Pathway. in *Epidermal Growth Factor* (Patel, T., and Bertics, P. eds.), Humana Press. pp 85-97
118. Lee, M.-H., and Murphy, G. (2004) *Journal of Cell Science* **117**, 4015-4016
119. Le Gall, S. M., Auger, R., Dreux, C., and Mauduit, P. (2003) *Journal of Biological Chemistry* **278**, 45255-45268
120. Murasawa, S., Mori, Y., Nozawa, Y., Gotoh, N., Shibuya, M., Masaki, H., Maruyama, K., Tsutsumi, Y., Moriguchi, Y., Shibasaki, Y., Tanaka, Y., Iwasaka, T., Inada, M., and Matsubara, H. (1998) *Circulation Research* **82**, 1338-1348
121. Gööz, M., Gööz, P., Luttrell, L. M., and Raymond, J. R. (2006) *Journal of Biological Chemistry* **281**, 21004-21012
122. Prenzel, N., Zwick, E., Daub, H., Leserer, M., Abraham, R., Wallasch, C., and Ullrich, A. (1999) *Nature* **402**, 884-888
123. Woo, S. B., Neet, K. E., and Whalen, C. (1998) *Protein Science* **7**, 1006-1016
124. He, X.-l., and Garcia, K. C. (2004) *Science* **304**, 870-875
125. Rothenberg, P., and Kahn, C. (1988) *The Journal of biological chemistry* **263**, 15546-15552
126. Pyne, N. J., Heyworth, C. M., Balfour, N. W., and Houslay, M. D. (1989) *Biochemical and Biophysical Research Communications* **165**, 251-256
127. Pyne, N. J., and Pyne, S. (2011) *Trends in Pharmacological Sciences* **32**, 443-450
128. Alderton, F., Rakhit, S., Kong, K. C., Palmer, T., Sambhi, B., Pyne, S., and Pyne, N. J. (2001) *Journal of Biological Chemistry* **276**, 28578-28585

129. Rakhit, S., Pyne, S., and Pyne, N. (2001) *Molecular pharmacology*
130. Dalle, S., Imamura, T., Rose, D. W., Worrall, D. S., Ugi, S., Hupfeld, C. J., and Olefsky, J. M. (2002) *Molecular and cellular biology* **22**, 6272-6285
131. Povsic, T. J., Kohout, T. A., and Lefkowitz, R. J. (2003) *Science Signalling* **278**, 51334
132. Amith, S. R., Jayanth, P., Franchuk, S., Siddiqui, S., Seyrantepe, V., Gee, K., Basta, S., Beyaert, R., Pshezhetsky, A., and Szewczuk, M. (2009) *Glycoconjugate Journal* **26**, 1197-1212
133. Finlay, T., Jayanth, P., Amith, S., Gilmour, A., Guzzo, C., Gee, K., Beyaert, R., and Szewczuk, M. (2010) *Glycoconjugate Journal* **27**, 329-348
134. Moughal, N. A., Waters, C. M., Valentine, W. J., Connell, M., Richardson, J. C., Tigyi, G., Pyne, S., and Pyne, N. J. (2006) *Journal of Neurochemistry* **98**, 1920-1929
135. Moughal, N. A., Waters, C., Sambhi, B., Pyne, S., and Pyne, N. J. (2004) *Cellular Signalling* **16**, 127-136
136. Lukong, K. E., Elsliger, M.-A., Chang, Y., Richard, C., Thomas, G., Carey, W., Tylki-Szymanska, A., Czartoryska, B., Buchholz, T., Criado, G. R., Palmeri, S., and Pshezhetsky, A. V. (2000) *Human Molecular Genetics* **9**, 1075-1085
137. Hinek, A., Pshezhetsky, A. V., von Itzstein, M., and Starcher, B. (2006) *Journal of Biological Chemistry* **281**, 3698-3710
138. Nan, X., Carubelli, I., and Stamatou, N. M. (2007) *Journal of Leukocyte Biology* **81**, 284-296
139. Yogalingam, G., Bonten, E. J., van de Vlekkert, D., Hu, H., Moshiah, S., Connell, S. A., and d'Azzo, A. (2008) *Developmental cell* **15**, 74-86
140. Rodriguez, J. A., Piddini, E., Hasegawa, T., Miyagi, T., and Dotti, C. G. (2001) *The Journal of Neuroscience* **21**, 8387-8395
141. Sasaki, A., Hata, K., Suzuki, S., Sawada, M., Wada, T., Yamaguchi, K., Obinata, M., Tateno, H., Suzuki, H., and Miyagi, T. (2003) *Journal of Biological Chemistry* **278**, 27896-27902
142. Papini, N., Anastasia, L., Tringali, C., Croci, G., Bresciani, R., Yamaguchi, K., Miyagi, T., Preti, A., Prinetti, A., Prioni, S., Sonnino, S., Tettamanti, G., Venerando, B., and Monti, E. (2004) *Journal of Biological Chemistry* **279**, 16989-16995
143. Daub, H., Weiss, F., Wallasch, C., and Ullrich, A. (1996) *Nature* **379**, 557-560
144. Werry, T. D., Sexton, P. M., and Christopoulos, A. (2005) *Trends in Endocrinology & Metabolism* **16**, 26-33
145. Yang, Y., and Yee, D. (2012) *Journal of mammary gland biology and neoplasia*
146. Huang, Y.-Q., and Pan, J.-X. (2012) *Zhongguo shi yan xue ye xue za zhi / Zhongguo bing li sheng li xue hui = Journal of experimental hematology / Chinese Association of Pathophysiology* **20**, 514-517